# FINAL REPORT

## Zeolite Coating System for Corrosion Control to Eliminate Hexavalent Chromium from DoD Applications

### SERDP Project WP-1342

AUGUST 2009

Yushan Yan
**University of California, Riverside, CA**

**SERDP**
DOD · EPA · DOE

| Report Documentation Page | | Form Approved<br>OMB No. 0704-0188 |
|---|---|---|

| 1. REPORT DATE<br>**AUG 2009** | 2. REPORT TYPE<br>**N/A** | 3. DATES COVERED<br>**-** | |
|---|---|---|---|
| 4. TITLE AND SUBTITLE<br>**Zeolite Coating System for Corrosion Control to Eliminate Hexavalent Chromium from DoD Applications** | | 5a. CONTRACT NUMBER | |
| | | 5b. GRANT NUMBER | |
| | | 5c. PROGRAM ELEMENT NUMBER | |
| 6. AUTHOR(S) | | 5d. PROJECT NUMBER | |
| | | 5e. TASK NUMBER | |
| | | 5f. WORK UNIT NUMBER | |
| 7. PERFORMING ORGANIZATION NAME(S) AND ADDRESS(ES)<br>**University of California, Riverside, CA** | | 8. PERFORMING ORGANIZATION REPORT NUMBER | |
| 9. SPONSORING/MONITORING AGENCY NAME(S) AND ADDRESS(ES) | | 10. SPONSOR/MONITOR'S ACRONYM(S) | |
| | | 11. SPONSOR/MONITOR'S REPORT NUMBER(S) | |
| 12. DISTRIBUTION/AVAILABILITY STATEMENT<br>**Approved for public release, distribution unlimited** | | | |
| 13. SUPPLEMENTARY NOTES<br>**The original document contains color images.** | | | |
| 14. ABSTRACT | | | |
| 15. SUBJECT TERMS | | | |

| 16. SECURITY CLASSIFICATION OF: | | | 17. LIMITATION OF ABSTRACT<br>**SAR** | 18. NUMBER OF PAGES<br>**87** | 19a. NAME OF RESPONSIBLE PERSON |
|---|---|---|---|---|---|
| a. REPORT<br>**unclassified** | b. ABSTRACT<br>**unclassified** | c. THIS PAGE<br>**unclassified** | | | |

# Contents

# 1. Performing Organizations



```
                        Dr. Y. Yan
                                          Mr. M. Boretz
                                          Ms. L. Arth
                                          Ms. C. Howard
```

| Dr. Y. Yan | Dr. P. Zarras | Mr. S. Smith | Dr. M. Tsapatsis |
|---|---|---|---|
| Mr. D. Beving<br>Dr. Y. Kim<br>Dr. R. Cai<br>Mr. R. Munoz<br>Mr. C. O'Neill | Ms. N. Anderson<br>Ms. C. Webber<br>Dr. A. Guenthner | Mr. M. Fleszar<br>Ms. Aisha Bishop<br>Dr. Gay Kendall | Dr. Z. P. Lai<br>Dr. S. Ghosh |
| | Mr. D. Harmston, NADEP | | |
| Zeolite coating<br>In-situ crystallization<br>Basic and standard characterization | Standard (Mil-spec) characterization<br>Polymer coating<br>Formulation/deposition | Basic coa ting characterization<br>Standard (Mil-Spec) characterization | Zeolite coating<br>Alternative deposition<br>Basic coa ting characterization |

Materials engineering/Chemical engineering /Inorganic chemistry/Polymer chemistry/Polymer physics/Physics

## 2. Project Background

**Corrosion control coa ting systems for DoD applications.** Corrosion costs associated with corrosion prevention and correction of corrosion-generated failures account for approximately 25% of the armed services' annual maintenance budgets, or more than $1 billion a year[1]. A majority of these costs is associated with compliance with new environmental regulations regarding worker safety and hazardous waste disposal. These costs have risen dramatically over the past several years – as high as 20% in some DoD facilities. This increase is responsible for a significant portion of noncompliance with new environmental regulations, systems downtime, and failure of mission readiness.

Current effective corrosion control coating systems for alloys and especially aluminum alloys used in DoD applications rely on extensive use of hexavalent chromium ($Cr^{+6}$) in conversion coatings and primers. *Table* 2-1 shows several current military coating systems used for corrosion inhibition on aluminum alloys. All coatings contain hexavalent chromium. As a surface pretreatment, chromium conversion coatings (CCC) were first introduced during the 1950s[2-5]. Since this time, they have found widespread use in both military and commercial applications. Within the DoD community, the CCC process is extensively used to enhance paint adhesion and corrosion inhibition. CCC has been used to effectively treat numerous metals such as aluminum, copper, cadmium, manganese and zinc. Hexavalent chromium is also widely used in the primers for corrosion control (*Table* 2-1). Unfortunately, $Cr^{+6}$ is toxic and carcinogenic[6]. Therefore, regulations regarding its use and disposal have become increasingly stringent. The current Permissible Exposure Limits (PEL) (50 $\mu g/m^3$) of $Cr^{+6}$ have been recommended to be reduced to 1.0 $\mu g/m^3$ by OSHA in order to meet the required low level of risk. Additionally, painting and depainting operations continue to be a significant source of hazardous waste for the DoD[7]. Hazardous waste generation and disposal from such operations are a significant source of painting operation costs. The National Emission Standards for Hazardous Air Pollutant (NESHAP)/Environmental Protection Agency (EPA) regulations are implementing new regulations for reducing chromate exposure for workers and will eventually eliminate its use altogether in the near future. Therefore, a new chromium-free coating system is critically needed to meet corrosion protection performance requirements in all DoD applications.

*Table* 2-1 Military coatings specifications (All coatings systems listed below contain chromates)

| MIL-Spec Description | |
|---|---|
| TT-2756 | solvent-based polyurethane self-priming topcoat |
| TT-P-2760 | solvent-based polyurethane flexible primer |
| MIL-P-53022 | solvent-based epoxy primer |
| MIL-P-53030 | water-reducible epoxy primer |
| MIL-PRF-85582 | water-reducible epoxy primer |
| MIL-PRF-23377 | solvent-based epoxy primer |
| DOD-P-15328 | wash pretreatment (primer) |
| DOD-P-5541 | chromate conversion coating |

**Corrosion resistant zeolite coatings**. Zeolites are crystalline inorganic polymers with a reduced molecular formula $mSiO_2\text{-}AlO_3$ ($1 \leq m \leq \infty$)[8]. At the atomic level, zeolites are constructed from $TO_4$ tetrahedra (T = tetrahedral atom, e.g., Si, Al); each apical oxygen atom is shared between two adjacent tetrahedra. Aluminum atoms usually are uniformly distributed within the polymer structure. According to Si/Al ratio, zeolite can be classified into two groups – high-silica (i.e., high Si/Al) and low-silica (i.e., low Si/Al). Zeolites, and especially high-silica zeolites are known for their thermal stability. Many zeolites are stable to 900 °C and some high-silica zeolites are stable up to 1400 °C without losing their crystalline structure[9]. All zeolites are stable to organic solvents and high-silica zeolites are stable to most mineral acids and react only with hydrofluoric acids[10]. Zeolites are inexpensive. Zeolites are non-toxic. Although not a high-volume application, zeolites are used in personal hygiene products such as odor removal gels and baby diapers. Very recently FDA has approved a medical application, which involves using zeolites as an oral contrast agent for magnetic resonance imaging[11].

Thus far, zeolite materials are most commonly used in particle form as catalysts (e.g., catalytic cracking for petroleum refining) and gas separation media (e.g., air separation into nitrogen and oxygen). Recently zeolite films have been prepared as membranes for separation applications[12]. All of these applications take advantage of the uniform microporosity of zeolites (3-13Å). In other words, zeolites are used in these applications as molecular sieves – sieving molecules according to their size with precision of a fraction of an angstrom. UCR has recently demonstrated for the first time that as-synthesized high-silica zeolite ZSM-5 coatings can be extremely corrosion resistant (*Figure* 2-1, *Figure* 2-2) [13, 14]. Syntheses of high-silica zeolites usually involve using an organic template (or structure-directing-agent) to crystallize the desired structure. These template molecules (e.g., tetrapropylammonium) are bulky and eventually trapped inside the zeolite structure. To free up the pore spaces for catalysis and separation applications, these trapped molecules are usually burned-out by high temperature calcinations (e.g., 500 ºC) in air or oxygen overnight. Therefore, as-synthesized zeolite coatings (without going through calcinations) can be non-porous (*Figure* 2-1c).

High-silica zeolite ZSM-5 coatings on aluminum alloy 2024-T3 (AA-2024-T3) have been shown to offer remarkably better corrosion resistance than chromate conversion coating and anodization coating in strong acids (Figure 2-2 a&b), bases (0.5 M NaOH, not shown), and pitting aggressive environments (*Figure* 2-2 c&d)[13, 14]. For example, there is no decrease of corrosion resistance after the zeolite coated AA-2024-T3 sample is immersed in 0.5 M $H_2SO_4$ for 10 days (*Figure* 2-2 b). The zeolite coating is chemically bonded to the aluminum alloys or other metals through condensation of surface hydroxyl groups[12]. Zeolite coating also has good thermal stability (e.g., 240 ºC) and thermal shock stability (e.g., fast thermal cycling between 240 ºC and – 70 ºC) and good adhesion under mechanical stresses (cutting, impact, and bending). Preliminary results have shown that the zeolite coatings have good paint compatibility and is compatible to polyurethane type paints[13]. They also have better abrasion resistance than anodization coatings. The coating thickness can be readily controlled between 0.5 to 50 μm according to specific needs.
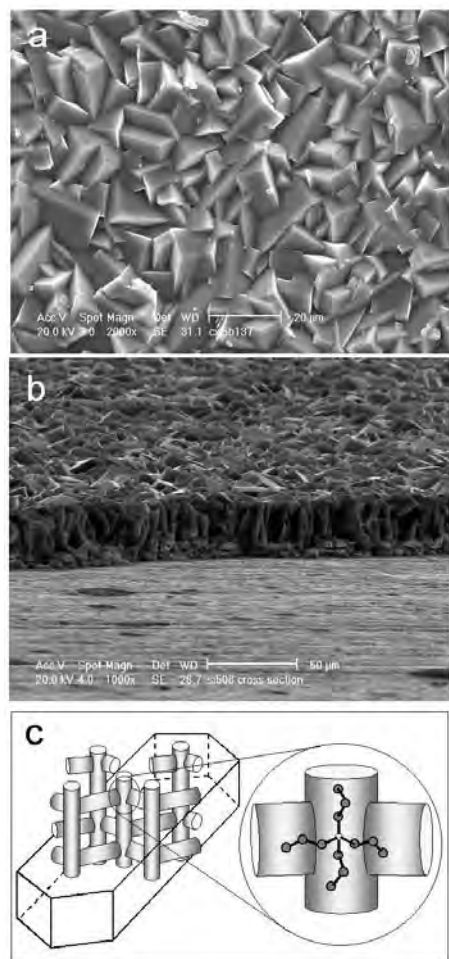
*Figure* 2-1 Scanning electron microscope (SEM) micrographs of an as-synthesized zeolite coating on Al-2024-T3, (a) top view and (b) cross-sectional view, (c) schematic of ZSM-5 pore system and location of the trapped template – tetrapropyl-ammonium (TPA) molecule. Open circle for nitrogen atom and solid circle for carbon atom, and hydrogen atoms were not shown. Ref.[13].
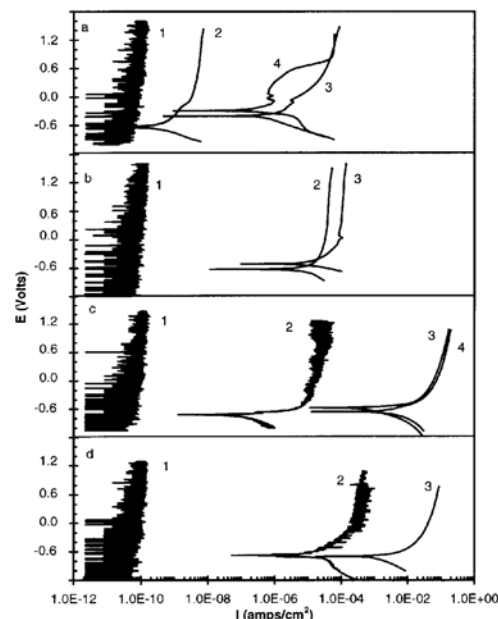


*Figure* 2-2 DC polarization curves of several coatings in different corrosive media. (1) zeolite coating on Al-2024-T3, (2) anodization coating on Al-5005 (sulfuric acid anodized and sealed by hot water, 18 μm thick, provided by Southern Aluminum Finishing, Atlanta, GA), (3) bare Al-2024-T3, (4) chromate conversion coating on Al-2024-T3 (submicron thick provided by Triple AAA plating, Inc. Bells, Texas); (a) 0.5 mol/L $H_2SO_4$ after immersion for 2 hours, (b) 0.5 mol/L $H_2SO_4$ after immersion for 10 days, (c) 0.5 mol/L NaCl/HCl (pH=1) after immersion for 2 hours, (d) 0.5 mol/L NaCl + 0.26 g/L $CuCl_2$ + HAc (pH=3) after immersion for 1 day. All tests at 25 °C with sweep rate of 1 mV/s, saturated calomel electrode and Solartron 1287 potentiostat. . Ref.[13].

Zeolite coating (line 1) provides better corrosion protection than chromate conversion coating and anodization coating in strong acid (a) and (b), strong base (0.5 M NaOH, not shown), and pitting aggressive solutions (c and d).

**Zeolite coating by *in-situ* crystallization.** The high-silica ZSM-5 coatings discussed above were prepared by *in-situ* crystallization process. *In-situ* crystallization here refers to a coating process in which the zeolite crystals making up the eventual polycrystalline coating are crystallized directly at the solid-liquid interface from a synthesis solution during the coating formation process (Figure 2-4)[12]. The synthesis solution used is a clear, *dilute* aqueous solution containing primarily molecular species of silicon and aluminum. The term "*in-situ* crystallization" originates from the fact that there are no preformed zeolite particles in the synthesis solution. The

*in-situ* crystallization coating process is an intrinsically simple (one-step) ***low temperature*** (60 – 180 ℃) hydrothermal process. The feature of low temperature deposition is important because it does not affect the mechanical properties of the alloys. Briefly, the substrate to be coated is immersed in the synthesis solution and any surface that is in contact with the synthesis solution during crystallization process receives a uniform coating. Since the dilute aqueous solution has very low viscosity (similar to water) and is consequently able to penetrate confined non-line-of-sight spaces, *in-situ* crystallization can selectively coat surfaces of complex geometry and in confined spaces (*Figure* 2-4 b)[13]. *In-situ* crystallization process is fast; the shortest deposition time is about 2 hours using conventional oven heating and 5-15 minutes with microwave heating[15]. For conventional oven heating, the reactor is loaded into an oven preheated at the crystallization temperature to start the crystallization. Thus a significant portion of the 2-hour heating goes to bring the temperature of the reaction mixture from ambient to the desired reaction temperature.
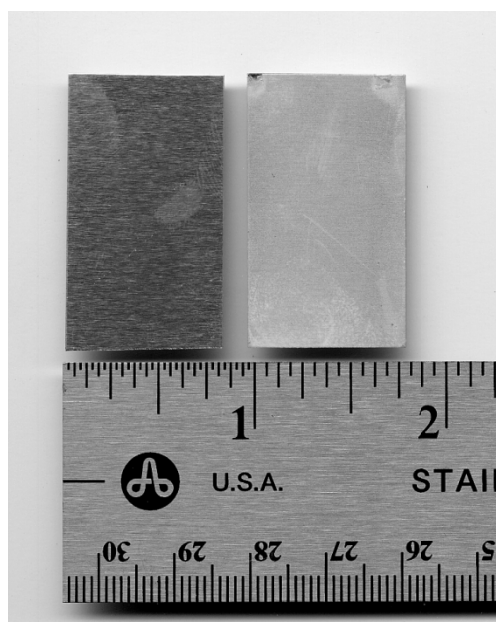


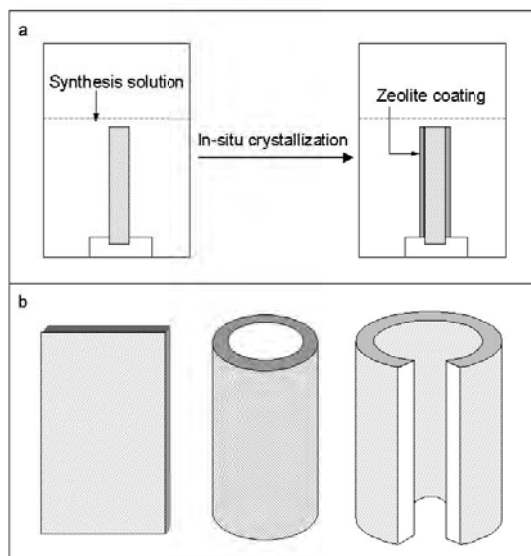Figure 2-3 Pictures of AA-2024-T3 coupons. Left is bare, right is ZSM-5 coated.



*Figure* 2-4 Schematics of an *in-situ* crystallization process and substrate geometries successfully coated. (a) *In-situ* crystallization process. (b) Substrates geometries – flat surface, inside and/or outside surfaces of a small tube (3 mm ID) and a curved narrow channel (3 mm channel width). Later on square channels of 500 um size were also successfully coated.

## 3. Objectives

The overall objective of the proposed project is to develop a new environmentally friendly zeolite coating system for corrosion control to eliminate hexavalent chromium in DoD applications without sacrificing performance. The specific goals of the project are as follows.

1) Development of zeolite coatings (see Tasks for details).
2) Demonstrate compatibility with current Military water-dispersible polyurethane topcoats.
3) Basic characterization and standard testing of zeolite and zeolite/topcoat systems and provide performance benchmarking with current chromium-containing DoD coating systems.
4) Fast technology transition.

## 4. Technical approach

This SERDP project will have four major thrusts: (1) development of zeolite coatings on DoD relevant alloys; (2) demonstrate compatibility of zeolite coatings with current Military water-dispersible polyurethane topcoats; (3) basic characterization and standard testing of zeolite/topcoat systems with benchmarking obtained from performance of current chromium-coating coating systems; (4) technology transition. Specifically, the following tasks will be carried out by the research team consisting of UCR, UMN, NAWCWD (China Lake), Army Benet Labs, and NADEP (North Island).

**Task 1: Zeolite coatings**

*Task 1-1: Extension of in-situ crystallization coating deposition process from AA-2024-T3 to other DOD relevant alloys such as AA-6061-T6, and AA-7075-T6, and steels (S1008, S4130, SS304)*

With support from US EPA, UCR has so far focused on 2x3 cm coupons to demonstrate that high-silica-zeolite (PSZ) coatings can be successfully deposited on AA-2024-T3, and the as-synthesized coatings are corrosion-resistant in strong acid, base, and pitting aggressive environments, and have good thermal and thermal shock stability, and good adhesion under mechanical stresses (cut, bending, and impact). For the proposed effort, it is important to show that the *in-situ* crystallization coating process can be extended to other DoD relevant alloys such as AA-6061-T6, AA-7075-T6, and cold rolled steel S-1008.

*Task 1-2: Scale-up in-situ crystallization coating deposition process from current 2x3 cm coupons to larger panels such as 3x6 inches*

With US EPA support, UCR's effort up to today has focused on 2x3 cm coupons because they are convenient to produce and adequate for the current research needs. By using small coupons, the amount of chemicals used can also be minimized. In the proposed effort, it is critical to demonstrate that the process can be scaled up. Large 3x6 inch panels are also needed for standard tests (e.g., ASTM and Mil-Spec as described in Task 4).

*Task 1-3&1-4: Develop alternative coating and coating deposition method*

The goal of this task is to develop alternative zeolite coatings (i.e., other than ZSM-5) and deposition process. The central requirements are ambient pressure, low temperature, and short deposition time. The process should also be convenient for repair should the original coating damaged. Two different deposition methods are being developed. The first one is a layer-by-layer deposition process using MCM-22 developed by UMN. The precursor of zeolite MCM-22, namely MCM-22(P), is a layered aluminosilicate. Layers in the as-synthesized MCM-22-(P) are weakly linked together with organic structure directing agents, Hexamethyuleneimine (HMI), along the [001] direction. Two-dimensional large channels are running in-plane of the MCM-22-(P) layers. However, the limiting apertures for transport perpendicular to the layers (along [001] direction) are 6MR's, i.e. defined by six interconnected $SiO_4$ tetrahedra. Thus, molecules like water and $O_2$ cannot penetrate along the c-axis. Upon calcination, MCM-22(P) condenses to MCM-22. On the other hand, layers in MCM-22(P) can be delaminated. After calcination, it

forms another material called ITQ-2. Either MCM-22(P) or MCM-22 particles are plate-like. Delaminated layers will be even thinner. We use these materials as building blocks to assemble a thin film by a chemical interaction based Layer-by-Layer method for corrosion protection. The second one is microwave-assisted ambient pressure ionothermal synthesis method using SAPO-11. In this method, ionic liquid was used instead of water, making it possible for zeolite synthesis at ambient pressure even at temperatures higher than 100 $^{\circ}$C since ionic liquid has negligible vapor pressure. Microwave radiation can accelerate the deposition process to fulfill the requirement of short deposition time.

## Task 2: Application of primer/topcoat or topcoat to zeolite coatings

The U.S. Army has developed a water dispersible polyurethane (U. S. Patent #5,691,410), which is currently being used by DoD for tactical and related support equipment. The water-dispersible (WD) chemical agent resistant coating (CARC) utilizes hydroxyl-functional polyurethane dispersions and water dispersible polyisocyanates. The U.S. Air Force has similarly developed a water dispersible polyurethane topcoat. Both Army and Air Force polyurethane topcoats will be applied to the zeolite coated alloys to demonstrate compatibility with these systems.

Primers and primer/topcoat systems currently in use by the military will also be applied to the zeolite coatings to demonstrate compatibility of the zeolite coating with existing systems. The different primers and topcoats and combinations to be tested are shown below.

| Primer | Topcoat |
|---|---|
| Mil-P-23377 I (chromated) | Mil-PRF-85285 |
| Mil-P-23377 I (non-chromated) | Mil-PRF-85285 |
| Mil-P-85582  (non-chromated) | Mil-PRF-85285 |
| | |
| Mil-P-23377 I (chromated) | none |
| Mil-P-23377 I (non-chromated) | none |
| Mil-P-85582  (non-chromated) | none |
| TT-P-2756 A (self-priming topcoat) | none |

## Task 3: Laboratory characterization and standard tests

***Task 3-1: Characterization of coating surfaces***. Quantitative surface characterization will be performed by Laser Scanning Confocal Microscopy (LSCM) and Atomic Force Microscopy (AFM). These methods provide non-destructive 2- and 3-dimensional imaging with no *a priori* surface preparation. Surface characterization of individual proposed layers will provide insights to total coating system performance (e.g., enhanced adhesion of topcoat to zeolite due to significant surface area available for bonding). LSCM and AFM will be used to obtain a quantitative measure of surface area, complexity (roughness, fractal dimension), and quality

(frequency/size of defects) of the following systems, having been applied to Al and steel substrates: (i) zeolite coating, (ii) zeolite/polyurethane topcoat system.

Surface characterization by LSCM and AFM will be repeated following sequential accelerated weathering exposures (see Task 3-4) of systems (ii) to quantitatively describe coating system degradation. Results will be benchmarked with current Army & Air Force pretreatment/primer/topcoat systems.

**Task 3-2: Instrumental analyses of coating degradation.** Several analytical techniques will be used to examine the degradation due to accelerated environmental weathering of zeolite/topcoat systems on aluminum alloy and steel substrates. These tests include thermal gravimetric analysis (TGA), Fourier transform infrared spectrometry (FTIR), thermal mechanical analysis (TMA), scratch tests and wear tests. In all cases, these tests will be conducted before, during and after accelerated service simulation testing. TGA is a technique which measures the weight of a sample as a function of temperature. TGA can effectively measure moisture, solvent, additive or plasticizer loss and the rate of thermal decomposition. FTIR can provide valuable information regarding the chemical nature and molecular structure of the material. This technique can provide information regarding the effects of drying and weathering on paints. TMA techniques can measure the coefficient of thermal expansion, stress relaxation, penetration, softening and glass transition temperature of thin films such as paint coatings, which will provide degradation profiles.

**Task 3-3: Quantitative/qualitative adhesion testing of coatings to substrates.** Current standard techniques for adhesion testing will be performed using ASTM qualitative adhesion testing such as the wet tape adhesion (FED-STD –141 method 6301) and dry tape adhesion (ASTM D3359). Benet Laboratories will apply semi-quantitative assessments of coating adhesion. They will use several techniques pioneered in their laboratories[16]. Adhesion Peel Testing (APT) and Dynamic Mechanical Analysis (DMA) will be utilized to evaluate the effects of surface pretreatments and coating process parameters on interfacial adhesion. Tests will be performed on zeolite and zeolite/topcoat systems.

**Task 3-4: Conduct accelerated service simulation testing.** Accelerated testing of all panels using novel zeolite and zeolite/topcoat systems and current military coatings as controls will be carried out using an Accelerated Corrosion Test Chamber. This chamber will provide precision testing such as 2000-hour salt-fog (ASTM B117) tests. If test panels meet this initial requirement, further testing will include acetic acid/salt spray (ASTM B287), copper accelerated salt spray (ASTM B368), corrodkote (ASTM B380), sulfur dioxide (ASTM B605) and GM 9540 tests. UV exposure tests will be performed on coated coupons following ASTM test 53-96 guidelines for 32 weeks.

**Task 3-5: Examine substrate degradation and corrosion inhibition.** The evaluation of the substrate corrosion, pitting, etc., will be evaluated using such techniques as eddy current, electrochemical impedance spectroscopy (EIS) and DC Polarization. Nondestructive eddy

current techniques will be used to measure electrical resistivity of the component structure to determine if corrosion has occurred. Eddy currents have been extensively used to measure the electrical resistivity of metals and have been very successful at determining cracks and corrosion[17]. EIS is a very sensitive technique to measure the corrosion barrier performance of a coating by measuring its electrical impedance. The charge transfer resistance obtained from this experiment provides an excellent indicator of the integrity of the coating and successfully predicts long-term corrosion behavior. This technique can effectively measure coating defects, water uptake, coating degradation and substrate corrosion. The technique measures various degradation processes in the coating, which causes absorption of electrical energy at different frequencies. This causes a time lag between the time-dependent excitation and response signals. These processes can be simulated by equivalent electrical networks. The frequency response generated from the EIS test is analyzed using a Bode plot, which can discriminate between different electrochemical processes. These plots provide detailed information about coating stability and degradation. They do not require any accelerating factors for testing and can be conducted *in-situ*.

***Task 3-6: Marine atmosphere tests.*** Zeolite and zeolite/topcoat systems will be field-tested in marine environment, and subsequently evaluated by all the relevant laboratory tests listed previously including adhesion. The coated coupons will be exposed to a marine environment both continuous and intermittent. The intermittent exposure tests will be performed at the NADEP located near coastal waters. If the panels pass this initial phase of testing, they will be subject to continuous exposure mounted on a navy vessel. Both these tests will provide initial verification of the robustness of the proposed coatings systems. Further studies for extensive field-testing will be developed as part of the transition study (Task 4).

***Task 3-7: Toxicology studies.*** Initial toxicology studies will focus on the Extraction Procedure (EP) Toxicity Test Method (EPTOX) (Method 1310A) and Toxicity Characteristic Leaching Procedure (TCLP) (Method 1311) for the analysis of potential byproducts from the zeolite-conductive polymer coatings. These tests are EPA approved to determine the leachates obtained from solid materials (Index to EPA Methods, ed. Peg Nelson, updated December 2001, SW-846 Manual, Chap 8.4-Methods for Determining Characteristics, April 1998), such as any potential small molecules that can be leached out of the coating into the environment.

## Task 4: Transition study of proposed technology

After successful completion of Task 3, a transition plan will be implemented. This plan will document all data from all laboratory tests. Once all technical data is assembled, it will provide a basis for a new MIL-spec for control of corrosion and elimination of hexavalent chromium. The cost-effectiveness data will also be documented and provided for fleet-wide study. This will allow an easy transition and dispersion of the data to other applications and maintenance sites for NAVAIR, AF and Army systems.

*Milestones and milestone owners*
The following milestones are built according to the federal fiscal year cycles. Milestone owners and the deadline are in parenthesis. **In case of multi-institutions as milestone owners, the first one is the lead institution**.

*Task 1-1: Extension of in-situ crystallization from AA-2024-T3 to AA-6061-T6, AA-7075-T6, S-1008*
    (1) Production of 2x3 cm ZSM-5 on AA-2024-T3, AA-6061-T6, AA-7075-T6, and S-1008. (*UCR 10/1/03*) → COMPLETED

*Task 1-2: Scale-up in-situ crystallization from 1x3 coupons to 3x6 panels*
    (2) Production of 3x6 ZSM-5 on AA-2024-T3 (*UCR 10/1/03*) → COMPLETED
    (3) Production of 3x6 ZSM-5 on AA-5052-H32, AA-6065-T6, AA-7075-T6 and S1008, (*UCR 10/1/04*) → COMPLETED and expanded to include ZSM-5 on S4130 and SS304-2b

*Task 1-3 and 1-4: Develop alternative zeolite and alternative deposition method (MCM-22)*
    (4) Production of 2x3 cm MCM-22 on AA-2024-T3 (*UM 10/1/03*) → COMPLETED
    (5) Production of 3x6 inches MCM-22 on AA-2024-T3 (*UM 10/1/05*) → COMPLETED
    (6) Production of 2x3 cm SAPO-11 on AA-2024-T3 *(UCR 1/31/08)* → THIS WAS AN ADDED TASK WITH SERDP PERMISSION AND COMPLETED

*Task 2: Application of primer/topcoat or topcoat to zeolite coatings*
    (7) Production of 3x6" ZSM-5/CARC Topcoat(Mil-PRF-64159) (**UCR, Benet, NAWCWD 10/1/05**) → COMPLETED
    (8) Production of 3x6" ZSM-5/topcoat [VOC-free topcoat (Deft product #55W-002, Deft, Irvine CA) and Self-Priming topcoat (TT-P-2756A from Deft, Irvine, CA)] (**UCR, NAWCWD 10/1/05**) → COMPLETED
    (9) Production of 3x6" ZSM-5/topcoat and ZSM-5/primer/topcoat (**UCR, NAWCW D 10/1/06**) → COMPLETED

*Task 3-1: Characterization of coating surfaces.*
    (10) Quantitative Surface Imaging by LSCM (**Benet** *10/1/05*) → COMPLETED
    (11) RMS Roughness (**Benet** *10/1/05*) → COMPLETED
    (12) Scaling Analysis & Optimized Filtering for LSCM Images (**Benet** *10/1/05*) → COMPLETED

*Task 3-2: Instrumental analyses of coating degradation.*
    (13) Dynamic mechanical analysis (**Benet** *10/1/05*) → COMPLETED
    (14) Quality Control testing method by DC Polarization on 3x6 inch zeolite coatings on AAs(2024-T3, 5052-H32, 6061-T6, 7075-T6) and steels (SS304, S4130, S1008)(**UCR** *10/1/06*) → COMPLETED
    (15) 3x6 ZSM-5 on AA-6061-T6, AA-7075-T6, and S-1008 (**Benet, NAWCWD, UCR 10/1/03**) → COMPLETED
    (16) 2x3 cm MCM-22 on AA-2024-T3 (**UM, UCR 10/1/03**) → COMPELTED
    (17) 3x6 MCM-22 on AA-2024-T3 (**UM, UCR 10/1/05**) → DROPPED

(18) 3x6" ZSM-5/topcoat system on AA-2024-T3 (**Benet, NAWCWD, UCR 10/1/05** ) → DELAYED BUT LATER COMPLETED

*Task 3-3: Quantitative/qualitative adhesion testing of coatings to substrates*
   (19) ASTM  D3359-2 adhesion test of ZSM-5 on AAs (2024-T3, 5052-H32, 6061-T6, 7075-T6)  (**UCR *10/1/04*)** → COMPLETED
   (20) Mechanical cutting test  of ZSM-5 on AAs (**UCR *10/1/04*)** → COMPLETED
   (21) Mechanical hole punching of ZSM-5 on AA-2024-T3(**UCR *10/1/04*)** → COMPLETED
   (22) ASTM D-2794-93 impact test (**UCR *10/1/05*)** → COMPLETED
   (23) ASTM D- 522-93a bending test (**UCR *10/1/05*)** → COMPLETED
   (24) ASTM G154-00a UV exposure (**UCR, Benet *10/1/06*)** → COMPLETED

*Task 3-4: Conduct accelerated service simulation testing*
   (25) ASTM B117 Salt-fog testing on bare zeolite coating (0.5 -2 um thick) on AA2024-T3 (3x6 inch) (**NAWCWD, 4/1/04)** → COMPLETED
   (26) ASTM  B117  Salt-fog  testing  on 3x6"  ZSM-5/CARC Topcoat(Mil-PRF-64159) (**NAWCWD *10/1/05*)** → COMPLETED
   (27) ASTM  B117  Salt-fog  testing  on  bare  zeolite  coating (7.5  um  thick,  no  QC)  on AA2024-T3 (3x6 inch) (**NAWCWD, 4/1/05)** → COMPLETED
   (28) ASTM  B117  Salt-fog  testing  on  bare  zeolite  coating  (7.5  um  thick,  with  QC)  on AA2024-T3 (3x6 inch) (**NAWCWD, 4/1/06)** → COMPLETED
   (29) ASTM B117  Salt-fog  testing  on ZSM-5/topcoat [VOC-free topcoat (Deft product #55W-002, Deft, Irvine CA) and Self-Priming topcoat (TT-P-2756A from Deft, Irvine, CA)] (**NAWCWD *10/1/05*)** → COMPLETED
   (30) ASTM B117 Salt-fog testing on machine scribed bare zeolite coating (7.5 um thick, with QC) on AA2024-T3 (3x6 inch) (**NAWCWD, 4/1/06)** → COMPLETED
   (31) ASTM  B117  Salt-fog  testing  on  ZSM-5/topcoat  and  ZSM-5/primer/topcoat (**NAWCWD *10/1/06*)** → COMPLETED
   (32) ASTM B117 Salt-fog testing on bare zeolite coating (4-5 um thick, with minimal QC) on 3x6 inch steels (SS304,S4130,S1008)  (**NAWCWD, 10/1/06)** → COMPLETED
   (33) ASTM B117 Salt-fog testing on machine scribed bare zeolite coating (4-5 µm thick, with minimal QC) on 3x6 inch steels (SS304 and S4130) (**NAWCWD, 6/20/08** ) → COMPLETED

*Task 3-5: Examine substrate degradation and corrosion inhibition. (UCR, NAWCWD, 4/1/07)* → *COMPLETED*

*Task 3-6: Marine atmosphere tests/EIS measurements/coating degradation studies. (UCR, NAWCWD, 4/1/07)* → *In progress*

*Task 3-7: Toxicology Studies (UCR, NAWCWD, 4/1/07)* → *DROPPED WITH PERMISSION FROM SERDP*

*Task 4: Transition Study of Proposed Technology (NAWCWD, NADEP, Benet, UCR, 4/1/07)* → *Considered finished for the project but will still be pursued*

## 5. Project Accomplishments

This is a final report for a project with duration of 5/2003 – 7/1/2008. We will follow the order of tasks. We use a simplified section heading for each task in most cases to save space, and for the details of each milestone please see section 4.

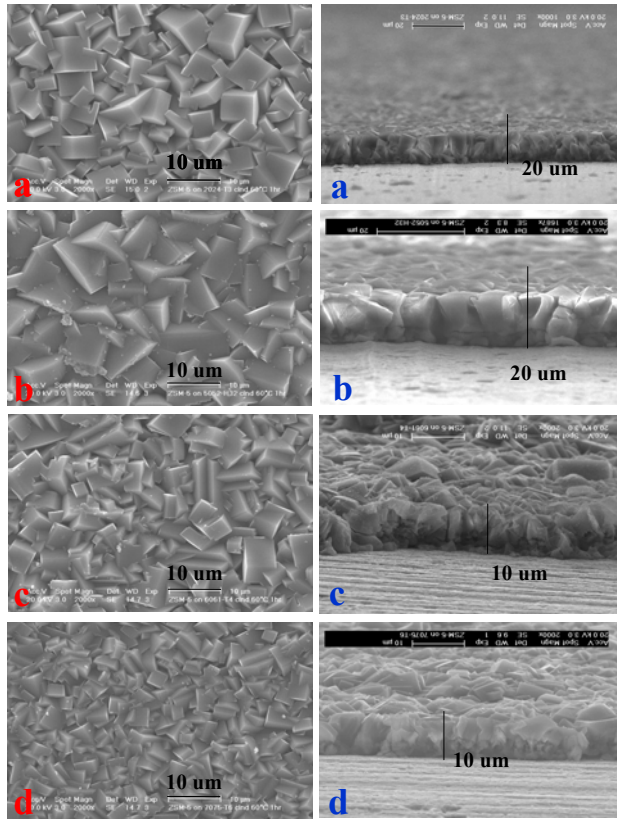## Task 1-1: Extension of ZSM-5 coating to other DoD alloys



*Figure* 5-1. SEM images of ZSM-5 coatings on aluminum alloys (a)AA-2024-T3, (b)AA-5052-H32, (c)AA-6061-T4, and (d)AA-7075-T6.
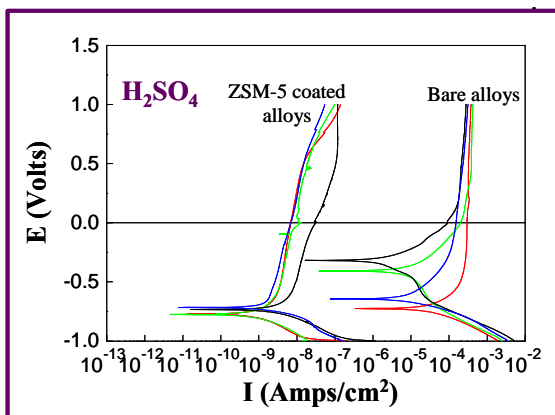
UCR has successfully extended ZSM-5 coating from AA 2024-T3 to AA-6061-T6, AA7075-T6 and steel SS1008 using 2x3 cm coupons. A universal solution composition and a universal deposition procedure were developed that produce high quality coatings on all of the aluminum alloys tested (2000, 5000, 6000, and 7000 series). Universal solution and deposition procedures are important as this eliminates the need to adjust the solution composition and deposition procedure to suit an individual alloy, and this means significant cost savings. The molar composition of the synthesis solution is TPAOH/0.16 : NaOH/0.64 : TEOS/1 : H2O/92 : Al/0.0018. Here TPAOH is for tetrapropylammonium hydroxide and TEOS for tetraethylorthosilicate. This is a fairly dilute aqueous solution and the deposition process produces uniform coating on the substrate with little bulk crystallization. The deposition was carried out in convection oven at 175 °C for 12-16 hours.

*Figure* 5-1 shows the scanning electron micrographs of ZSM-5 coatings on AA-2024-T3, AA-5052-H32 (not required by the project), AA-6061-T4, and AA-7075-T6. The coatings are polycrystalline, continuous, and well adhered to the substrate. Thickness varies from 7-10 um.

The corrosion resistance of the ZSM-5 coatings on these aluminum alloys are measured in acid, base and pitting aggressive media and their polarization curves are shown in *Figure* 5-2. Clearly, good corrosion resistance was obtained on all of these coatings and in all of the media tested.

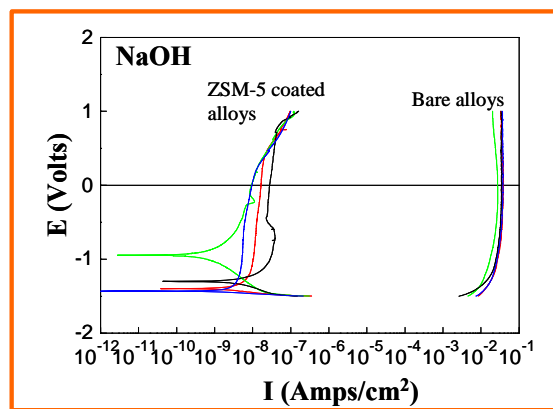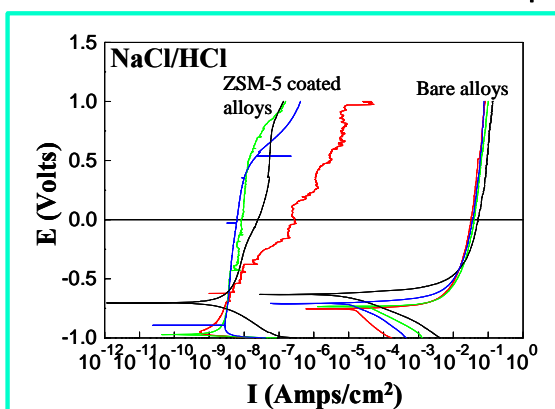Figure 5-2 Polarization curves of ZSM-5 coatings on AA2024-T3, AA-5052-H32, AA-6061-T4, and AA-7075-T6 in acid (H₂SO4), base (NaOH) and NaCl solutions.

## Task 1-2: Scale up the deposition process to 3x6" panels from 2x3 cm coupons

UCR successfully scaled up the coating process from 2x3cm coupons to 3x6" panels (ZSM-5 on AA-2024-T3) in October 2003. This allows the performance of many ASTM and Mil-spec testing. The same chemical solution (TPAOH/0.16 : NaOH/0.64 : TEOS/1 : H2O/92 : Al/0.0018) was used on the large 3x6" panels as for the small 2x3cm" coupons. And the deposition was also carried out in a convection oven at 175 °C for 12-24 hours. The reactor used was a simple standard steel autoclave with a Teflon liner from Parr Instruments. The substrate was suspended from a Teflon bridge at the top of the liner (*Figure* 5-3a). The scale up had little impact on deposition chemistry. The coatings are extremely uniform (*Figure* 5-3b) and have excellent adhesion. The coatings are very flexible.
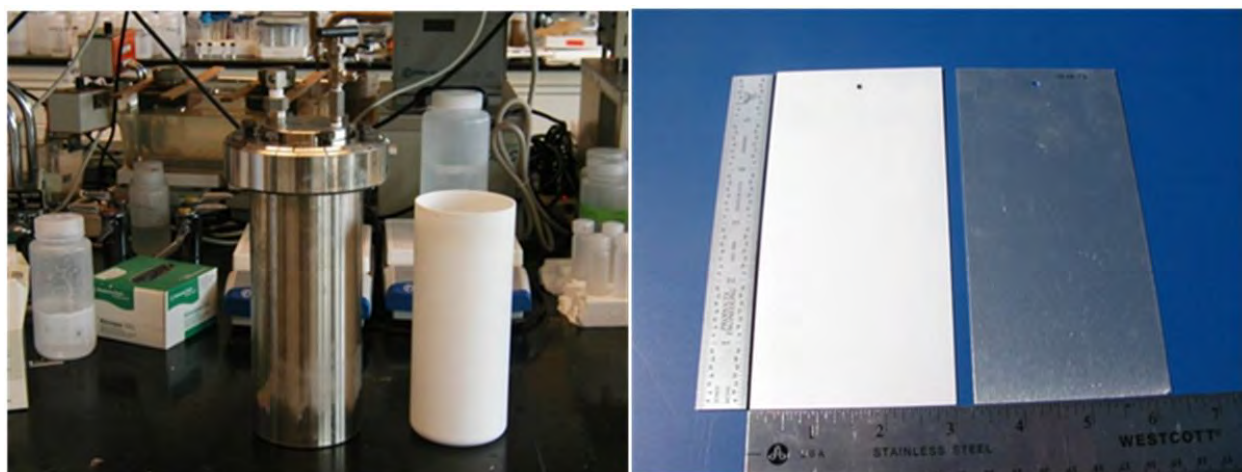


*Figure* 5-3 (a) A commercial Parr autoclave was used as the reactor; with white Teflon liner, (b) Optical images of bare AA-2024-T3 (right) and ZSM-5 coated AA-2024-T3 (left).

We have gone through three evolutions of zeolite coating syntheses on the 3" x 6" AA-2024-T3 coupons (*Figure* 5-4). Each generation of zeolite coating was salt fog tested by ASTM B117 (results shown later in this report).

By adjusting the solution to surface area ratio and crystallization time, we can produce uniformly coated 3x6"panels of variable but controlled thicknesses. We have investigated the coating corrosion properties at several thicknesses (0.5, 2, 4.5, 7.5, 11, and 13 um thick). Salt fog tests (ASTM B117) were performed on zeolite coated AA-2024-T3 (0.5 um [Generation – 1] and 7.5 um thick [Generation - 2 & 3]) and on scribed coatings (7.5 um thick [Generation – 3]) (see testing results in later sections).

## Evolution of zeolite coatings on metal alloys

### Evolution of zeolite coatings on AA-2024-T3 (and other AAs)

Generation – 1
- 0.5 um thick (no optimization and no QC)
- Poor salt-fog performance of bare zeolite on AA-2024-T3
- Actions
  - Developed protocols for producing coatings of various thickness (e.g., 0.5, 2.0, 4.5, 11, 13 um)
  - Decided to use 7.5 um as the new benchmark (Generation-2 and -3 coatings)

Generation – 2
- 7.5 um thick (no optimization)
- Inconsistent salt-fog performance of bare zeolite on AA-2024-T3
- Actions
  - Optimize zeolite coating synthesis
  - Implement QC testing on zeolite coatings (DC Polarization in 5 wt% NaCl)

Generation – 3
- 7.5 um thick (limited optimization – aging time and DC Polarization in 5 wt% NaCl testing for QC)
- Excellent DC Polarization performance in 5 wt% NaCl
- Consistently excellent salt-fog performance of bare zeolite on AA-2024-T3

### Evolution of zeolite coatings on steels (SS-304-2b, S4130, S1008)

Generation – 3 (same synthesis methods as Generation – 3 for zeolite on AAs)
- 4-6 um thick (no optimization specific for zeolite on steels and no routine QC testing)
- Excellent DC Polarization performance in 5 wt% NaCl
- Good to excellent salt-fog performance of bare zeolite on steels

*Figure* 5-4 Evolution of zeolite coatings on metal alloys.

The scale up and application of Generation - 3 zeolite coatings was successfully expanded to other DoD aluminum alloys (AA-5052-H32, AA-6061-T6, and 7075-T6) and to several steels (SS304-2b, S4130, and C1008). These have all been tested by DC Polarization in 5 wt% NaCl, showing excellent corrosion resistance (results and details shown later in this report).

*Figure* 5-5 shows the scanning electron micrographs of Generation – 3 ZSM-5 coatings on S1008, S4130 and SS304-2b (S4130 and SS304-2b not required by the project). The coatings are polycrystalline, continuous, and well adhered to the substrate. Thickness varies slightly from 4 - 5 um.

Five zeolite coated panels of each steel (SS30-2b, S4130, and C1008) with zeolite thickness of about 5 um salt fog tested (ASTM B117) at China Lake (results and details shown later in this report).

Key features and milestones of zeolite coating technology:
- Simple alkaline detergent solution pretreatment adequate for all metals
- Immerse metal in 3 grams Alconox® per 400 ml de-ionized $H_2O$ at $60^oC$ for 30 minutes
- Single zeolite chemical formulation adequate for all metals
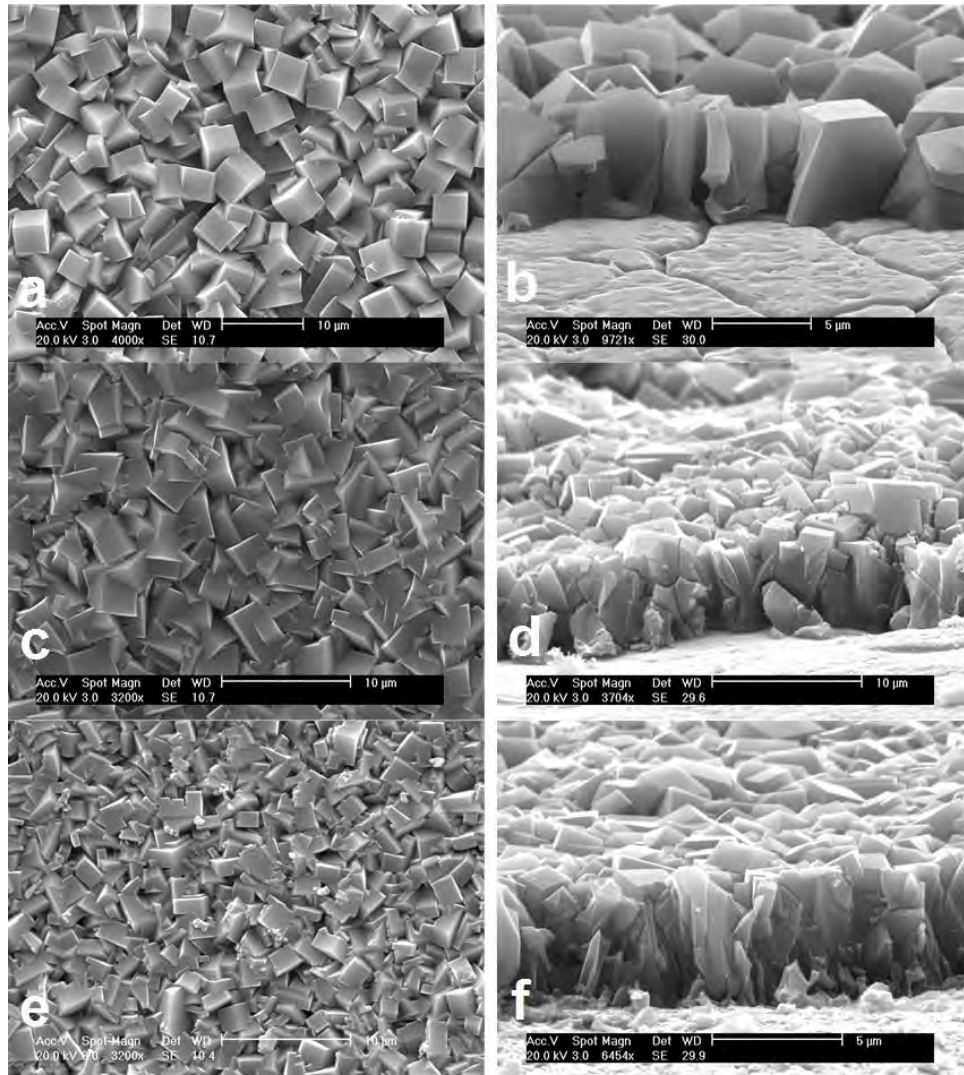- TPAOH/0.16 : NaOH/0.64 : TEOS/1 : H2O/92 : Al/0.0018

*Figure* 5-5 SEM images of ZSM-5 coatings (4 - 5 um thick) on steels. SS304-2b (a, b); S1008 (c, d); S4130 (e, f)

## Task 1-3 & 1-4: Alternative zeolite and deposition process

The central goal of this task is to develop a coating process that is low pressure, low temperature, and short deposition time.

### Layer by layer deposition of MCM-22

MCM-22 and its precursor MCM-22(P) are microporous aluminum silicates reported by Mobil researchers[18]. In MCM-22(P), the structure directing agent, hexamethyleneimine, is located between layers. By special treatments, MCM-22(P) can be delaminated leading to a new aluminosilicate, ITQ-2[19]. The delaminated material was reported to be stable at high temperatures (in excess of 500°C). On the other hand, by calcination the silicate layers in MCM-22(P) condense to form MCM-22 (structure code MWW). Based on their framework structures, the limiting apertures for transport perpendicular to the layers (along [001] direction) are 6MR's, i.e. defined by six interconnected $SiO_4$ tetrahedra. Molecules like water and $O_2$ cannot penetrate along the c-axis. Therefore, the primary idea of this project is to prepare a dense c-oriented MCM-22 film which is practically impermeable and thus suitable for the corrosion protection purpose.

*Synthesis of MCM-22(P)*

Layered MCM-22(P) precursor was prepared using hexamethylenimine (HMI, Aldrich), silica (Aerosil 200, Degussa), sodium aluminate (56% $Al_2O_3$, 37% $Na_2O$ Carlo Erba), sodium hydroxide (98% Prolabo), and deionized water[18]. More specifically a sample with Si/Al = 50 was prepared as follows: 0.239g of sodium aluminate and 0.826g of NaOH were dissolved in 103.498g of $H_2O$ by magnetic stirring for few minutes, then 6.373g of HMI were added slowly leading to a yellowish solution, and finally 7.86g of $SiO_2$ were added very slowly under continuous stirring. After 30 minutes of vigorous stirring, the very viscous final gel was poured into a 60-ml Teflon lined stainless-steel autoclave and treated at 408K for 11 days, rotating at 60 rpm. After cooling down the autoclaves quickly, the samples were centrifuged at 10,000 rpm and washed with water until pH < 9. Typical particle morphology of as-synthesized MCM-22(P) is shown in *Figure* 5-6. Most particles are plate-like with dimensions of about 1µm in width and length and less than 100nm in thickness. Some particles curl. The x-ray diffraction pattern on the right verifies that the synthesized materials are MCM-22(P).
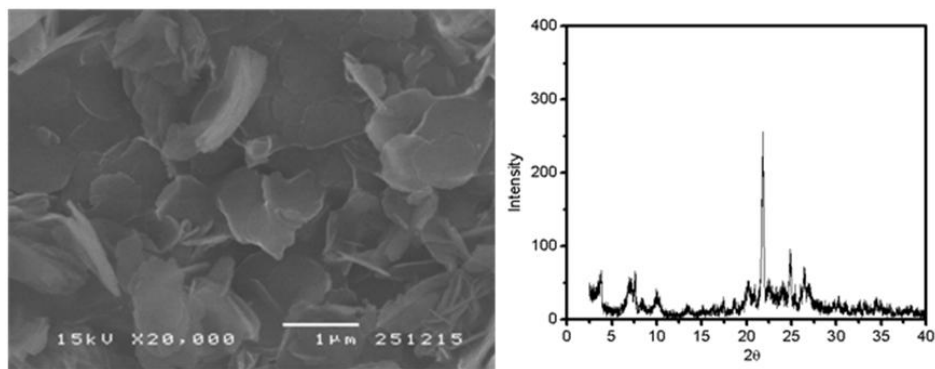


*Figure* 5-6 MCM-22(P) as made for 11 days at 135ºC, before calcination or swelling.

*Condensation of MCM-22(P) to MCM-22 and avoidance of agglomeration*
To ensure good dispersion and to avoid agglomeration during calcination, MCM-22(P) particles were first filtered and then calcined in a way analog to that reported in ref[20]. First, 5g of MCM-22(P) wet cake was well-dispersed into 20ml DI water by stirring for one hour followed by ultrasonication for another one hour. The suspension was filtered by high-density polyethylene filter tips (POREX) with particle retention size of 5μm, and then diluted to a total volume of 100ml. The solution was stirred at room temperature for another one hour before 10g of acrylamide (AM, Aldrich) and 0.1g of N, N'-methylenebisacrylamide (MBAM, Aldrich) were added inside. The mixture was further stirred for about 30 minutes until all the water-soluble organic monomers completely dissolved. Then 0.25g of $(NH_4)_2S_2O_8$ was added to the solution under stirring. Finally the solution was placed in an ultrasonicator for one hour. During sonication the solution will become warm and the organic monomers will be polymerized to form a white hydrogel with the MCM-22(P) particles trapping inside. The hydrogel was dried at 90°C overnight before it was carbonized under nitrogen (150cc/min) at 540°C for 2 hours (heating rate 2°C /min) and then calcined at 540°C for 3 hours under air (150cc/min).

*Figure* 5-7 shows the SEM image and the x-ray diffraction pattern of particles after calcination. Most crystals have the plate-like shape with similar dimensions to the as-synthesized MCM-22(P) crystals. The x-ray diffraction pattern confirms that the MCM-22(P) crystals condensed to MCM-22 during calcination.
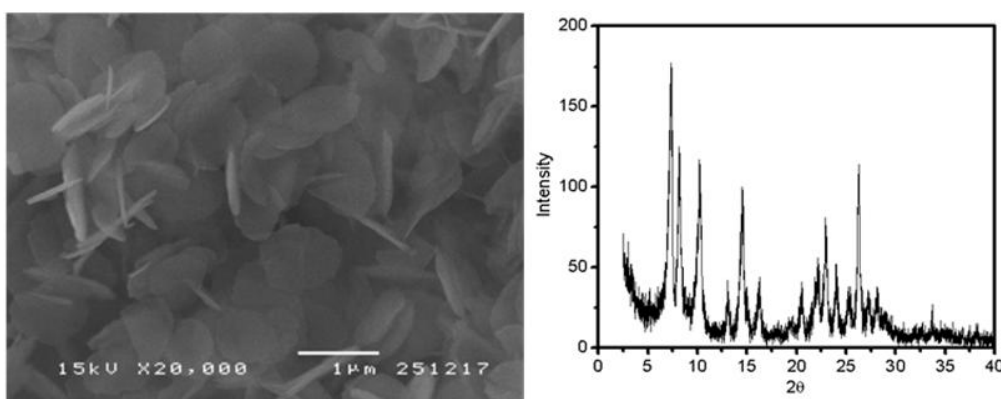


*Figure* 5-7 MCM-22 crystals. A) SEM image of particles after calcination at 540ºC in air for 3 hours; B) X-ray diffraction pattern.

*Exfoliation of MCM-22(P) to ITQ-2*

The exfoliation procedure involves two steps, that is, swelling under the interaction of surfactants followed by exfoliation provoked by ultrasonication. After compared the swelling procedures in ref.[21] and ref.[22], we adopted the following procedure. First, 3.05g cetyltrimethylammonium bromide (CTAB surfactant, Aldrich), 4.16g deionized water and 6.60g tetrapropylammonium hydroxide (TPAOH, 1M in water, Aldrich) were mixed together and stirred for 1 hour to form a slurry. Then 1.00g MCM-22(P) cake was added to the slurry under stirring. Swelling was processed by refluxing the mixture at 80°C for 20 hours. The excess surfactant was dissolved by adding about 10 drops of concentrated hydrochloric acid until the pH of the mixture was less than 2. The mixture was stirred for another 1 hour before the remained powder was collected by filtration. The collected powder was dried at 90°C overnight. XRD pattern of the powder was taken at this point. Exfoliation of the dry powder was carried out by first re-disperse the powder (~1g) into 40g of deionized water. The solution was then ultrasonicated for 2 hours. Powder was collected from the solution by centrifuging at the speed of 15000rpm.

XRD patterns of the MCM-22(P) powder before swelling, after swelling and after exfoliation are shown in *Figure* 5-8, respectively. As pointed out in ref.[22], a successful swelling can be roughly determined from changes in the XRD patterns according to the following criteria.

1) General hkl reflections shift to lower 2θ angles or disappear altogether.
2) hk0 reflections remain invariant.
3) A prominent 001 peak emerges around 5.0-5.5nm d-spacing, possibly accompanied by higher order peaks at appropriate positions.



*Figure* 5-8 XRD patterns of MCM-22(P) powder before swelling, after swelling and after exfoliation.

As can be seen from *Figure* 5-8, the XRD pattern before swelling is the typical pattern for MCM-22(P)[19]. After swelling, the [001] peak moves to a lower 2θ angle with d-spacing of about 4.5nm. The [002], [101] and [102] peaks disappear, while the [100] peak remains. All of these changes roughly obey the rules as stated above, thus suggesting a successful swelling. After ultrasonication, all reflections disappear. Considering the exfoliation process is carried out in a chemically mild condition, we think the layers are exfoliated instead of completely destructed. If this is true, the exfoliated layers will also be out of the detection limit of SEM. Other techniques, such as Small Angle X-ray Scattering, AFM or TEM, are necessary and going to be used in future studies.
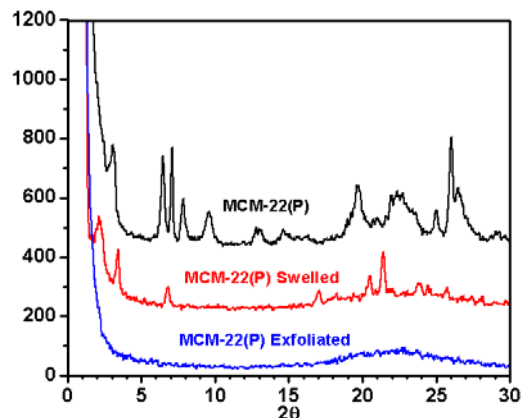
*Layer-By-Layer deposition*

The deposition procedure is mainly based on a chemical-interaction method which is originally developed by Ha and coworkers[23]. We extended this method in our previous work to make a b-oriented silicalite-1 seed monolayer on α-alumina supports and satisfactory results were obtained[23]. The procedure can be easily adapted here for the purpose of depositing MCM-22 particles to aluminum alloy surface for corrosion protection. In this method, first a mesoporous silica layer is coated on top of the support to provide a smooth and common functional surface. Then a silane coupling agent, 3-chloropropyltrimethoxylsilane, was used to covalently link the plate-like MCM-22 particles to the silica surface. The silane coupling agent has two functional groups, i.e., chloro and methoxyl, with one reacting to the silica surface and the other reacting to the MCM-22 particle surface. Extra MCM-22 particles can be removed by sonication, and therefore after each coating, an almost close-packed monolayer can be obtained. The procedure can be repeated to make the films with two layers, three layers and so on to increase coverage.

An image of the mesoporous silica layer is shown in *Figure* 5-9A, which shows that shallow dents in the original substrate surface can be leveled off by the mesoporous layer and the entire surface is much smoother than before. However, the corrosion results showed this mesoporous silica layer was rather detrimental than beneficial for corrosion protection. Since XPS results show that there is an oxide layer on the aluminum alloy surface which can also provide enough functional groups for deposition, therefore this mesoporous layer can be eliminated.
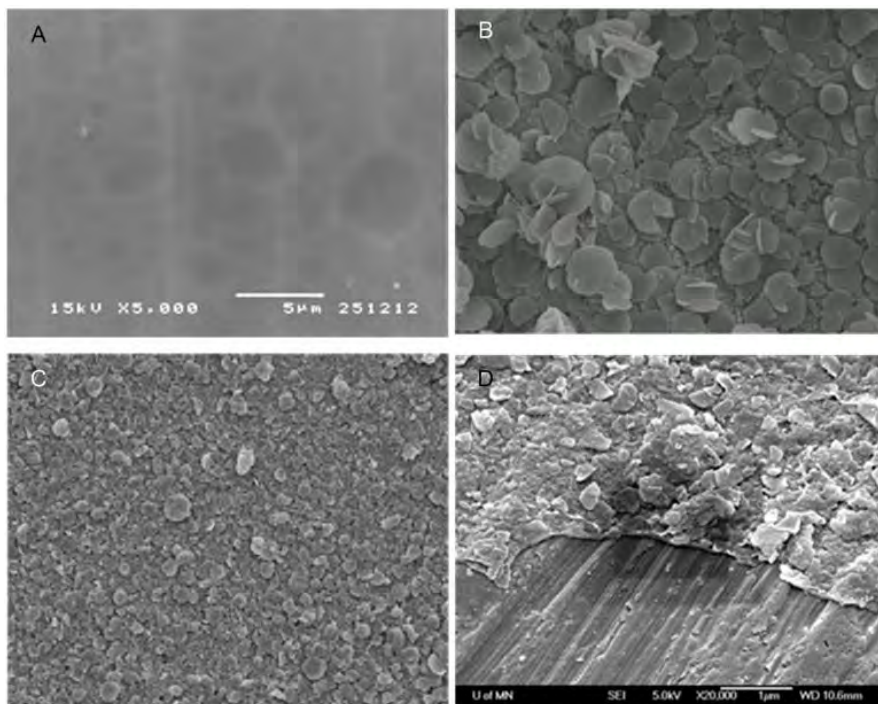


*Figure* 5-9 A) SEM image of the mesoporous layer; B) SEM image of the MCM-22 layer after one time deposition; C) SEM image of the MCM-22 film after three times deposition; D) Cross view of the MCM-22 film after three times deposition.

*Figure* 5-9B shows a SEM image of the MCM-22 layer after one deposition. The deposit is almost a close-packed monolayer. Most crystals retain their plate-like shape without breakage or

curling, and attach to the substrate surface with their flat surfaces and therefore the obtained film is c-oriented. After adopting the special treatment during calcination, the film is much smoother with few agglomerates bigger than 10µm. *Figure* 5-9C shows the MCM-22 film after 3 depositions and *Figure* 5-9D the corresponding cross view. Film coverage improves substantially without loss in orientation by repeating the deposition process. The film is very smooth. From the cross view, the film thickness is less than 100 nm even after 3 depositions.

We have demonstrated our successful efforts on the synthesis of MCM-22(P) and MCM-22 particles with the desired plate-like shapes. The particle size is about 1 µm in diameter and less than 100 nm in thickness. Significant progress was also made regarding the exfoliation of MCM-22(P) to ITQ-2 and the elimination of big agglomerates during the calcination process. The film after one-time deposition is almost a close-packed and c-oriented monolayer. Without loss of the film orientation, the coverage of the film increases substantially by repeating the deposition process. The thickness of the film after three-time deposition is still less than 100nm. Therefore, the goal to make a thin, compact, and c-oriented MCM-22 film is very close, although the compactness of the film and the reproducibility of the procedure still need to be improved.

To improve the compactness of the film, we will use uncalcined MCM-22(P) crystals or ITQ-2 crystals instead of MCM-22 crystals to make the film. The film will then be condensed by calcination to eliminate gaps between layers and thus to improve the compactness of the film.

Significant corrosion protection is demonstrated by coating a substrate with alternating layers of zeolite particles and mesostructured surfactant-templated silica. The UMN team developed and optimized a coating process that involves deposition of plate-like particles of zeolite MCM-22 on a substrate by chemical attachment under sonication. DC-Polarization tests, conducted in acid ($H_2SO_4$) as well as in salt (NaCl) solution at UC Riverside, show consistent and reproducible results of polarization current density of the level achieved by use of chromate conversion coatings. *Figure* 5-10 shows an overview of the layer-by layer deposition process and *Figure* 5-11 shows a typical MCM-22 film with silica aerosol coating.

The sequence of processes[19-24] to prepare the samples for DC polarization test is described on the left side of *Figure* 5-11. MCM-22 particles were deposited using chemical attachment under sonication[21, 22] on the polished aluminum plates following experimental protocol (**1**). The deposition of MCM-22 was followed by deposition of surfactant-silica composite by aerosol coating using the experimental protocol (**2**). Samples MN107, 108, prepared using these steps, were tested for corrosion protection. Other samples were subjected to additional coating cycles. The substrate was calcined at 300ºC (experimental protocol (**3**)) in order to generate enough hydroxyl groups for the reaction based deposition of MCM-22 particles. Another deposition of MCM-22 particles, this time without sonication, was performed following experimental protocol (**4**), followed by coating with surfactant silica composite layer using procedure (**2**). At this stage samples MN 122, 123, 124, 125 were tested for corrosion protection. Other samples were calcined at 300 ºC using procedure (**3**) for an additional deposition cycle yielding samples MN 126, 127, 128, 129.
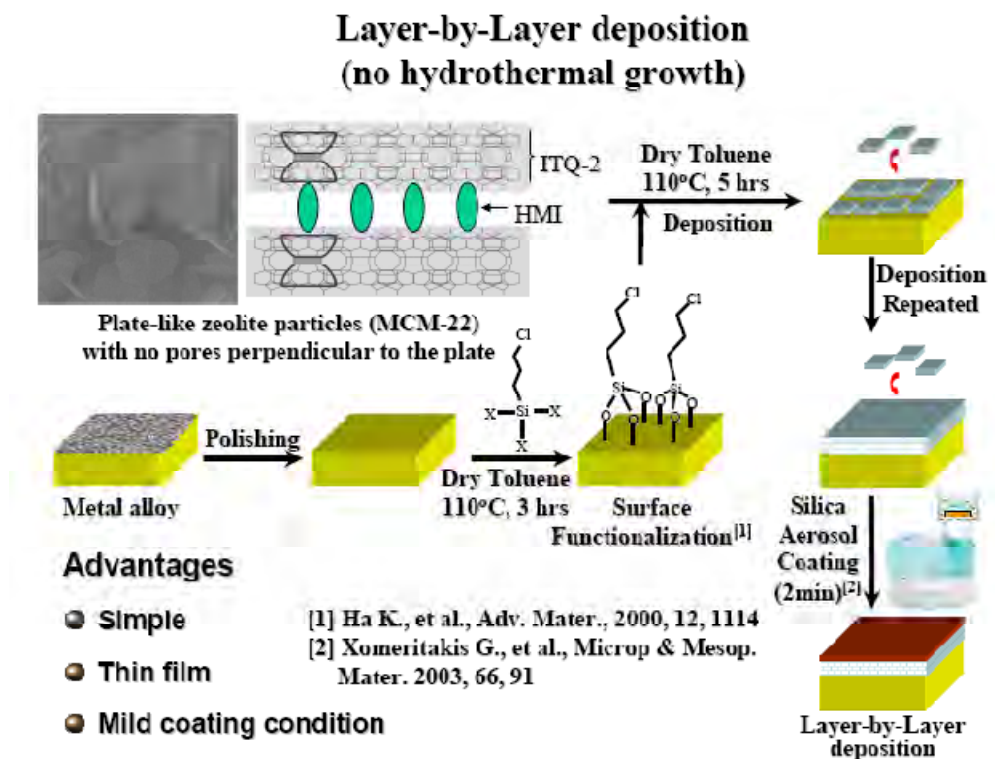
*Figure* 5-10 Overview of the Layer-by-Layer deposition process.
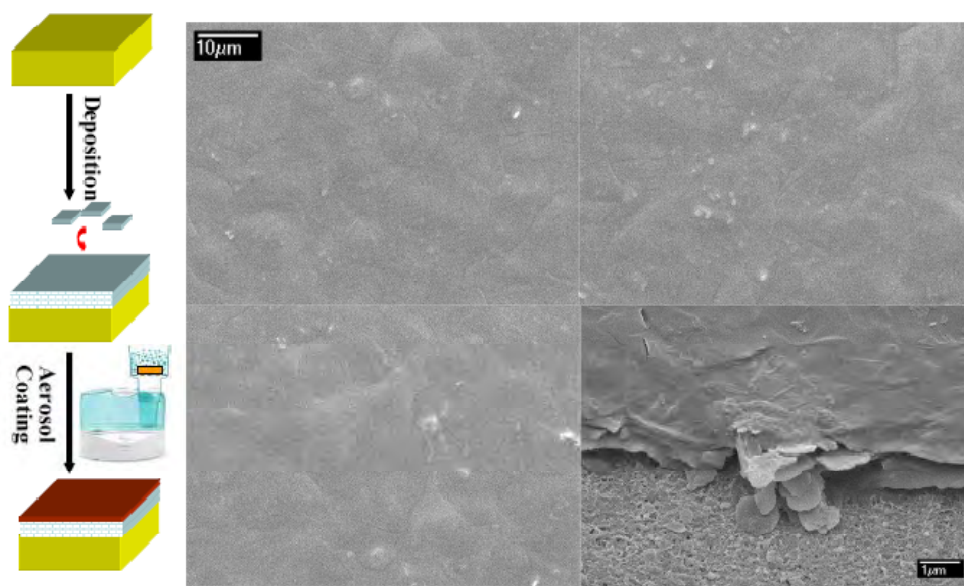


*Figure* 5-11 MCM-22 film with silica aerosol coating

DC polarization test results performed in 0.5 M $H_2SO_4$ are shown on the right side (top) of *Figure* 5-12. Sample MN 108 with one layer of MCM-22 and one layer of surfactant-silica composite shows corrosion protection action. The corrosion protection performance improved progressively with additional layer of MCM-22 as observed in samples MN 122 and MN 124

(both with two coatings of MCM-22 and surfactant-silica composite) and samples MN 127 and MN 129 (both with three coatings). Our findings demonstrate that as the number of deposited layers increases, the level of corrosion protection is enhanced considerably.

DC polarization tests in 0.1M NaCl solution were also performed for the samples prepared in the same manner as described above and shown in *Figure* 5-12 (right side – bottom). Samples MN 123 and MN 125 (with two MCM-22 layers and two aerosol coatings) show comparable or higher degree of corrosion protection as compared to the samples MN 126 and MN 128 which have an additional layer of MCM-22 and silica. Therefore, in contrast to the measurements in $H_2SO_4$, it appears that for NaCl there is an optimum corrosion protection action exhibited by films with two layers of MCM-22.
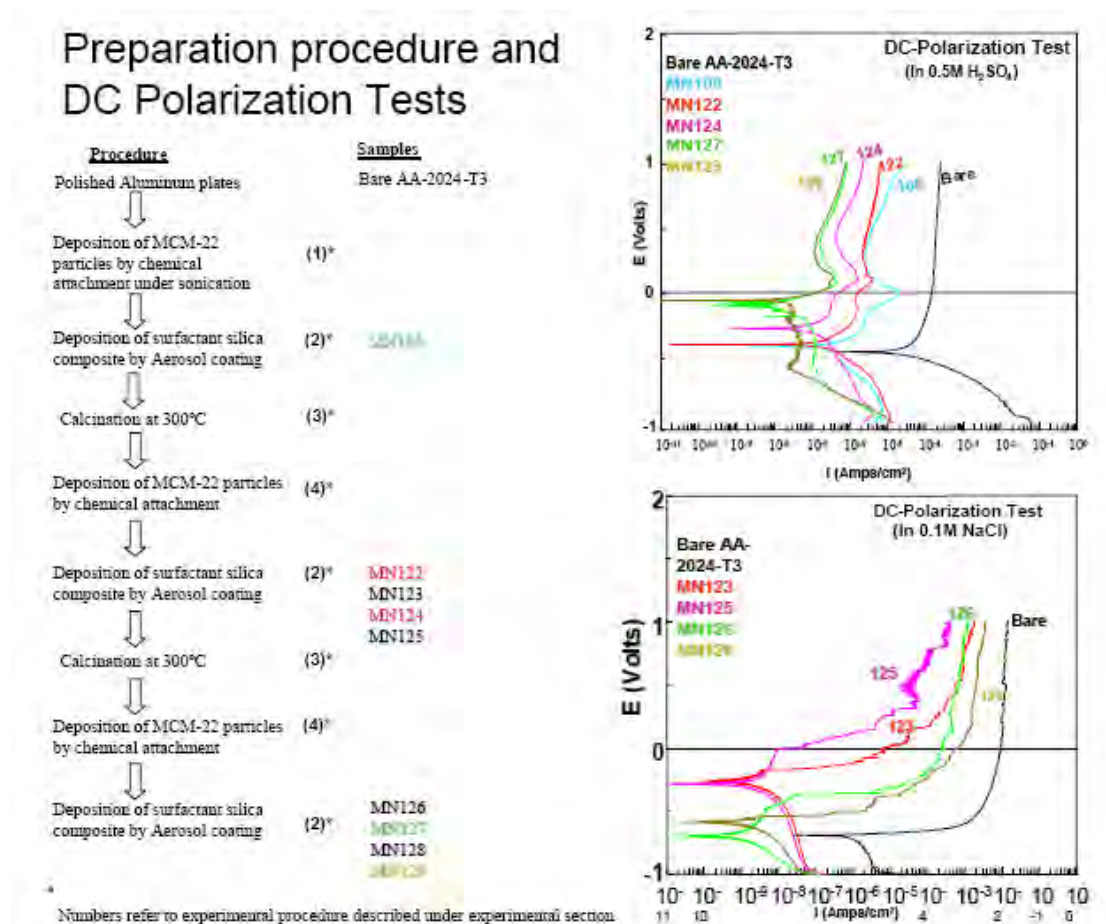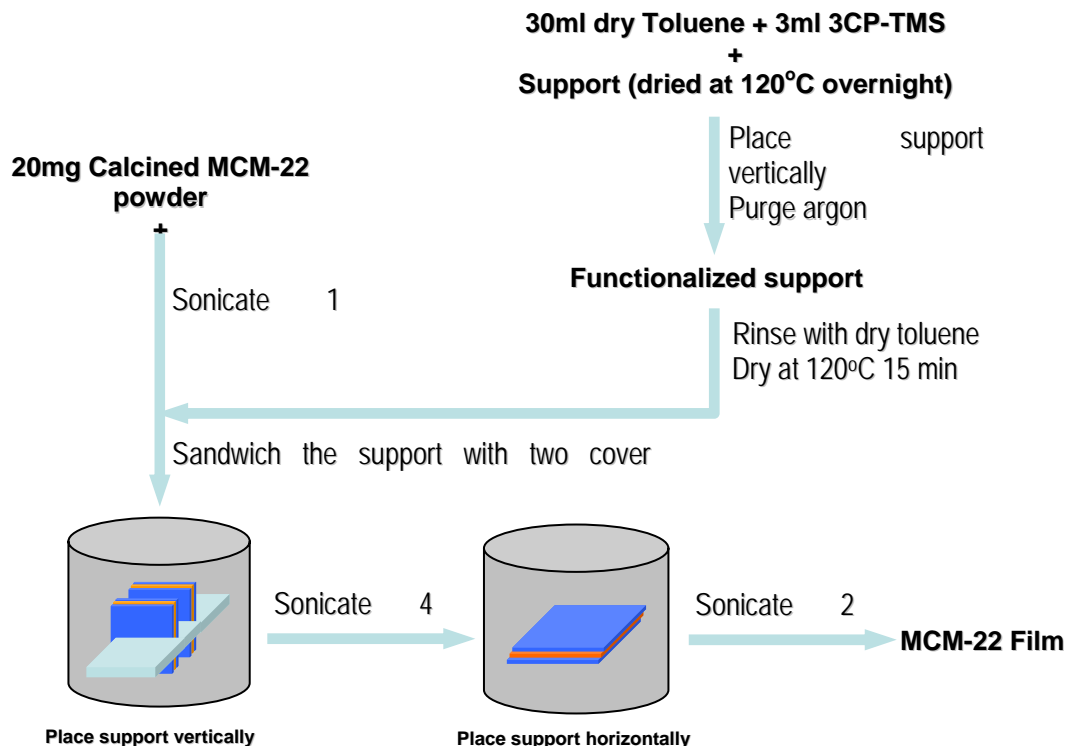


*Figure* 5-12 Preparation procedure and DC-Polarization Tests in 0.5M $H_2SO_4$ and 0.1M NaCl

*Experimental Section*

**Procedure (1): Deposition of MCM-22 particles by chemical attachment under sonication**



**30ml dry Toluene + 3ml 3CP-TMS**
**+**
**Support (dried at 120°C overnight)**

Place support vertically
Purge argon

**20mg Calcined MCM-22 powder**
**+**

Sonicate    1

**Functionalized support**

Rinse with dry toluene
Dry at 120°C 15 min

Sandwich the support with two cover

Sonicate    4    Sonicate    2    **MCM-22 Film**

**Place support vertically**        **Place support horizontally**

Prior to seed deposition the polished supports were dried at 120 °C overnight in a drying oven, apparatus required during the experiments were dried at 80 °C at least overnight prior to the experiments. The substrate which was supported by a Teflon holder was loaded vertically into a specially designed glass reactor which was under continuous purge with argon. First, 30 mL of dry toluene and then 3 mL of 3-chloropropyltrimethoxysilane were quickly transferred to the reactor from argon-purged containers. The reactor was then closed and connected to a water-cooled condenser (15 °C). The solution was refluxed for 3 h at 110°C under a gentle argon stream.  After this, the support was taken out, washed in fresh toluene and dried for about 15 min at 120 °C.

In a separate step 20 mg of precalcined MCM-22 seeds and 50 mL of dry toluene were charged into a dry reactor under argon flow. The suspension was sonicated for 1hour (seed dispersion) after which the functionalized support was then quickly introduced into this suspension under argon purge. The support was positioned vertically sandwiched between two cover glasses using a combed shaped Teflon holder. The reactor was then closed and placed in a sonicator (Branson 1210, 50/60 Hz) for 4 minutes sonication. Subsequently the seeded support was removed from the seed suspension, and placed horizontally. Further this was sonicated for 2 minutes. Finally, the supports were taken out of the reactor and rinsed in fresh toluene in order to remove multilayered crystals.

**Procedure (2): Deposition of surfactant silica composite by aerosol coating**

**14.24g Brij 56 + 308.64g H₂O + 31.66g TEOS + 12.77g HNO₃ (0.07M)**

Sonicate 3 hrs
Age 1 hr

**Coating Sol**

Coat 1 min
Dry

**Aerosol coating**

A sol was freshly prepared each time aerosol coating was carried out as follows. 14.24 g. Brij-56 was mixed with 308.64 g water, 31.66 g TEOS and 12.77 g 0.07 M $HNO_3$ in a capped Pyrex bottle. The mixture was sonicated (Branson 1210, 50/60 Hz) for 3 h resulting in a turbid but homogeneous sol. This sol was aged for about 1 h and then charged into a humidifier (kaz).

The supports were placed horizontally onto wire gauze (polished side up) and exposed to an aerosol cloud generated by the underlying humidifier into an enclosed space that housed the gauze and supports. This allowed heavy aerosol droplets to settle on the support surfaces. After the coatings, the supports were left to dry overnight.

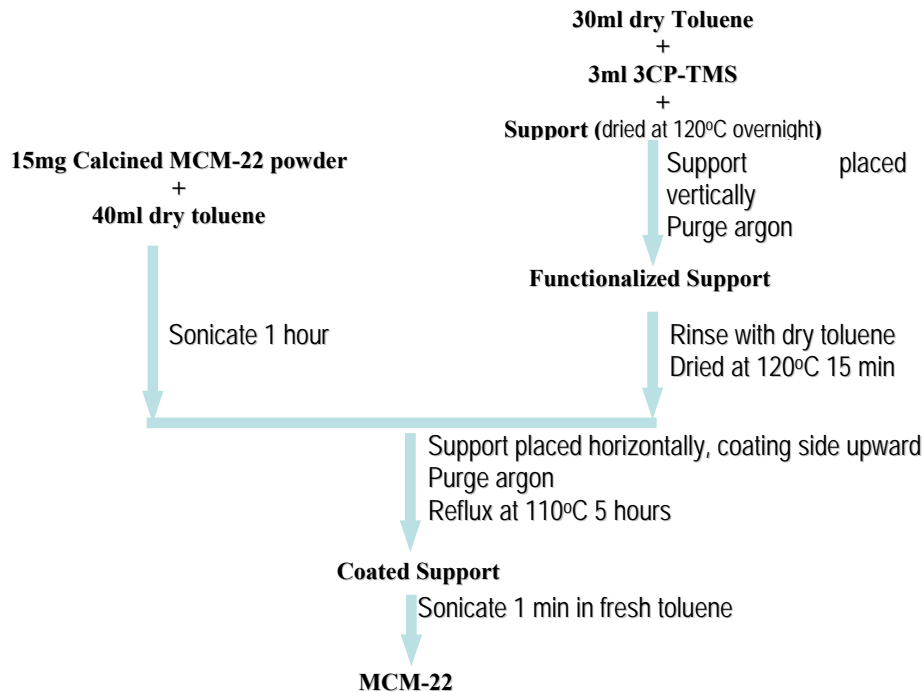## Procedure (3): Calcination at 300°C
The films were calcined in air at 300°C for 4 hours with a 0.5°C/min ramp rate.

## Procedure (4): Deposition of MCM-22 particles by chemical attachment
Prior to seed deposition the polished supports were dried at 120 °C overnight in a drying oven, apparatus required during the experiments were dried at 80 °C at least overnight prior to the experiments. The substrate which was supported by a Teflon holder was loaded vertically into a specially designed glass reactor which was under continuous purge with argon. First 30 mL of dry toluene and then 3 mL of 3-chloropropyltrimethoxysilane were quickly transferred to the reactor from argon-purged containers. The reactor was then closed and connected to a water-cooled condenser (15 °C). The solution was refluxed for 3 h at 110 °C under a gentle argon stream. After this the support was taken out, washed in fresh toluene and dried for about 15 min at 120 °C.

In a separate step 15 mg of precalcined MCM-22 seeds and 40 mL of dry toluene were charged into a dry reactor under argon flow. The suspension was sonicated for 1hour (seed dispersion) after which the functionalized support was then quickly introduced into this suspension under argon purge. The support was positioned horizontally using a Teflon holder with the functionalized silica layer facing upwards. The mixture was refluxed for 5 h at 110 °C. The reactor was then closed and placed in a sonicator (Branson 1210, 50/60 Hz) for 1 min sonication to get a substrate with MCM-22 deposit.

```
                                              30ml dry Toluene
                                                     +
                                              3ml 3CP-TMS
                                                     +
                                       Support (dried at 120ºC overnight)
```

**15mg Calcined MCM-22 powder**
**+**
**40ml dry toluene**

Support      placed vertically
Purge argon

**Functionalized Support**

Sonicate 1 hour

Rinse with dry toluene
Dried at 120ºC 15 min

Support placed horizontally, coating side upward
Purge argon
Reflux at 110ºC 5 hours

**Coated Support**

Sonicate 1 min in fresh toluene

**MCM-22**

## Microwave-assisted ionothermal synthesis of SAPO-11

Ionothermal synthesis uses ionic liquid instead of water as the solvent. An ionic liquid is a substance that only consists of ions and has a melting temperature below 100 $^o$C. The most significant advantage of this method is that the whole process can be carried out in an open vessel rather than in a sealed Teflon$^®$-lined autoclave; consequently, the syntheses occur at ambient pressure due to the negligible vapor pressure of ionic liquid even at an elevated temperature. SAPO-11 is one of the first successful example for zeolite ionothermal synthesis[25], which was prepared under ambient pressure in a convection oven for 68 h at 150 $^o$C using 1-methyl 3-ethyl imidazolium bromide ([emim]Br) as both solvent and template. This recipe is also successful under microwave heating where only one hour was needed for the crystallization due to the rapid microwave absorption of ionic liquids[26]. The primary idea of this project is to prepared a SAPO-11 coating on AA 2024-T3 using ionothermal synthesis and microwave radiation, which presents a short time, ambient pressure deposition process for zeolite.

*Synthesis of SAPO-11 coating on AA 2024-T3*

A synthesis mixture with molar composition: $32[emim]Br:1Al(OC_3H_7)_3:0.25$tetraethyl orthosilicate (TEOS)$:3H_3PO_4:0.8HF$ was prepared and then stirred for 4 h at 100 $^o$C. AA 2024-T3 substrates were pretreated by an Alconox detergent solution. The substrate was then fixed vertically inside the synthesis mixture in the Teflon vessel designed for MARS5 (CEM Co.) microwave reaction system. The unsealed vessel was then quickly heated to 150 $^o$C and held at the temperature for 2 h under microwave radiation. After the synthesis, the coated sample was thoroughly washed with DI water and acetone and dried with compressed air. The synthesis procedure was repeated once or twice with fresh synthesis solution. SAPO-11 coatings on AA 2024-T3 are confirmed by the X-ray diffraction (XRD) (Fig.5-13c). No other by-products are found. The preferred orientation is evident for the SAPO-11 coatings. AEL consists of a 10-

membered ring (0.40 ×0.65 nm) channel parallel to the c-axis of the crystal. The strong (002) reflection peak in the SAPO-11 XRD pattern indicates that the one-dimensional channels are perpendicular to the Al alloy surface.
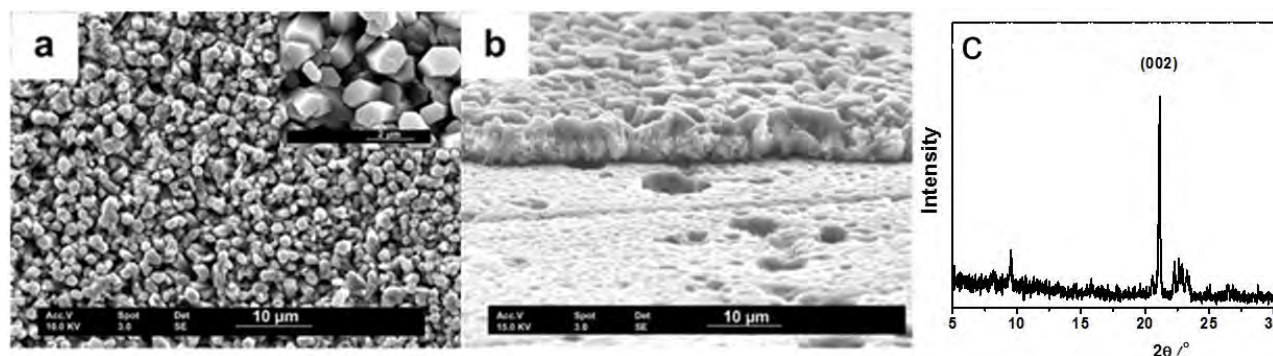


*Figure* 5-13 SEM pictures and XRD pattern of SAPO11 on AA 2024-T3

*BTSM-MEL coatings*

It can be seen from the cross-sectional SEM picture of SAPO-11 coating (*Figure* 5-13b) that the film consists of two major components: the dense barrier layer adjoining the metal and a porous layer extending from the barrier layer to the outer surface of the film, which is similar to the anodized film of Al alloys. This kind of structure has the advantage of being able to be dyed. In order to obtain the maximum corrosion resistance, the porous coating must be sealed. A nano-zeolite filled silane was used as the sealing agent. Several aspects were considered for choosing it: (1) silane has very good adhesion properties, which can act as a binder layer between zeolite coating and the polymer topcoat; (2) silane film itself has good corrosion resistance for Al alloys;[27] (3) nano-particle filled silane films offer better mechanical properties and MEL nanocrystal filled silane films also improve the corrosion resistance.

A dilute 1,2-bis(triethoxysilyl)methane (BTSM) solution was prepared by adding silane to a DI water and ethanol mixture. The volume ratio of BTSM:DI water:Ethanol was 1:1:20. Acetic acid was then added to adjust the pH of the solution in the range of 4.5~5. The solution was then stirred at room temperature for aging at least 24 hours before a MEL gel was added. MEL concentration in the solution was about 20 ppm. The SAPO-11 coated sample was polished on a Buehler, Ecomet 3 grinder-polisher using 0.05 μm silica slurry and thoroughly cleaned with DI water and acetone under sonication. Then the nanoparticle suspension was spun on it at room temperature on a Laurell spin coater. Afterward, the sample was heated at 80 $^o$C overnight and then 200 $^o$C for 30 min.
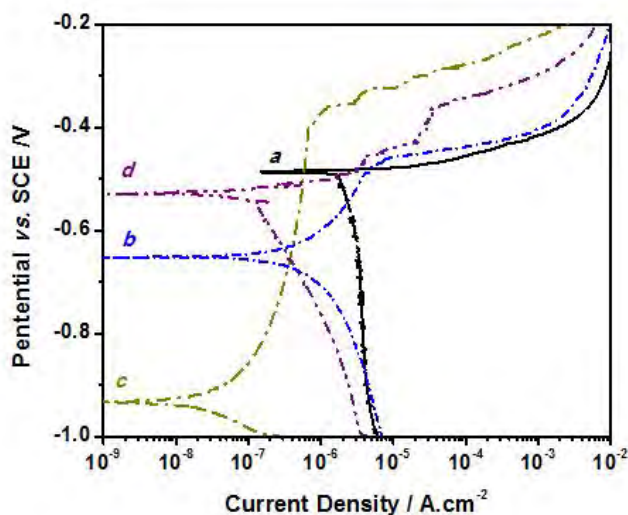
*DC polarization test*

DC polarization testing was carried out with Solartron potentiostat SI 1287 in a three-electrode Flat Cell (Princeton Applied Research Model K0235) with a Pt counter electrode and a saturated calomel electrode (SCE) as the reference electrode. The corrosive medium was 0.1 mol/L NaCl aqueous solution. The samples were immersed in the corrosive medium for 30 min prior to the DC polarization test with a sweep rate of 1 mV/s.

*Figure* 5-14 shows that bare AA 2024-T3 pits at its open circuit potential (OCP) (ca. -0.5 $V_{SCE}$). That is, the pitting corrosion occurs once the metal is immersed in the corrosive media. This OCP corrosion is related with the intermetallics of Cu in Al matrix and the presence of Cl⁻ in the electrolyte. OCP of SAPO-11 (ca. -0.65 $V_{SCE}$) coated samples are more negative than bare AA 2024-T3, which means the AEL coatings inhibit the OCP corrosion of the samples. The corrosion current density of SAPO-11 coated samples is about two orders of magnitude smaller than that of the bare Al alloy. The pitting potential is slightly higher than the OCP of AA 2024-T3, which means the favored sites for pit initiation, mostly the copper intermetallics, are at least partially covered by the SAPO-11 coatings. The BTSM-MEL modified SAPO-11 coating has very good corrosion resistance. The OCP is more negative than -0.9 V and the corrosion current is less than $10^{-8}$ mA/cm$^2$. The pitting potential also increases to -0.4 V, even higher than the pure Al at similar conditions[28]. The DC polarization behavior of BTSM-MEL spin-on coating directly on bare AA 2024-T3 is also tested. It does show good corrosion resistance but the combination of SAPO-11 coating and BTSM-MEL sealing shows the best anticorrosion performance in this work.

## Task 2. Zeolite/topcoat systems

We have gone through three evolutions of zeolite coating syntheses on AA-2024-T3 (see Task 1-2, *Figure* 5-4). The primer and/or topcoat systems applied to the zeolite coatings is organized based on the different zeolite generation on which the primer and/or topcoat was applied.

Much of the poor adhesion of the CARC topcoat (MIL-PRF-64159) to Generation-1 zeolite coatings has been contributed to the fact of no QC for the synthesis and the thinness of the zeolite coatings (0.5-2 um thick). The first Generation-3 zeolite coatings (7.5 um thick) were painted with a VOC-free topcoat (5 samples) or a self-priming topcoat (5 samples) and had extremely non-uniform topcoat application and blistering occurred after 168 hours of salt-fog exposure. The VOC-free and self-priming topcoats were applied at Deft (Irvine, CA) in a trial run (The visit by UCR to Deft was primarily aimed to observe and learn the deposition technique) and ASTM standards were not followed. Our latest testing of zeolite (Generation – 3) coatings with primer and/or topcoat applications showed that coating systems with chromated primers with and without topcoat had no delamination from the zeolite surface after 3100 hours of salt-fog exposure.

### Zeolite (Generation - 1)

CARC topcoat (Mil-PRF-64159)
Five aluminum 2024-T3 panels were coated with zeolite of 0.5-2 um thick at UCR and delivered to China Lake. The panels were then sent to the Army Research Laboratory (ARL) to be coated with CARC topcoat. The panels were coated on one side with the CARC topcoat (Mil-PRF-64159) and coated with primer on the other side to keep corrosion from contaminating the salt fog chamber. These panels were then scribed and tested in salt-fog (ASTM B117, see Task 3.4 for details).

Results: No adherence of the CARC topcoat to zeolite.

### Zeolite (Generation - 2)

No zeolite/topcoat or zeolite/primer/topcoat system was tested for the Generation – 2 zeolite coatings. Salt fog testing of the bare zeolite coatings (Generation – 2) was performed (see results in Task 3.4).

### Zeolite (Generation - 3)

VOC-free topcoat (Deft product #55W-002, Deft, Irvine CA) and Self-Priming topcoat (TT-P-2756A from Deft, Irvine, CA)
Once the 7.5 um thick ZSM-5 coating samples were developed and chosen as the benchmark, they were applied with topcoats at Deft (Irvine CA) in a trial run (The visit by UCR was primarily aimed to learn the deposition technique). Five panels were applied with VOC-free topcoat and five panels were applied with self-priming topcoats. These panels were then sent to China Lake for salt-fog testing (ASTM B117). The results showed blistering of topcoats after 168 hours salt-fog exposure (See Task 3.4 for details).

Zeolite/Primer, Zeolite/Primer/Topcoat and Zeolite/Topcoat

Forty nine (49) zeolite (Generation – 3) coated AA-2024-T3 panels were prepared and painted by Deft (Irvine, CA), following ASTM guidelines. *Figure* 5-15 shows the matrix of primers and topcoats applied to the zeolite coating.



*Figure* 5-15 Primers and topcoats applied to zeolite coatings following ASTM and MIL specs.

Salt-fog (ASTM B117) and adhesion (wet and dry) testing were performed at NAWC, China Lake (See Task 3.4 for details).

## Task 3.1: Laser Scanning Confocal Microscopy (LSCM) characterization of coating surfaces

- **Quantitative Surface Imaging by LSCM**

UCR initially provided six samples of the high-silica ZSM-5 zeolite coating on 2024-T3 Al substrates with the following nomenclature: M, Q, P, 8, H, and K. Three samples each of the high-silica ZSM-5 zeolite coating on 2x3 cm of 2024-T3 Al, 6061-T6 Al, and 7075-T6 Al substrates with the following nomenclature: A, B, and C for each system were later received for further analysis. All samples were imaged using the LSCM under 2000x magnification. *Figure* 5-16 and *Figure* 5-17depict the optical and height mappings and surface profiles of systems 8 and P. *Figure* 5-18 depicts regions of the surface on coating H where there is an "over-growth" of the zeolite coating. *Figure* 5-19 and *Figure* 5-20 depict the optical, height mappings, and filtered surface profiles of the zeolite coating system on 6061-T6 Al and 7075-T6 Al substrates.
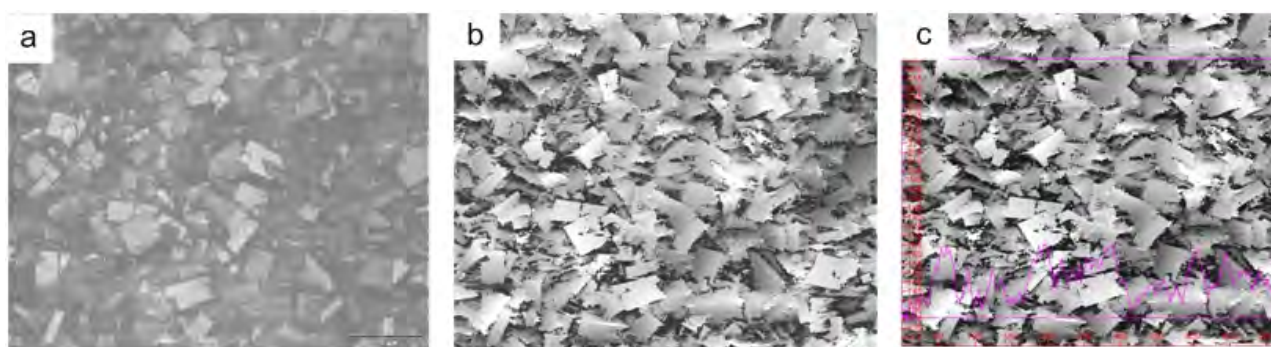


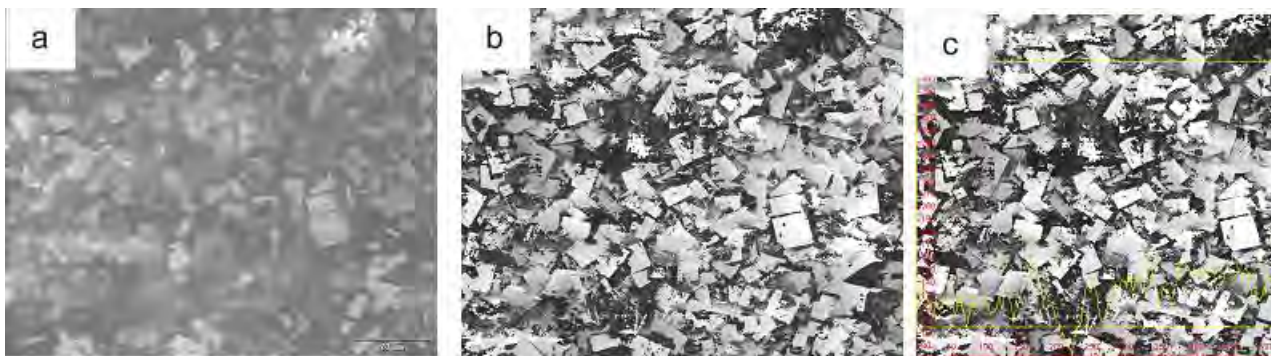*Figure* 5-16 LCSM Optical (a), Height Mapping (b), and Surface Profile (c) of Coating 8



*Figure* 5-17 LCSM Optical (a), Height Mapping (b), and Surface Profile(c) of Coating P

Surface profiles in *Figure* 5-18c, *Figure* 5-19c and *Figure* 5-20c suggest that there is an effect of the Al substrates on the surface morphology of the zeolite coating.
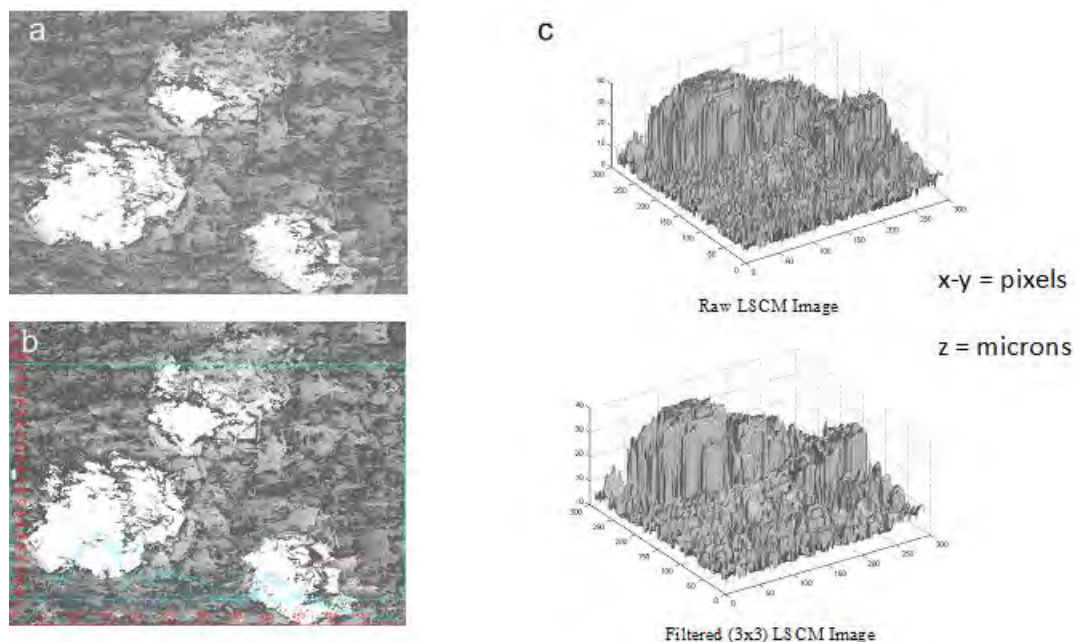
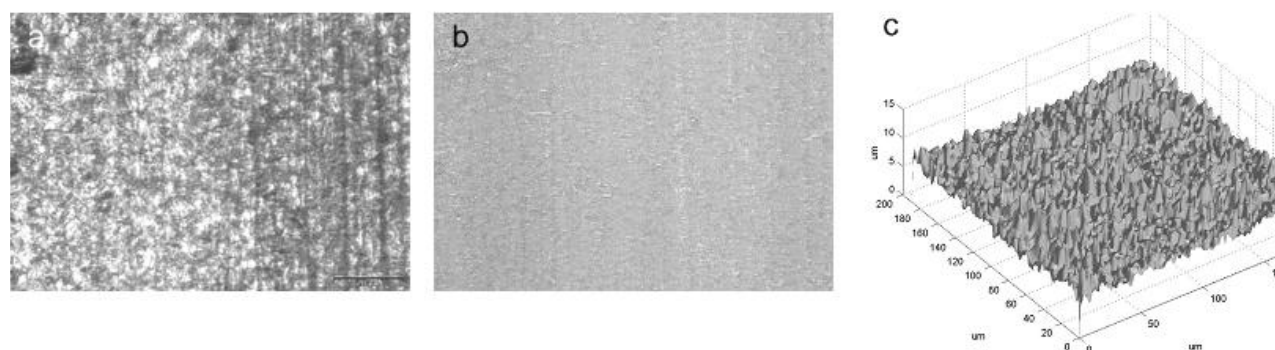*Figure* 5-18 Mapping (a), Surface Profile (b), and 3-dimensional Images (c) of coating H



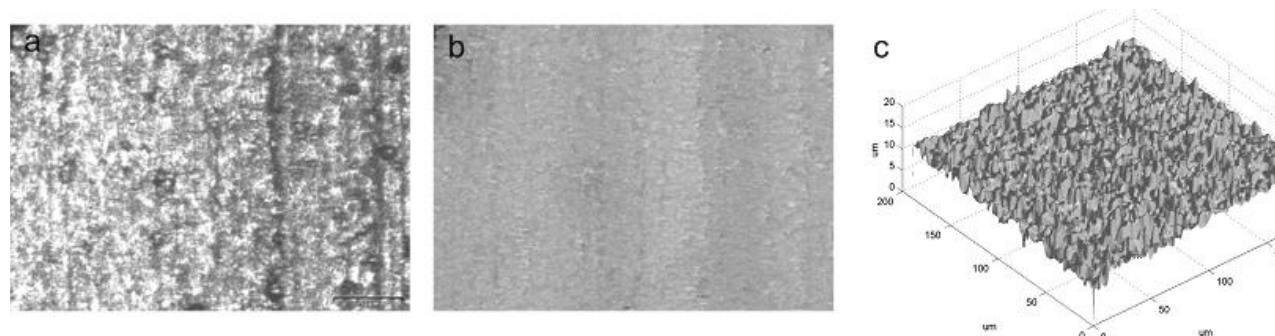*Figure* 5-19 (a)LCSM Optical, (b)Height Mapping, and (c) Surface Profile of Zeolite Coating on 6061-T6 Al



*Figure* 5-20(a)LCSM Optical, (b) Height Mapping, and (c) Surface Profile of Zeolite Coating on 7075-T6 Al

**RMS Roughness**

Coating roughness measurements were calculated to obtain information on coating surface structure. Analysis of RMS roughness suggests that there is a difference in surface roughness between the three Zeolite coatings systems. ***Table*** 5-1 lists RMS roughness values for each coating system.

*Table* 5-1 Surface Roughness for ZSM-5 on different Al alloy substrates

|  | 2024-T3 | 6061-T6 | 7075-T6 |
|---|---|---|---|
| A | 1.15±0.01 | 0.80±0.03 | 1.17±0.05 |
| B | 1.59±0.01 | 0.92±0.34 | 0.92±0.06 |
| C | 2.73±0.10 | 1.29±0.07 | 1.05±0.06 |

On large scale, the ZSM-5 coating on 2024-T3 Al has the largest structural fluctuations (1-3 $\mu m^2$), which yield higher roughness values. Moreover, these results suggest that the ZSM-5 coating on 6061-T6 Al and 7075-T6 Al substrates have similar structural morphologies.

- **Scaling Analysis & Optimized Filtering for LSCM Images**

The scaling analysis technique employed for this analysis was developed to obtain measures of changes in surface morphology to gain insight into small-scale surface structural changes. The roughness of the coating surface was characterized in terms of scaling exponents to obtain power- law correlations.
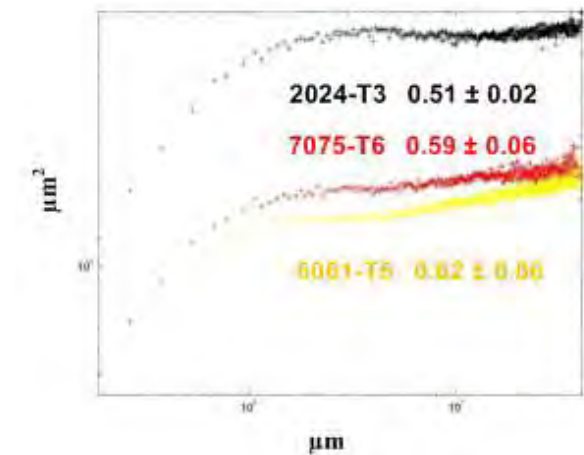


The roughness ($w$, the average RMS deviation in surface heights from a center plane) is measured for increasing areas of $l^2$ where the dependence of the roughness on $l$ gives rise to a power law relation characterized by the roughness exponent $\alpha$ at time $t$:

$$w_L(l,t) \sim l^\alpha$$

$\alpha$ is obtained from the scaling dependence of the local width on $l$:

$$w_L^2(l,t) \equiv \left\langle \left[ h(x,t) - h_l(x,t) \right]^2 \right\rangle_x$$

*Figure* 5-21 Local scaling for LSCM filtered images ($\alpha$ value shown inside)

$h(x,t)$ is the height of a single-valued surface at location x, $h_l(x,t)$ is the average height of the local data at time t, $t$ is the exposure time, and $l$ is the size of local surface patches.

*Figure* 5-21 shows the results of local scaling analysis applied to LSCM data collected from ZSM-5 coated 2024-T3, 6061-T6 and 7075-T6 Al samples. As with all analyses in this study, the results represent averages of three different scans for each sample. Results show that there is not

a significant difference in complexity (fractal dimension) between the three zeolite-substrate systems, however there is a large deviation between the three in surface roughnesses. The zeolite coating on the 2024-T3 Al substrates have the highest roughness values, which suggests that this coating would perform the best as an adhesive pre-coat for CARC coatings.

The roughness exponent α represents the coating's small-scale structural changes (denoted by the linear region in *Figure* 5-21). These fluctuations occur within a 1 μm scaling region. Outside of this region there is no longer a correlation between independent surface structures and large-scale surface changes are measured (RMS roughness).

Atomic Force Microscopy (AFM) was not employed in this study due to limitation in height deviations of the microscope. The surface area that can be imaged using AFM is limited to 100 $\mu m^2$ with at most a 7 μm variation in heights. The variation in heights of the surfaces used in this study are >6 μm. Previous work has shown that a 5x5 median filter of the LSCM image can be used to mimic the resolution of the AFM. However in this study, a 3x3 median filter is sufficient to remove artifacts on the surface structure. A more rigorous filter may result in a loss of information.

## Task 3.2: Instrumental analysis of coating degradation

- **Dynamic mechanical analysis**

Dynamic Mechanical Analysis employs the application of thermal analytical techniques to measure physical properties such as modulus, heat capacity and linear coefficient of thermal expansion of the zeolite coatings. It is believed that this data will lend some insight into the adhesion of the coating to the substrate.

The coated specimens will be analyzed in two ways. The first set of experiments will apply a static stress scan, where the applied load will increase at a constant rate over time. The second set of experiments will apply a constant or increasing force at a constant frequency; this testing will occur at various frequencies. All experiments will be completed with both 3 point bending and single cantilever methods. The idea is to see if the composite or combined modulus of the coated samples shows any effect due to varying adhesion at the interface between the samples, when compared to independent modulus of the bare substrate and of the bare coating and if there any effect on the modulus resulting from changes in interface adhesion of the coating.

*Figure* 5-22 shows results from DMA analysis of the zeolite coating on 2024 Al vs. bare 2024 Al. Both have been tested in static stress. The modulus has been measured but has to be correlated against the zeolite coating without the Al substrate. Moreover, the effect of varying coating thickness has to be addressed.
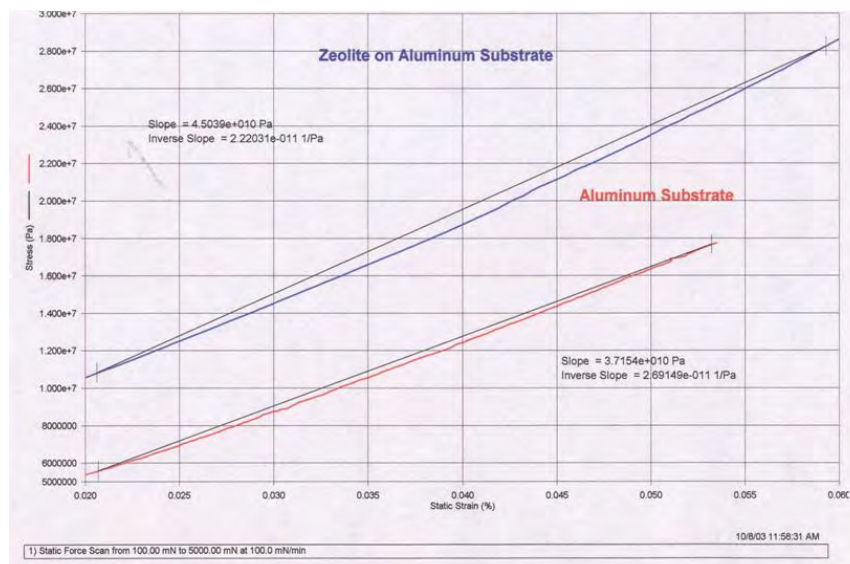


*Figure* 5-22 Stress/Strain curves for Zeolite on 2024-T3 Al & Bare 2024-T3 Al

- **DC Polarization quality control testing development**

For small 2x3 cm coupons we had been using epoxy to seal off the edges before electrochemical testing (*Figure* 5-23). This has been effective for coupons, but this means the large panel has to be cut into small pieces for electrochemical tests.



*Figure* 5-23 2x3 cm coupon sealed by epoxy before electrochemical tests.

To preserve the zeolite coated panels and to be able to characterize the same panel with both DC Polarization and EIS, as well as other tests such as salt-fog and UV exposure, we are using a test procedure which only requires a small scratch on one side of the panel for electrical contact for the DC Polarization and EIS tests (*Figure* 5-24). This small cut can be easily sealed and put on the back side in the salt-fog tests. This allows us to correlate the DC Polarization and EIS results with salt-fog or UV exposure results. We can also use this quick and almost non-destructive method as quality control for the coatings. We can also use this setup to check the uniformity of the coating by testing several spots on the same panel. Thus far it has been shown that our panels have uniform corrosion resistance. We have found that coatings synthesized together in the same reactor perform almost identically under electrochemical and mechanical testing. As a result, we routinely only perform quality control on one of the synthesis pair prior to additional sample testing (i.e. salt fog and UV exposure).



*Figure* 5-24 Left: Corrosion test cell that can test a 3x6" panel without sacrificing the panel. Right: Zeolite coated panel with scratch on one side for electrical connection.

DC Polarization testing procedure for quality control of zeolite coated samples

A small area of bare metal substrate is exposed on one side of the zeolite coated panel for electrical connection with copper conducting tape when panel is used as working electrode. A standard corrosion test cell is used as shown in *Figure* 5-24 Left. Three 1 cm$^2$ locations are tested on the same side of electrical connection: 1" from top of panel (top), 3" from top of panel (middle) and 5" from top of panel (bottom). The corrosion media used is 5 wt% NaCl (0.856M NaCl), test areas were in contact with corrosion media 5 minutes prior to testing.
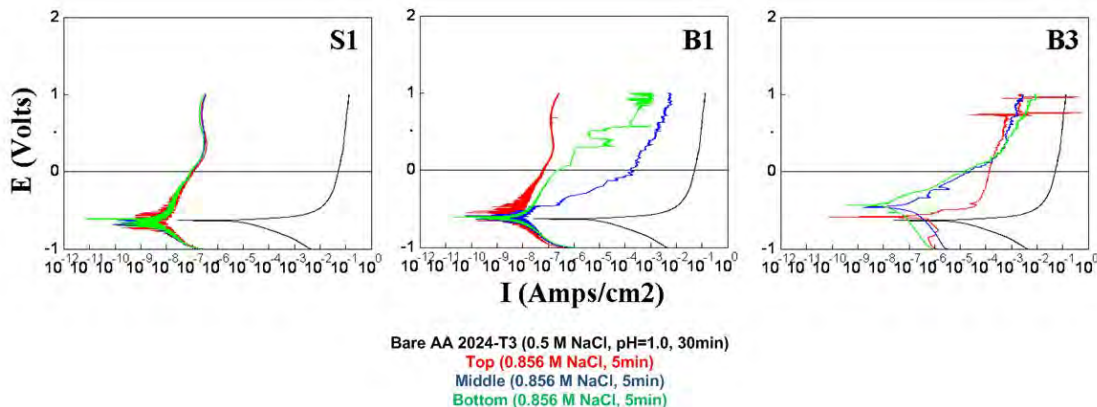
Bare AA 2024-T3 (0.5 M NaCl, pH=1.0, 30min)
Top (0.856 M NaCl, 5min)
Middle (0.856 M NaCl, 5min)
Bottom (0.856 M NaCl, 5min)

*Figure* 5-25  Representative DC Polarization profiles of the 15 zeolite coated panels sent to China Lake for salt fog testing.  S1 – actual DC polarization profile of S series, sample 1; B1 – actual DC polarization profile of B series, sample 1; B3 – actual DC polarization profile of B series, sample 3.
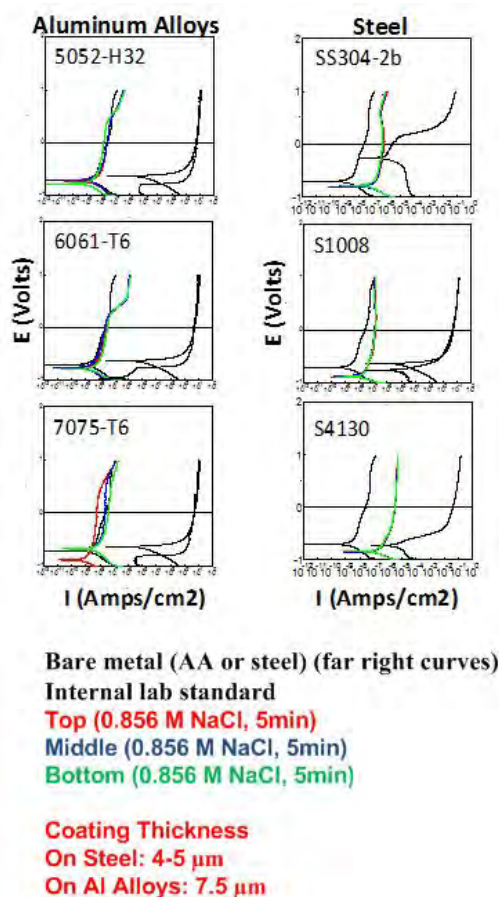


Bare metal (AA or steel) (far right curves)
Internal lab standard
Top (0.856 M NaCl, 5min)
Middle (0.856 M NaCl, 5min)
Bottom (0.856 M NaCl, 5min)

Coating Thickness
On Steel: 4-5 μm
On Al Alloys: 7.5 μm

*Figure* 5-26  Representative DC Polarization profiles in 0.856 M NaCl of aluminum alloys and steels.

We sent 15 zeolite coated panels to China Lake with 5 of them DC polarization tested on the back and shown to have excellent corrosion resistance (S series) (*Figure* 5-25, S1), 5 samples that were not tested but synthesis twins of S samples (A series), and 5 samples (B series) whose twins were tested by DC Polarization and shown to have medium (*Figure* 5-25,B1) to low corrosion current ($10^{-3.5}$ A/cm$^2$) (*Figure* 5-25, B3).  All 15 panels passed 2205 hours of salt fog testing (salt fog results shown later in this report).

To date we have synthesized hundreds of zeolite coated panels, greater than 99% of the coatings exhibit polarization profiles similar those in *Figure* 5-25.  Specifically, greater than 93% have polarization profiles similar to S1 and less than 7% demonstrate polarization profiles within the range of B1 and B3 from *Figure* 5-25.

DC Polarization testing in 5 wt% NaCl as a quality control measure prior to salt fog testing appears to be an excellent predictor of salt fog performance for zeolite coated panels.  It is likely that as long as there is not a complete loss of passivation during the DC Polarization testing the panels will pass 2000 hours exposure to salt fog.

DC Polarization testing in 5 wt% NaCl was also

performed on zeolite coatings (7.5 um thick) on other aluminum alloys (AA-5052-H32, AA-6061-T6, AA-7075-T6) and zeolite coatings (4-5 um thick) on 3 different steels (S1008, S4130 and SS304-2b) *Figure* 5-26.

**Task 3-3: Quantitative/qualitative adhesion testing of coating to Al & steel substrates**
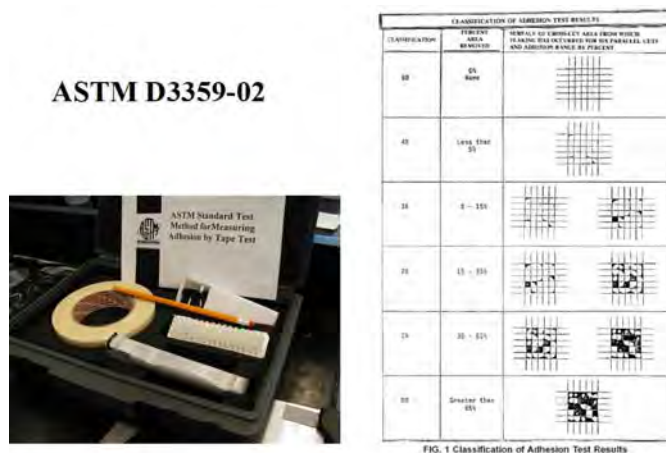
- **ASTM D3359-02 adhesion test**



*Figure* 5-27 ASTM D3359-02 test kit (left) and the rating protocol (right)

| Substrate | Coating | Rating |
|---|---|---|
| Al-2024 | ZSM-5 | 5B |
| Al-2024 | Calcined ZSM-5 | 5B |
| Al-5052 | ZSM-5 | 5B |
| Al-5052 | Calcined ZSM-5 | 5B |
| Al-6061 | ZSM-5 | 5B |
| Al-6061 | Calcined ZSM-5 | 5B |
| Al-7075 | ZSM-5 | 5B |
| Al-7075 | Calcined ZSM-5 | 5B |

*Figure* 5-28 Adhesion rating on ZSM-5 coatings on aluminum alloys and a representative optical image of the ZSM-5 coating on AA-6061 after adhesion test.

UCR has carried out adhesion test according to ASTM D3395-02 on ZSM-5 coating on AA-2024-T3, AA-5052-H32, AA-6061-T4, and AA-7075-T6. This is a dry adhesion test involving cross-cutting through the coating to the substrate with a multi-blade knife followed by adhesive taping and peeling. Then the cut areas were examined using a low magnification glass (x6). The test kit and the rating protocol according to the damages are shown in *Figure* 5-27. 5B is the highest rating under this protocol. ZSM-5 coatings on all of the aluminum alloys tested received a rating of 5B (Table in *Figure* 5-28). Although the ASTM D3395-02 protocol does not require a high magnification microscope, we examined the cuts under high magnification microscope (x2000), and extremely clean cuts were revealed. There were no chipping and cracking into the coating after the cutting operation. This is a clear indication that the coatings are strongly adhered to the substrate. High temperature calcination was also performed to see if the coating would behave differently. 5B rating was retained for all of the samples after calcination at 400 °C for 2 hours.

- **Mechanical cutting tests**

To test the properties of the zeolite coating under mechanical stress, zeolite coated panels were cut using a standard lab shear (*Figure* 5-29a). The cut area was examined by SEM (*Figure* 5-29b& c). It can be seen that the cut was very clean, having no clack formation and propagation into the coating.
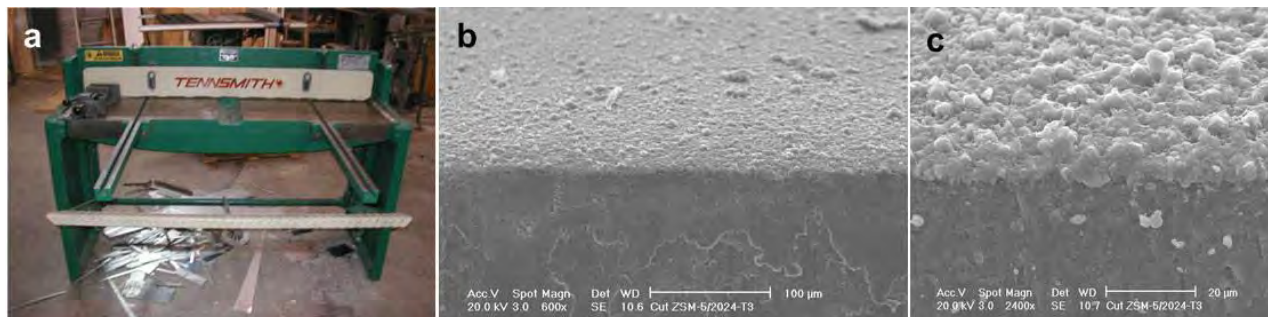
*Figure* 5-29(a) Lab shear for cutting metal sheets, (b) SEM of the cut of ZSM-5 coating on AA-2024-T3 at low magnification, (c) SEM of the cut of ZSM-5 coating on AA-2024-T3 at high magnification.

- **Mechanical hole punching**



*Figure* 5-30 Photograph of a ZSM-5 coated AA-2024-T3 panel with punched holes

The ZSM-5 coated AA-2024-T3 3x6" panels were punched using standard punch in a machine shop. Very clean holes were generated (*Figure* 5-30). Similar results were obtained on ZSM-5 coating on carbon steel S-1008. The edge of the hole was examined by SEM, and was found that no crack was formed along the cutting edge, showing excellent adhesion and mechanical properties of zeolite coating.

- **ASTM D-2794-93 impact test**

Impact tests according to ASTM D-2794-93 were performed on ZSM-5 coated AA-2024-T3 panels. Tests were performed on 2 um and 7.5 um thick coatings showing no crack formation or delamination of the zeolite coating.
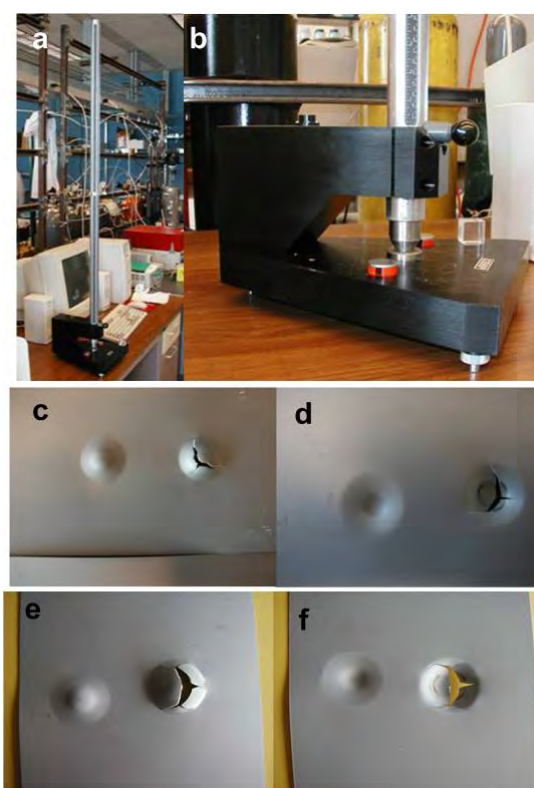


*Figure* 5-31 Photographs of the ASTM D-2794-93 impact setup from Gardner (a and b), impacted area of the 2 um thick ZSM-coated AA-2024 panel (c and d for each side, and left mark for impact from 1 ft and right mark for impact from 2 ft) and impacted area of the 7.5 um thick ZSM-coated AA-2024 panel (e and f for each side, and left mark for impact from 1 ft and right mark for impact from 2 ft)

Photos of the experimental apparatus and the impacted area are shown in *Figure* 5-31. Clearly, when the impact is not enough to break the panel, it generates a dent that shows no

cracking of zeolite coatings. Once the impact is large enough, then both the coating and the panel were broken.

- **ASTM D 522-93a bending test**

To examine the flexibility and adhesion of the zeolite coating, ZSM-5 coated AA-2024-T3 panels were tested according to ASTM D 522-93a. Basically the zeolite coated panels were bent around a metal cone and the coating experiences different degrees of bending at different heights along the cone. Tests were performed on 2 um and 7.5 um thick zeolite coatings. For both the 2 um and 7.5 um thick coatings, no cracking of the coating was observed along the whole height of the cone (*Figure* 5-32)
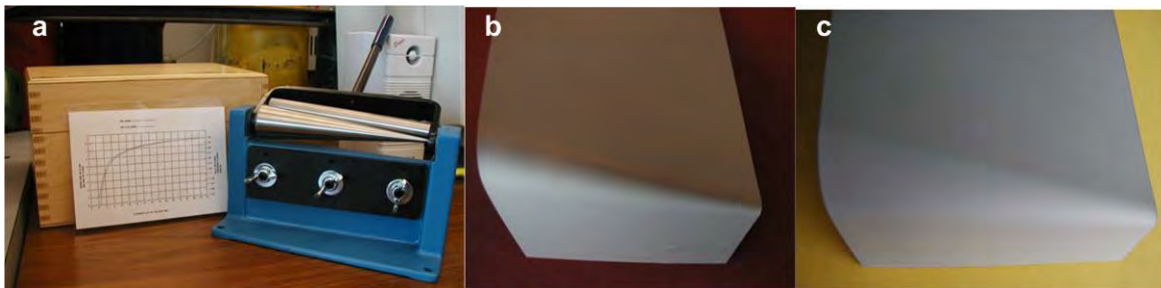


*Figure* 5-32  Photos of the apparatus for ASTM D 522-93a bending test (a); bent 2.0 um thick ZSM-5 coated AA-2024-T3 (b); bent 7.5 um thick ZSM-5 coated AA-2024-T3 (c).

- **ASTM G154-00a UV exposure**

Ten panels of 7.5 um thick zeolite coated AA-2024-T3 were sent to Benet Labs for UV testing following ASTM G154-00a.  Five panels were continuously exposed for 32 weeks and then tested by DC Polarization in 5 wt% NaCl (*Figure* 5-34).  Another 5 panels were removed from UV exposure at 7.23, 16, and 32 week intervals for DC Polarization testing in 5 wt% NaCl at UCR (*Figure* 5-35).  Each of the 10 panels was tested by DC Polarization (*Figure* 5-33) prior to be being shipped to Benet Labs.  The DC Polarization testing procedure was described previously and the test setup is shown in *Figure* 5-24.

The legend for the line designations for Figure 5-33, Figure 5-34, and Figure 5-35 is shown in Figure 5-35 (bottom panel).  In each Figure, one of the DC Polarization test sets has the line designations labeled. Figure 5-34 shows the DC Polarization in 5 wt% NaCl profiles of the five zeolite coated AA-2024-T3 coupons after 32 weeks of continuous UV exposure compared to the DC Polarization profiles prior to UV exposure. There was no decrease in corrosion resistance after 32 weeks continuous UV exposure.  In all cases the polarization profiles after UV exposure for 32 weeks showed improved corrosion resistance, reflected in a decrease in current density and more vertical traces for anodic passivity as compared to the polarization profiles before UV exposure.  The DC Polarization profiles of sample 3-21-05 (*Figure* 5-34) before and after UV exposure exemplifies the improved corrosion resistance following UV exposure. Five zeolite coated AA-2024-T3 panels were tested by DC Polarization in 5 wt% NaCl after incremental UV exposure (7.23, 16, 32 weeks) and their polarization profiles compared with those taken before UV exposure (*Figure* 5-35).  The purpose of the incremental UV exposure and DC Polarization testing at each interval is to monitor the effects of UV exposure on corrosion resistance at different exposure times.  Increased corrosion resistance was observed after 7.23 weeks UV

exposure for all five samples and continued to improve with longer UV exposure times. Sample 3-16-05 (*Figure* 5-35) was only UV exposed for a total of 16 weeks to provide a sample at a shorter UV exposure time for future comparative analyses.
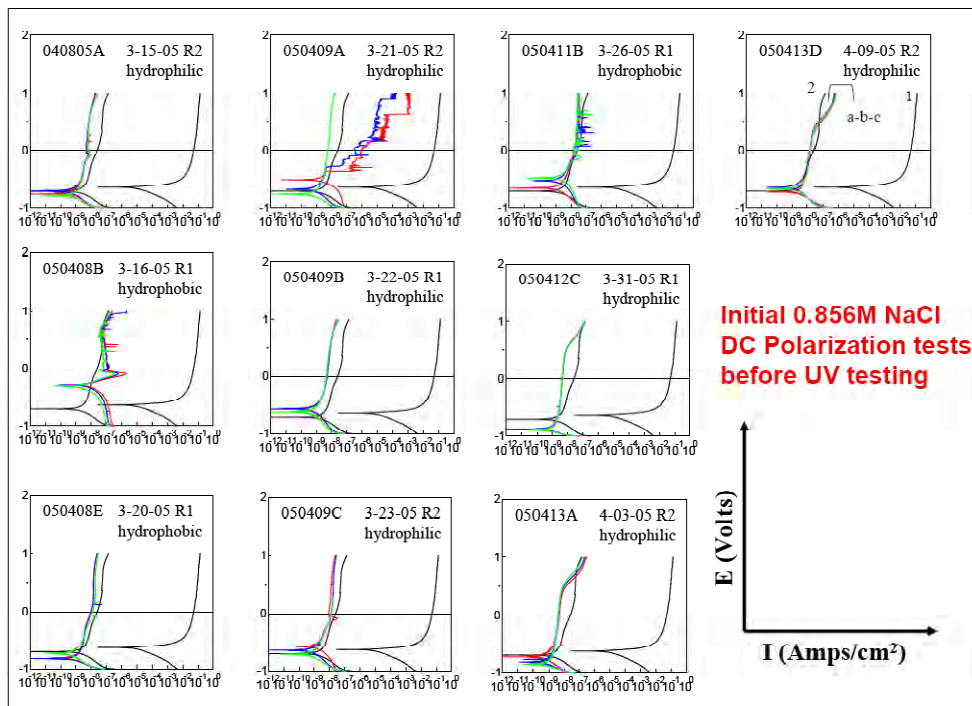
*Figure* 5-33 DC Polarization profiles of each zeolite coated AA-2024-T3 prior to UV exposure. See *Figure* 37 (bottom panel) for line designation legend
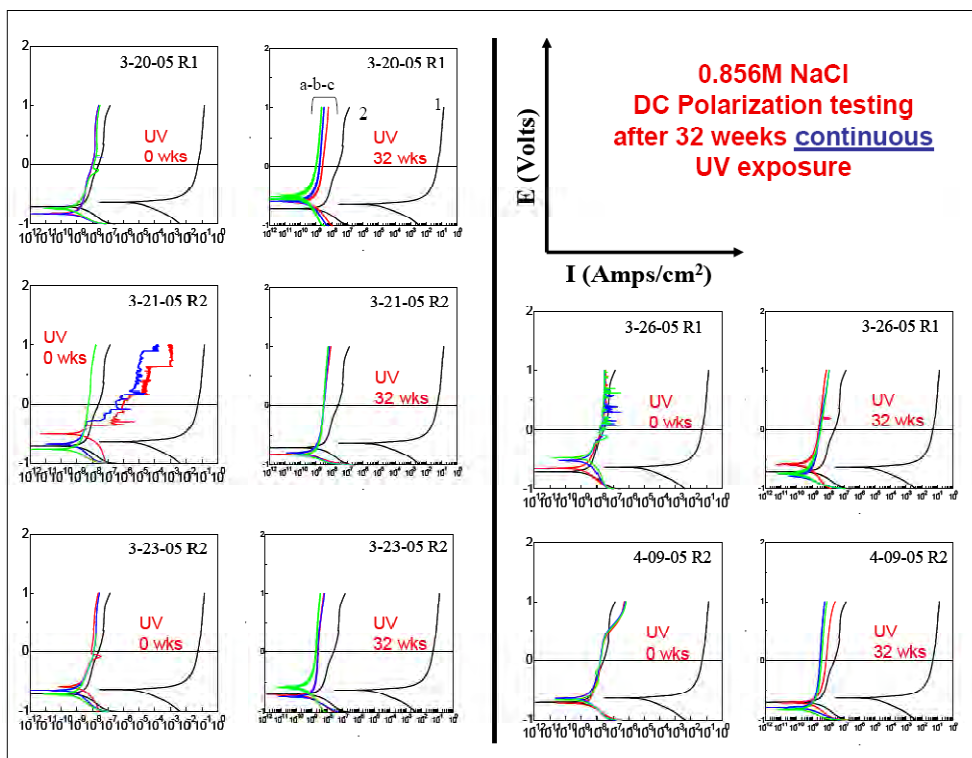


*Figure* 5-34 DC Polarization profiles of zeolite coated AA-2024-T3 prior to and after 32 weeks continuous UV exposure. See *Figure* 37 (bottom panel) for line designation legend
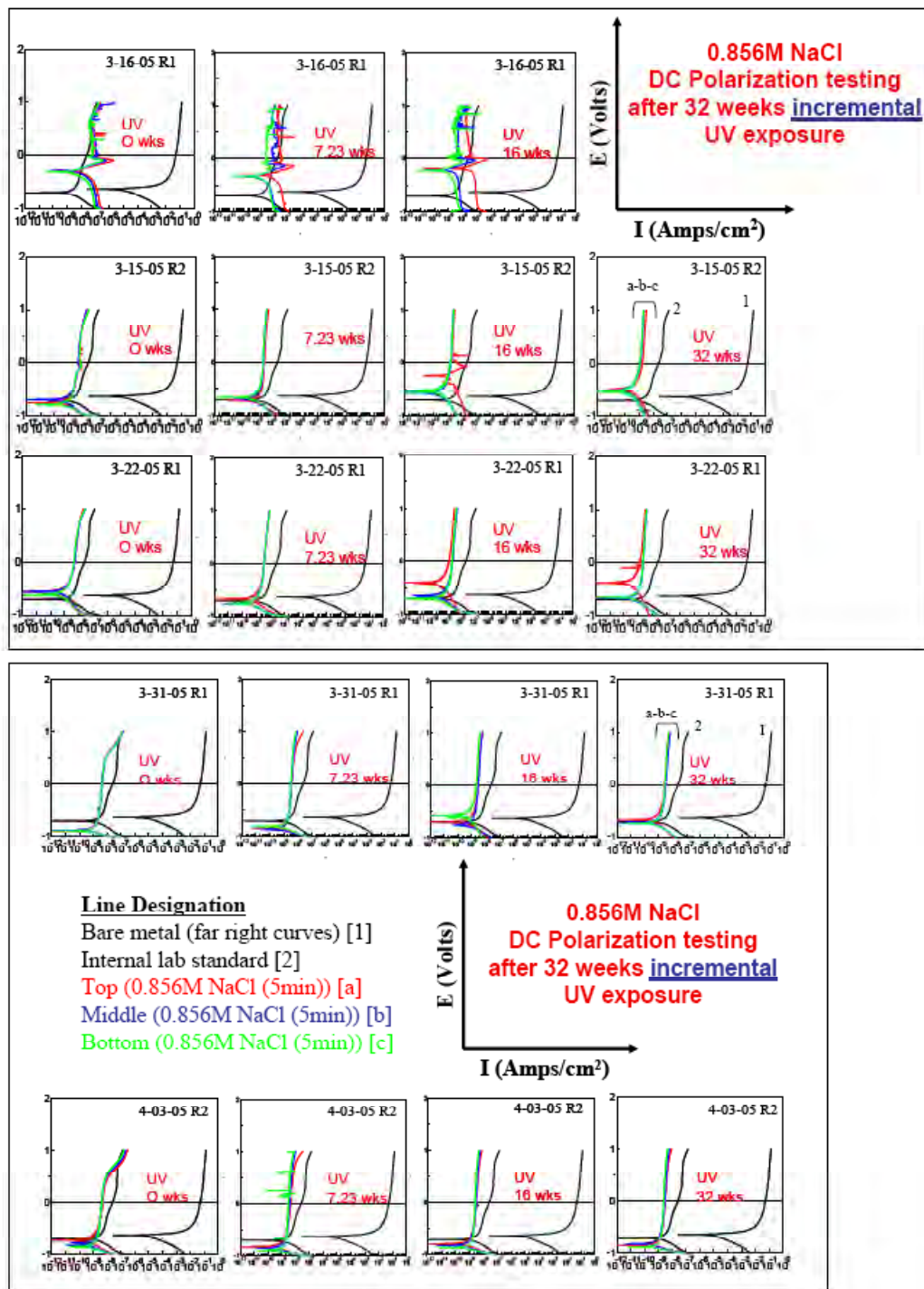
*Figure* 5-35 DC Polarization profiles of zeolite coated AA-2024-T3 prior to and after 7.23, 16, and 32 weeks UV exposure.

**Task 3-4: Conduct accelerated service simulation testing**

ASTM B117 Salt-fog testing on bare zeolite coating

Initial salt fog testing on thin (0.5 um to 2 um thick) (Generation-1) zeolite coatings and coatings generated from differentially aged synthesis solutions during our coating optimization phase had inconsistent results, yielding many non-passing samples.  During that process we optimized our synthesis process where we can reproducibly generate uniform zeolite coatings of variable, but controlled, thickness (0.5 um to greater than 13 um).  Coating performance is virtually identical between panels that are coated simultaneously in the same reactor. We have developed a quick, minimally invasive DC Polarization testing regimen (described previously in section 3.2) for quality control monitoring of zeolite coatings prior to salt fog testing.  Currently, greater than 99% of zeolite coatings (7.5 um thick) produced will pass a very demanding DC Polarization quality control test in 5 wt% NaCl.

Following our optimized zeolite synthesis process, zeolite coatings (7.5 um thick) on AA-2024-T3 samples were salt fog tested for over 2000 hrs at China Lake with all samples passing.  Salt fog testing (1000 hours) of machine scribed zeolite coatings (7.5 um thick) demonstrated that rust, if present, was confined to the scribed area and there was no delamination of the zeolite.

*Generation-1 coatings (0.5 – 2.0 um thick) on AA-2024-T3:*

Five zeolite coated panels (0.5 um thick) were tested for corrosion performance as a pretreatment according to Mil-C-81706, which requires the coating to be free from corrosion after 336 hours (2 weeks) of salt fog exposure.  *Figure* 5-36 were taken of the zeolite panels after 336 hours of exposure.
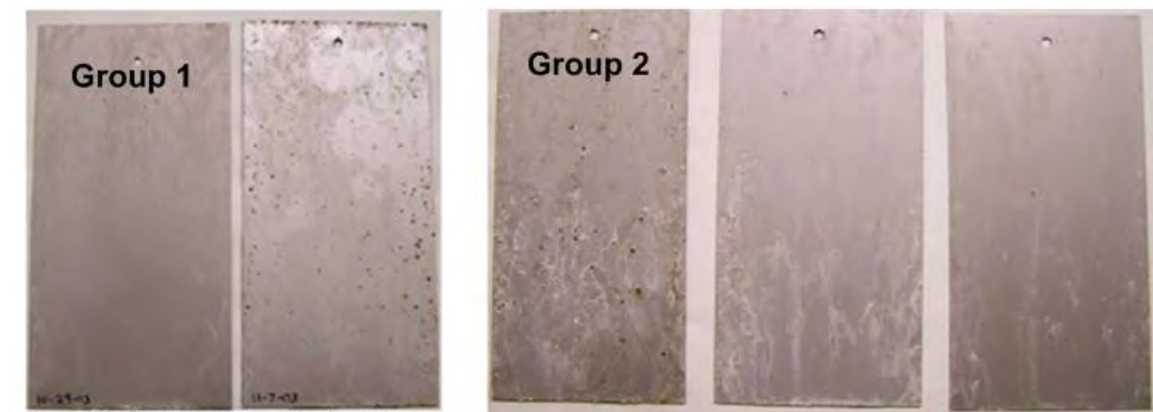


*Figure* 5-36 Zeolite coated panels after 336 hours of salt fog exposure

Three (Group 2) of the five panels have a significant number of corrosion spots while two (Group 1) of the panels show very few corrosion spots. Based on these results new panels with a thicker zeolite coating were decided to be tested.

*Generation-2 coating (7.5 um thick)*

Five zeolite-coated aluminum 2024-T3 panels with 7.5 um thickness (with 3 different aging times of the deposition solution) were sent to China Lake for testing under neutral salt fog conditions, according to ASTM B-117. We thought 7.5 um would be a good thickness to start and likely to strike a balance between corrosion resistance and mechanical properties. The panels were in three different bundles, each with a different date, their preparation date. The dates indicated on the packages were 2-25-04 (two panels), 2-27-04 (two panels) and 3-1-04 (one panel). **The panels w ith the same date w ere pr oduced in the same reactor. Thus the consistency of perfo rmance amo ng 2-25 and 2-27 w ill show that the coat ing depositio n procedure is very reproducible.** The panels were labeled with permanent ink on one side (used as the back side) with the corresponding dates that were on the packaging. The packages that contained two panels with the same date were given "a" and "b" designations.

The panels were placed in a salt fog chamber on May 11 at 10:30 a.m. At intervals of 168 hours and 336 hours of exposure, the panels were rinsed with deionized water, dried, examined and photographed.

With one exception, all of the panels had a uniform appearance before exposure testing began. Panel 2-27-04b had a small streak that was grey in appearance but was slightly more reflective or shiny than the rest of the coating. See *Figure* 5-37 and *Figure* 5-38.



*Figure* 5-37 Panels 2-27-04a, 2-27-04b, and 3-1-04 before exposure

*Figure* 5-38 Close up of non-uniform coating section on panel 2-27-04b before exposure.

The streak or non-uniformity did not adversely affect the coating performance during the test.

The sole criterion by which a conversion coating is determined to "pass" the salt fog test is that there are to be no visible signs of corrosion whatsoever for a specific duration of exposure. Two critical times of inspection are 168 hours (1 week) and 336 hours (2 weeks). Many military systems require 336 hours of corrosion resistance but some systems require only 168 hours. Of the five panels tested, four passed the 168 hour inspection with no signs of corrosion while one panel designated as 3-1-04, was severely pitted (*Figure* 5-39).

.
After one week of salt fog exposure, another difference was observed on panel 2-27-04b (other than the streak in the coating). Immediately after removing panels from the salt fog, they were rinsed with DI water. A significant portion of panel 2-27-04b had surface property differences; specifically it did not wet evenly. There were other very small areas on other panels that would not wet evenly but they were significantly smaller than the sections on panel 2-27-04b. Darker sections seen in *Figure* 5-40, down the left side, are the areas that had differences in surface wetting from the rest of the coating.

The panels were returned to the salt fog chamber and evaluated after 1000 hrs of exposure. Panels 2-27-04a and 2-27-04b (*Figure* 5-41) are still passing and show no signs of corrosion.

Although panels 2-25-04a (*Figure* 5-43) and 2-25-04b (*Figure* 5-44) had some pitting corrosion on the surface after 336 hours of exposure, they were tested further to determine if the pitting corrosion would worsen and delaminate the coating. The number of areas of pitting did not significantly increase on the surface and the coating around these areas remained intact. There is no sign of filiform corrosion, blistering or delamination. (*Figure* 5-42)

The zeolite coating shows great promise as a viable conversion coating. It appears that although a pit can form within the coating, the corrosion does not undercut, delaminate or cause blistering in the surrounding coating; instead the corrosion area is limited in size.

Coating resistance and performance are virtually identical between panels that are coated simultaneously in the same reactor.

*Figure* 5-41 Panels 2-27-04a and 2-27-04b after 1000 hours of exposure



*Figure* 5-42 Panels 2-25-04a and 2-25-04b after 1000 hours of exposure



*Figure* 5-43 Panel 2-25-04a and 2-25-04b after 336 hours of exposure.



*Figure* 5-44 Close up of panel 2-25-04a after 336 hours of exposure

*Generation-3 coatings*

Based on the previous testing results, it appears that 7.5 um thick coating has sufficient corrosion resistance. Therefore we decided to focus on 7.5 um coatings. We produced 25 zeolite coated panels with 15 of them without topcoat and 10 with topcoats. The topcoats were applied by Deft in a trial run in their facility. The S series have been examined on the back by DC Polarization using the almost non destructive method described in Task 3-2 and shown to have excellent corrosion resistance. Series B are the non-tested (by DC Polarization) twins of the S samples. Series A are the non tested twins of 5 panels that showed medium corrosion resistance (sulfuric acid, $10^{-4}$ A/cm$^2$).

- **Generation-3 coatings (7.5 um thick) on AA-2024-T3**

ASTM B117 on zeolite coated AA2024-T3 panels:
Based on the previous testing results, it appears that 7.5 um thick coating has sufficient corrosion resistance.  Therefore we decided to focus on 7.5 um coatings.  15 zeolite coated panels were

sent to China Lake for neutral salt fog testing (ASTM B117). The S series have been examined on the back by DC Polarization in 5 wt% NaCl using the almost non destructive method described in Task 3-2 and shown to have excellent corrosion resistance (*Figure* 5-25, S1). Series A are the non-tested (by DC Polarization) twins of the S samples. Series B are the non tested twins of 5 panels that showed medium corrosion resistance by DC Polarization (*Figure* 5-25, B1 & B3). All 15 zeolite panels passed 2205 hours of salt spray exposure. *Figure* 5-45, *Figure* 5-46 and *Figure* 5-47 are of the three sets of zeolite panels after 1000 hours salt fog exposure and *Figure* 5-48, *Figure* 5-49 and *Figure* 5-50 are of the three sets of panels after 2205 hours salt fog exposure. Discoloration can be seen on the bottom corners of several panels which are due to color transfer of the wood that is used to hold the panels at the required 6° angle.
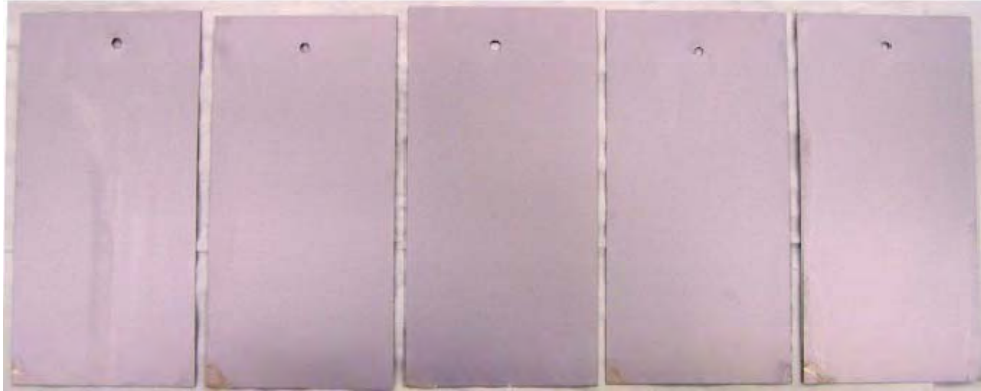
*Figure* 5-45 Panels A1-A5 after 1000 hours of salt fog exposure. Panel surfaces are alternating smooth and rough from A1 to A5



*Figure* 5-46 Panels B1-B5 after 1000 hours of salt fog exposure. Panel surfaces are alternating smooth and rough from B1 to B5.



*Figure* 5-47 Panels S1-S5 after 1000 hours of salt fog exposure. Panel surfaces are alternating rough and smooth from S1 to S5.

After the zeolite panels were inspected and photographed after 1000 hours they were returned to the chamber for further exposure, for a total of 2205 hours.

*Figure* 5-48 Panels A1-A5 after 2205 hours of salt fog exposure.  Panel surfaces are alternating rough and smooth from A1 to A5
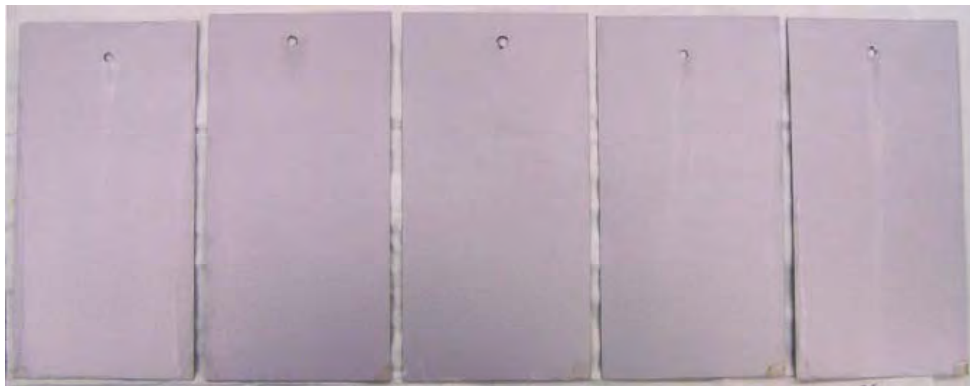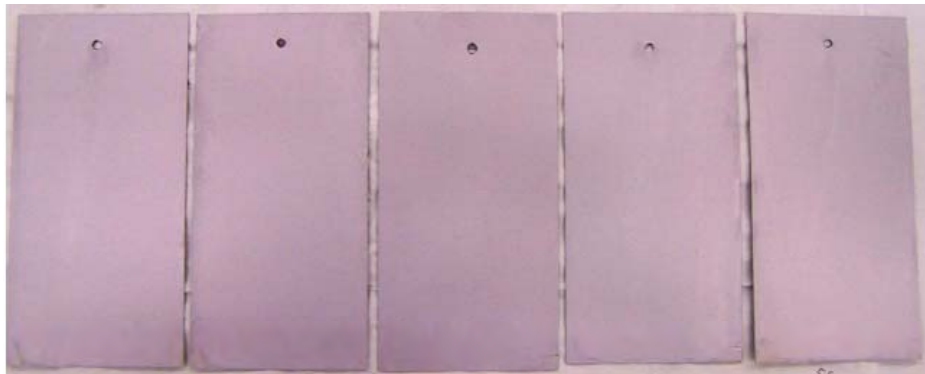


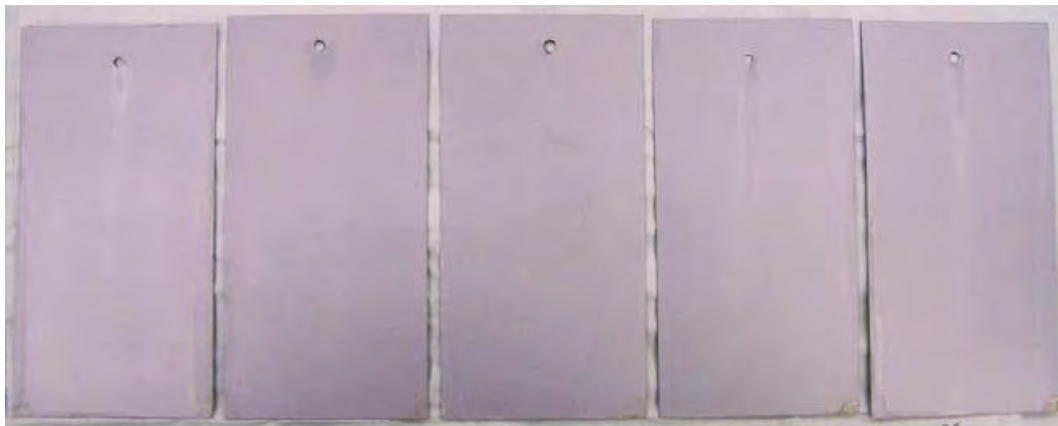*Figure* 5-49 Panels B1-B5 after 2205 hours of salt fog exposure.  Panel surfaces are alternating smooth and rough from B1 to B5



*Figure* 5-50 Panels S1-S5 after 2205 hours of salt fog exposure.  Panel surfaces are alternating rough and smooth from S1 to S5.

After 2200 hours of exposure, the only visible signs of corrosion were small areas along the outer edges of the panels designated S1-S5.
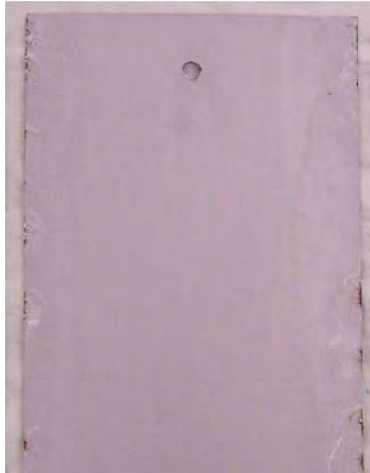
*Figure* 5-51 Visible corrosion along the edge of panel S2 after 2205 hours of exposure

The beginnings of corrosion along the outside edges of the panels, "edge effects", are neglected within 0.25" when rating a coating according to pass/fail criteria. After 2205 hours of exposure the most significant corrosion, seen in *Figure* 5-51, is neglected and the coating meets passing criteria. All of the zeolite coatings were considered passing after the removal from the chamber after 2205 hours of exposure.

The edge effects were only observed on the S series. These samples had a small area of zeolite removed on the back side, exposing the metal substrate. None of the back sides of the samples being salt fog tested were sealed. *Figure* 5-52(left) shows the back side of sample S2 after 2205 hours of testing. The right panel shows a similar zeolite sample with a small area of zeolite removed, exposing the bare metal prior to salt fog testing. The severe corrosion on the bare metal observed after the salt fog test and the fact that only those samples that had zeolite removed to expose bare metal demonstrated edge effects suggests that the edge effects may be caused by the bare metal corroding. If the backs of samples that have had bare metal exposed for quality control testing are sealed prior to salt fog testing, the edge effects observed may be eliminated.



*Figure* 5-52 Back side of sample S2 from S series after 2205 hours salt fog testing (left panel), Non-salt fog tested zeolite panel with small area of zeolite removed, exposing bare metal (right panel).

ASTM B117 testing on scribed zeolite coated AA-2024-T3 panels:
Five (5) zeolite coated panels were machine scribed at Deft (Irvine, CA), and then exposed to neutral salt fog testing for 1000 hours. *Figure* 5-53 shows that the only visible corrosion was within the scribe and that there was no delamination or pealing of the coating.
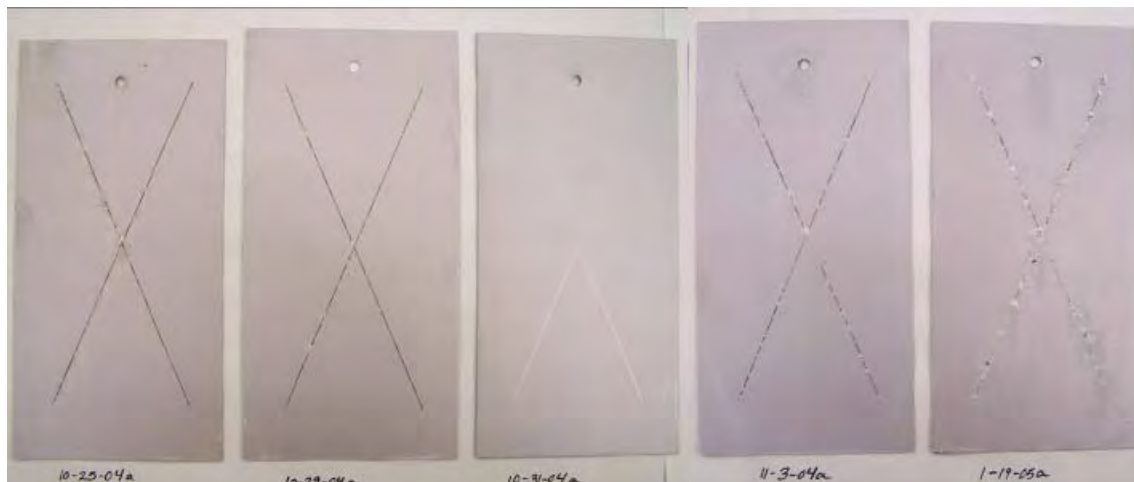
*Figure* 5-53 Machine scribed Panels after 1000 hours of salt fog exposure

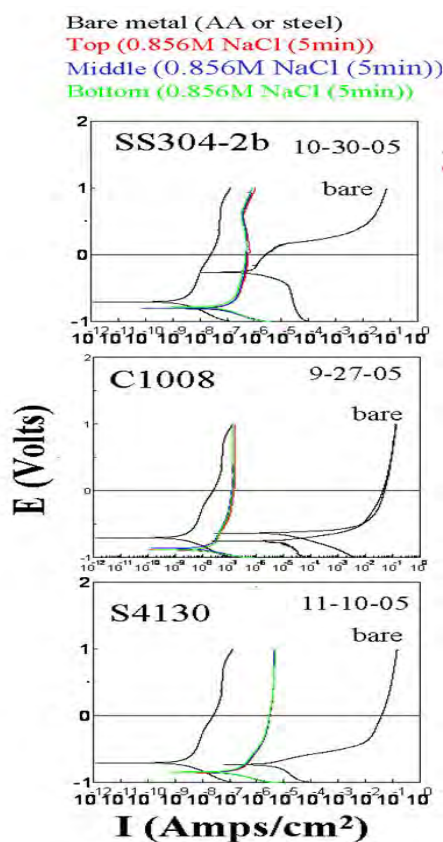- **ASTM B117 testing of zeolite coated steels (2006)**



*Figure* 5-54 Representative DC Polarization quality control curves of 5 um think coatings on steels in 5 wt% NaCl . The far left black curve in each panel is an internal lab standard used for comparative purposes

Fifteen (15) zeolite coated samples (5 each of SS304-2b, S4130, and C1008) with a coating thickness of about 5 um were given to China Lake on November 18, 2005 for salt fog testing (ASTM B117). We are testing a thinner zeolite coating of 5 um instead of our previous 7.5 um thick zeolite coatings for two reasons. The first reason is that the zeolite coated steel panels or their twins have undergone DC Polarization quality control testing in 5 wt% NaCl, demonstrating excellent corrosion resistance (*Figure* 5-54). Secondly, we want to determine the thinnest coating that can match the excellent corrosion protection throughout 2205 hours of salt fog testing of the 7.5 um thick coatings on AA-2024-T3.

The criteria used to determine coating failure on steel panels was that visible edge corrosion could have no more than 1/8 inch of creep from the edge of the coating and no more than 5 pits within the coating. After 168 hours of exposure, all of the steel samples were passing with the exception of 1 of the 5 1008 steel panels. After 336 hours of salt fog exposure, all of the samples were passing with the exception of 2 of the 5 1008 steel panels. After 552 hours of exposure, multiple failures became evident within the 4130 steel panel set

as well as the 1008 steel panel set.  The 304 stainless steel set began to fail after 3000 hours of exposure.  *Table* 5-2 is a summary of the bare zeolite on steel panel performance data.

*Table* 5-2 Salt fog testing (ASTM B117) results for zeolite coatings on steels (2006)

| Alloy | Coating | Results |
|-------|---------|---------|
| S1008 | Zeolite only | 0 failures at 48 hours<br>2/5 failures at 168 hours<br>3/5 failures at 672 hour<br>3/5 failures at 1056 hours<br>5/5 failures at 1584 hours |
| S4130 | Zeolite only | 0 failures at 168 hours<br>1/4 failures at 336 hours<br>1/4 failures at 672 hours<br>4/4 failures at 1056 hours |
| SS304 | Zeolite only | 0 failures at 1584 hours<br>2/5 failures at 3100 hours |

Carbon steel S1008:

The 1008 steel panels in *Figure* 5-55 had good protection overall after 168 hours of exposure.  Two of the 3 panels had small pits resulting in visible red rust.  The panels tested for over 1000 hours to look for zeolite coating delamination and further pit formation.  The same panels are seen in *Figure* 5-56 after 1056 hours of exposure.  Once a pit had formed, the corrosion increased, as expected, but the zeolite did not delaminate from the panel.  It is clear from these photos that the zeolite was still protecting the majority of the surface area on 3 of the 5 panels after 1000 hours.
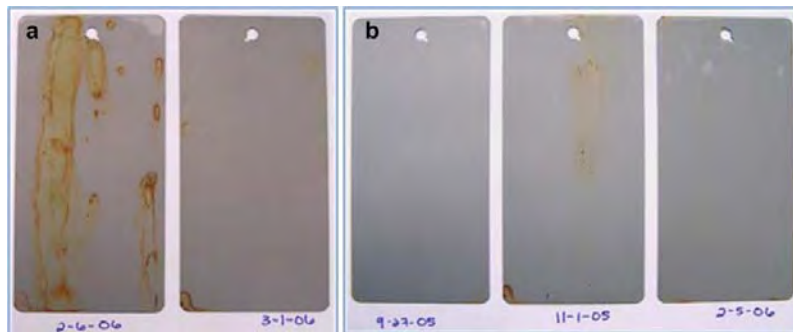


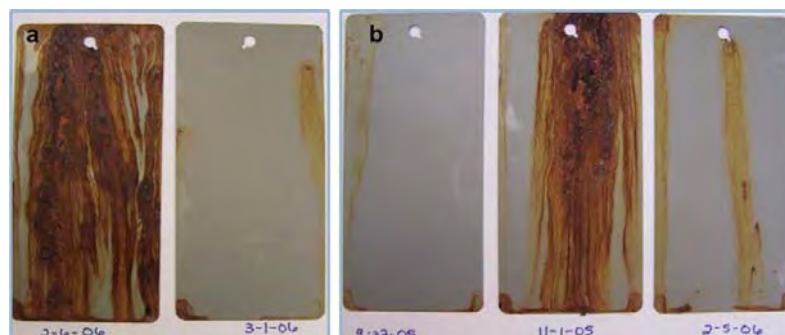*Figure* 5-55 Zeolite coated 1008 steel after 168 hours of exposure



*Figure* 5-56 Zeolite coated 1008 steel after 1056 hours of exposure

High-strength steel S4130:

The 4130 steel panels seen in *Figure* 5-57 had no failures after 168 hours of exposure. After 672 hours only one of the panels had pitting. Although the surfaces of the majority of the panels were corrosion free after 1056 hours of exposure, there were at least 5 corrosion pits present on each panel (*Figure* 5-58).
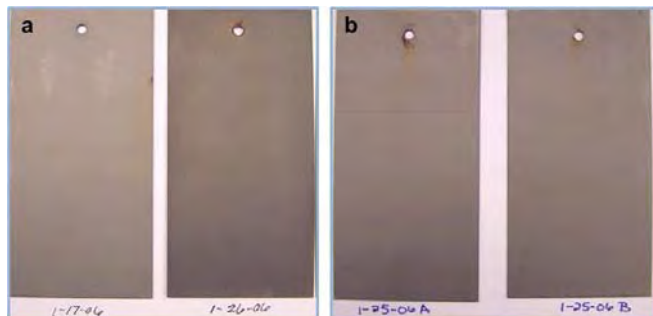


*Figure* 5-57 Zeolite coated 4130 steel after 168 hours of exposure
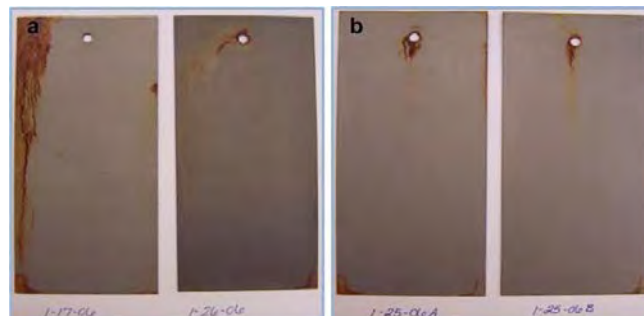
*Figure* 5-58 Zeolite coated 4130 steel after 1056 hours of exposure

Stainless steel SS304-2b:

The 304 stainless steel panels just began to show sign of corrosion geminating from the edge of the hole in the panel after 3100 hours of exposure (*Figure* 5-59).

The protection of steel panels under salt fog conditions exceeds most military requirements. An increase in zeolite coating thickness may increase protection times even further by reducing corrosion pit formation.
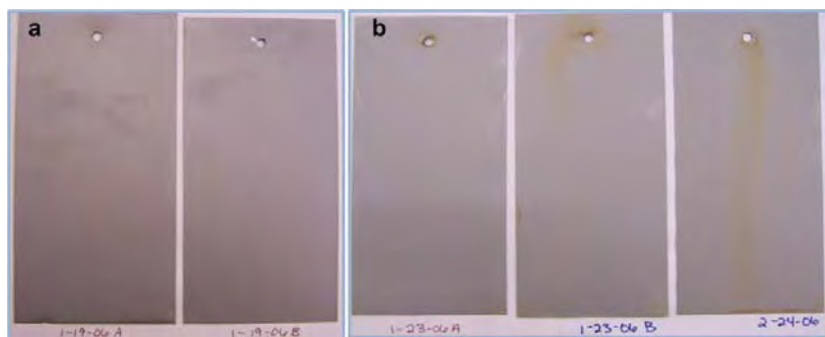


*Figure* 5-59 Zeolite coated 304 SS after 3100 hours of exposure

- **ASTM B117 testing of zeolite coated steels (2008)**

Another fifteen zeolite coated samples (5 each of SS304-2b, S4130, and C1008) with a coating thickness of about 5 um were tested by China Lake on March 12, 2008. Three different controls were used. The C1008 steel was Zn phosphate coated with MIL-DTL-11195. The SS304-2b received a nitric acid passivation and the S4130 was Cd plated.

The C1008 sets were scribed. The zeolite coated samples failed by 24 hours of salt fog (Figure 5-60). The controls failed as well (Figure 5-61). Three out of the five zeolite coated SS304-2b samples passed 2376 hours of salt fog (Figure 5-62). All of the nitric acid passivated controls passed 2376 hours test (Figure 5-63). The zeolite coated S4310 samples failed after 500 hours of salt fog (Figure 5-64), while the Cd plated counterpart passed (Figure 5-65). The results were summarized in Table 5-3.

Table 5-3 Salt fog testing (ASTM B117) results for zeolite coatings on steels (2008)

| Steel Coating | | Results |
|---|---|---|
| C1008 | Zeolite (Scribed) | Failed by 24 h |
| C1008 | Zn phosphate and coated with MIL-DTL-11195(Scribed) | Failed by 24 h |
| SS304-2b | Zeolite | 3/5 passed 2376 h |
| SS304-2b | Nitric acid passivation | 5/5 passed 2376 h |
| S4130 | Zeolite | Failed by 504 h |
| S4130 | Cd plated | Passed by 504 h |

Figure 5-60  Scribed Zeolite coated C1008 after 24 hours of exposure



Figure 5-61 Scribed   C1008 (Zn phosphate coated with MIL-DTL-11195) after 24 hours of exposure



Figure 5-62 Zeolite coated SS304-2b after 2376 hours of exposure
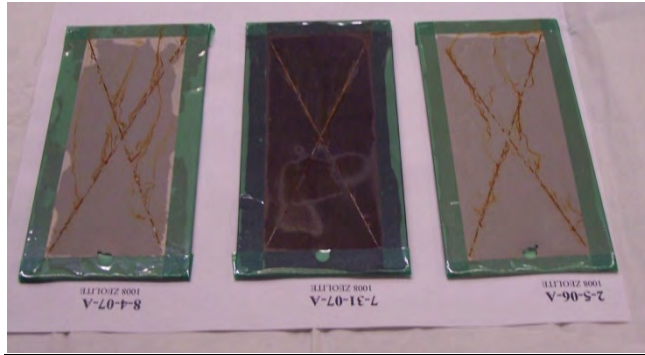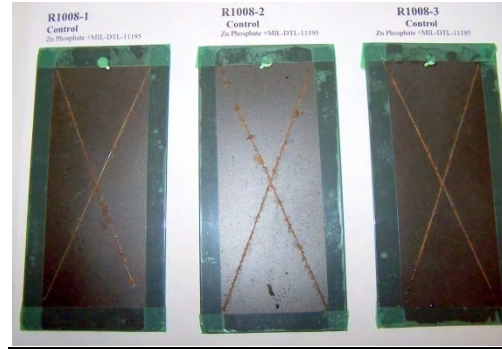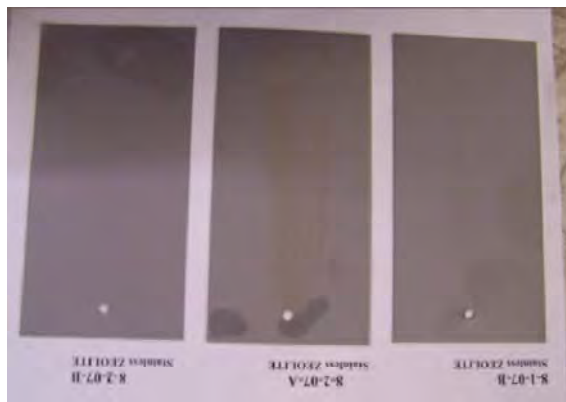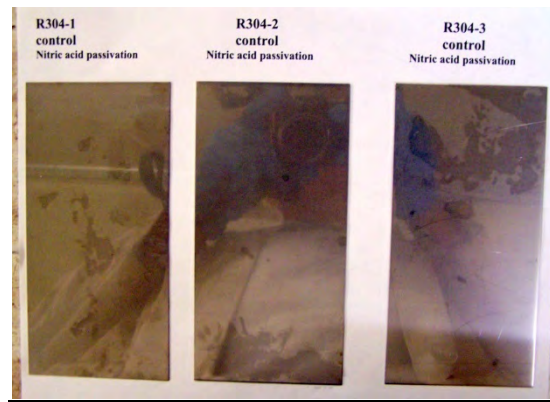


Figure 5-63 Nitric acid passivated SS304-2b after 2376 hours of exposure



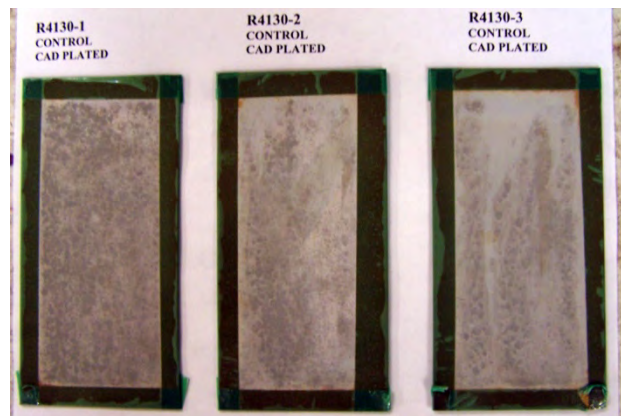Figure 5-64  Zeolite coated S4130 after 504 hours of exposure



Figure 5-65  Cd plated S4130 after 504 hours of exposure

ASTM B117 Salt-fog testing on zeolite coating systems

*Generation-1 coating (0.5 – 1.0 um thick):*



*Figure* 5-66 Aluminum panels coated with zeolite and CARC topcoat after 19 hours of salt fog exposure

Aluminum 2024-T3 panels were coated with zeolite of 0.5-2 um thick at UCR and delivered to China Lake. The panels were then sent to the Army Research Laboratory (ARL) to be coated with CARC topcoat. The panels were coated on one side with the CARC topcoat (Mil-PRF-64159) and coated with primer on the other side to keep corrosion from contaminating the salt fog chamber.

The painted panels were scribed in an "X" configuration and placed into the chamber while held at 15° from vertical. The unpainted panels were placed in the chamber 6° from vertical. The panels were exposed to a salt fog according to ASTM B-117.



*Figure* 5-67  Exposed zeolite surface after 524 hours of exposure after CARC removal.

Unpainted zeolite panels were also used to test the zeolite performance as a pretreatment.

All panels were first inspected after 19 hours of exposure. Upon initial inspection, it was evident that the CARC coating did not adhere to the zeolite (*Figure* 5-66).

Although the CARC topcoat did not appear to be compatible with the zeolite directly, the primer adhered to the test panels and there were no signs of delamination between the primer and zeolite. Another test using primer and topcoat may show that the zeolite coating performs well in a coating system. Because the topcoat came off of the panels very cleanly, the excess paint was trimmed away and the panels were allowed to remain in the salt fog chamber to test effects on the zeolite coating alone. After 524 hours of exposure, the bulk zeolite coating showed almost no corrosion except where the coating had been scribed (See *Figure* 5-67). Another interesting and positive aspect of the coating is that the corrosion that can be seen within the scribed areas did not migrate and damage the bulk coating.

*Generation-3 coating (7.5 um thick)*

<u>VOC-free topcoat (Deft product #55W-002, Deft, Irvine CA) and Self-Priming topcoat (TT-P-2756A from Deft, Irvine, CA)</u>

Based on the previous testing results, it appears that 7.5 um thick coating has sufficient corrosion resistance. Therefore we decided to focus on 7.5 um coatings. We produced 25 zeolite coated panels with 15 of them without topcoat and 10 with topcoats. The topcoats were applied by Deft in a trial run in their facility. Five panels were applied with VOC-free topcoat (Deft product #55W-002, Deft, Irvine CA) and five panels were applied with self-priming topcoat (TT-P-2756A from Deft, Irvine, CA). Three of each of the topcoated panels were then sent to China Lake for salt-fog testing (ASTM B117). The S series have been examined on the back by DC Polarization using the almost non destructive method described in Task 3-2 and shown to have excellent corrosion resistance. Series B are the non-tested (by DC Polarization) twins of the S samples. Series A are the non tested twins of 5 panels that showed medium corrosion resistance (5 wt% NaCl, $10^{-4}$ A/cm$^2$).

From initial observation of the panels painted with the VOC-free formulation, there were significant differences between the surfaces of the paint. Two of the panels had a smooth appearance while one had a rough "orange peel" look (*Figure* 5-68a&b). During the scribing process, one coating peeled away from the scribed area. (*Figure* 5-68**c**)
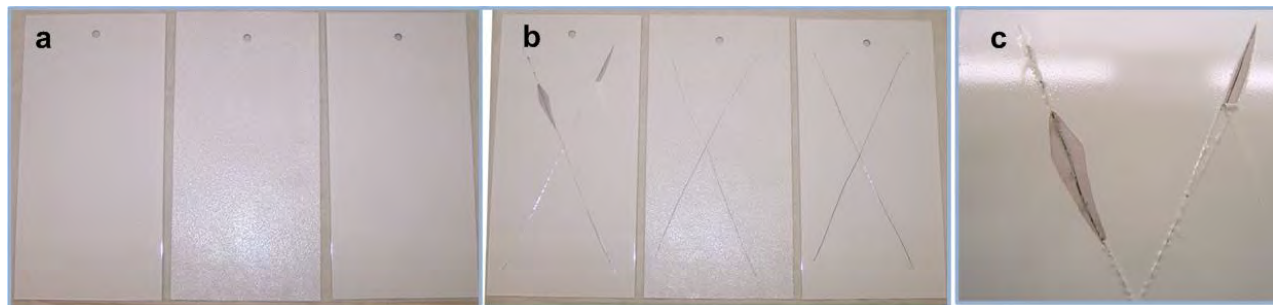


*Figure* 5-68 Zeolite panels 6-5-04, 6-10-04a and 6-10-04b with VOC-free self-priming topcoat before scribing (a) and after scribing (b). (c) close up view of zeolite panel 6-5-04 with topcoat

Three panels with designations 8-1-04, 10-16-04a and 10-16-04b were painted with a solvent-based self-priming topcoat. The panels had a uniform appearance and showed no peeling or delamination during the scribing process.

All painted panels were placed in the chamber at an angle of 15° from vertical. After 168 hours (1 week) of exposure all painted panels had some degree of blistering between the zeolite and the paint along the scribe and significant blistering on the outer edges of some panels. Although blistering is a



*Figure* 5-69 Panel 10-16-04b coated with (a) a VOC-free topcoat and (b) a solvent-based topcoat after 168 hours of salt fog exposure

performance failure for this test, the panels remained in the chamber for a total of 336 hours. The severity of the blistering increased and the panels were removed from the test. *Figure* 5-69 are photos of blistering areas after 168 hours of exposure of the VOC-free topcoat and the solvent-based topcoat, respectively.

The poor performance of these topcoats is contributed in part to their application to the zeolite coatings. Neither ASTM nor MIL specs were followed during the topcoat application; they were applied as part of a demonstration of the topcoat application process. Based on these results, MIL specs will be adhered to during future primer and/or topcoat application.

Zeolite/Primer, Zeolite/Primer/Topcoat and Zeolite/Topcoat

Forty nine (49) zeolite coated AA-2024-T3 panels were prepared and painted by Deft (Irvine, CA), following ASTM guidelines. *Figure* 5-15 shows the matrix of primers and topcoats applied to the zeolite coating following MIL specs.

Aluminum 2024-T3 panels, coated with zeolite, were painted and tested in a salt fog environment according to ASTM B-117. Panels were tested with primers alone, primers and topcoat, and one set was tested with a self-priming topcoat. The primers include Mil-PRF-23377 Type I Class C (control), Mil-PRF-23377 Type I Class N and Mil-PRF-85582 Type I Class N. The topcoat applied over the primers was a Mil-PRF-85282 and the self-priming topcoat was a TT-P-2756A.
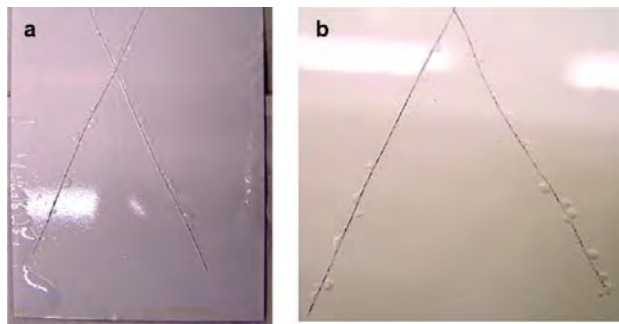
Primed and painted panels were scribed with a 4-inch "X" which exposed bare metal before being placed into the test chamber. The panels were inspected at various time intervals, including 168 hours, 336, hours, 552 hours, 672 hours, 1056 hours, 1584 and 3100 hours. It should be noted that during the first two weeks of the test, a city-wide power failure caused the chamber to lose power for approximately 4 days. Once power was restored, the chamber was calibrated and the test resumed.

Coating delamination and corrosion was evident on some samples in the early stages of the test. The corrosion is thought to be due to flexing of the aluminum panels causing coating breaches. The samples that were provided were less than 0.032 in thickness. While handling, it was obvious that the panels were flexing. Possible cracking of the zeolite coating may have lead to corrosion within the bulk of some of the samples.

*Table* 5-4 summarizes the performance data of the tested coating systems. It should be noted that the test was stopped after 3100 hours.

*Figure* 5-70 are of the panel sets that had the chromated Mil-PRF-23377 Type I primers applied. After 3100 hours of exposure, the scribed areas were free of corrosion and the coating did not show signs of delamination from the zeolite surface.

Corrosion is evident within the scribed areas of the panel sets in *Figure* 5-71. The panels had the non-chromated Mil-PRF-23377 Type I primer. These panels failed after 336 hours of exposure.

Table 5-4 Summary of performance and exposure time

| Alloy | Primer | Topcoat | Result |
|---|---|---|---|
| Al 2024-T3 | Mil-PRF-23377 Type I Class C | Mil-PRF-85285 | Passing at 3100 hours |
| Al 2024-T3 | Mil-PRF-23377 Type I Class N | Mil-PRF-85285 | Partial failure at 168 hours<br>Complete Failure at 336 hours |
| Al 2024-T3 | Mil-P-85582 Type I Class N | Mil-PRF-85285 | Failure at 168 hours due to delamination |
| Al 2024-T3 | Mil-PRF-23377 Type I Class C | None | Passing at 3100 hours |
| Al 2024-T3 | Mil-PRF-23377 Type I Class N | None | Partial failure at 168 hours<br>Complete Failure at 336 hours |
| Al 2024-T3 | Mil-P-85582 Type I Class N | None | Failure at 500 hours |
| Al 2024-T3 | ---------- | TT-P-2756A | Failure at 168 hours due to delamination |



Figure 5-70 Zeolite coated 2024-T3 aluminum with Mil-PRF-23377 Type I Class C primer (a) without and (b) with Mil-PRF-85285 topcoat after 3100 hours of exposure.
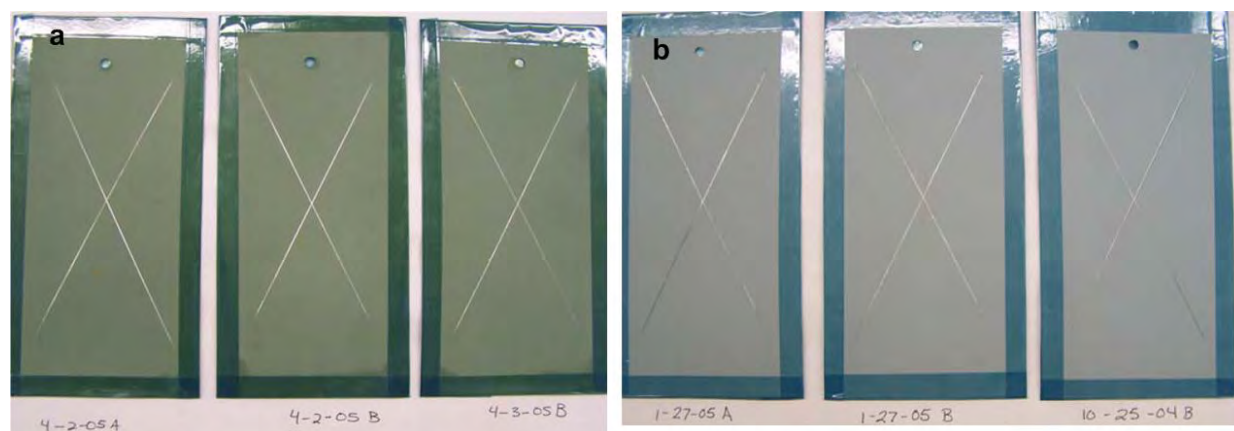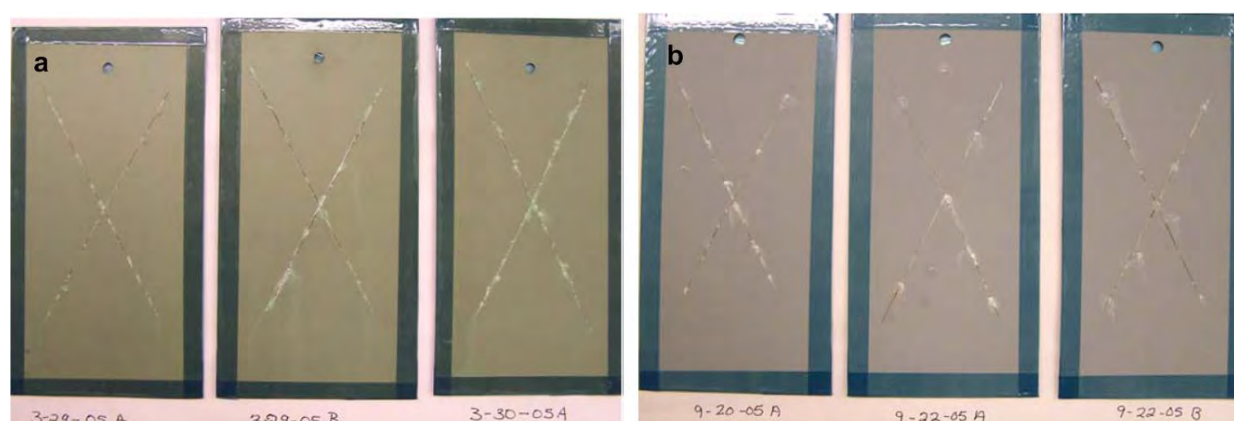


Figure 5-71 Zeolite coated 2024-T3 aluminum with Mil-PRF-23377 Type I Class N primer (a) without and (b) with Mil-PRF-85285 topcoat after 336 hours of exposure.

In *Figure* 5-72, corrosion is evident within the scribe on the 3-25-05A panel after 336 hours of corrosion. Failure was observed after 500 hours of exposure.

Delamination between the coating system and the zeolite is evident in the scribed areas of the panels that contained the Mil-PRF-85582 Type I Class N primer and Mil-PRF-85285 topcoat (*Figure* 5-73). The adhesion of the primer to the zeolite surface was affected by the addition of the topcoat.

The self-priming topcoat was delaminating from the zeolite surface and there was corrosion present within the scribes after 168 hours of exposure to the salt fog (*Figure* 5-74).
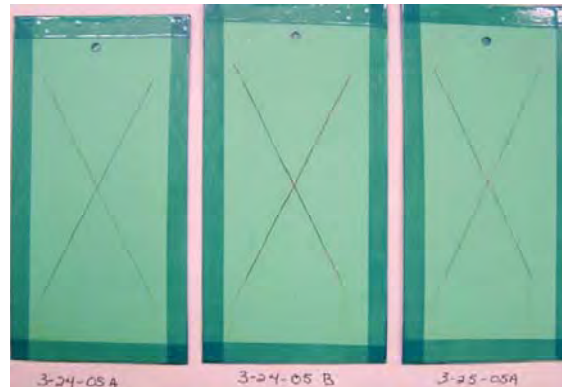
*Figure* 5-72 Zeolite coated aluminum 2024-T3 with Mil-PRF-85582 Type I Class N primer after 336 hours of exposure
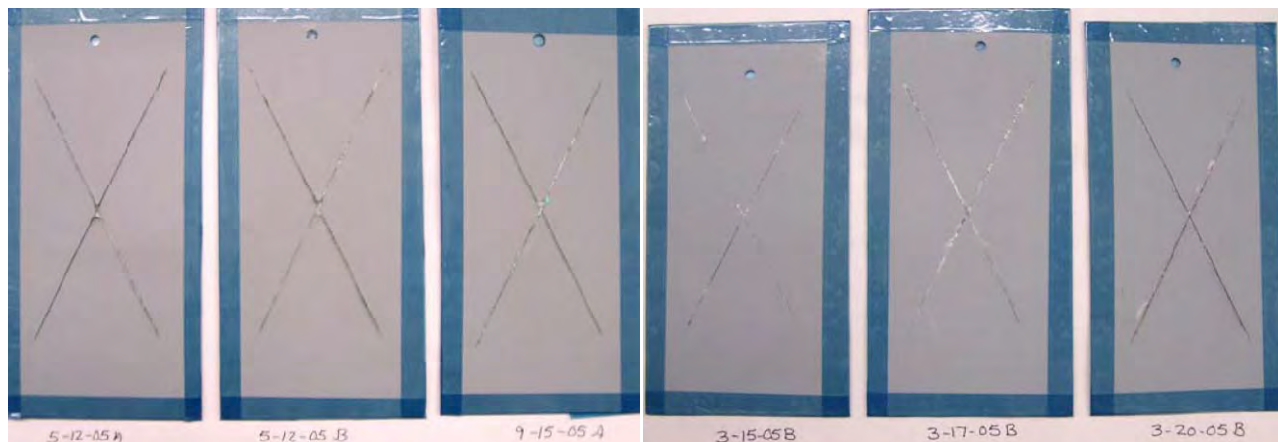
*Figure* 5-73 Zeolite coated aluminum 2024-T3 panels with Mil-PRF-85582 Type I Class N primer and Mil-PRF-85285 topcoat after 168 hours of exposure

*Figure* 5-74 Zeolite coated 2024-T3 aluminum with self-priming topcoat TT-P-2756A after 168 hours of exposure

## Summary

The bare zeolite coating offers excellent corrosion protection on 2024-T3 aluminum in the accelerated weathering tests. The reproducibility of the zeolite deposition process is excellent. A simple alkaline detergent solution pretreatment is used for all aluminum alloys and steels. A single chemical formulation is used for generating zeolite coating on all metals. If the coating is breached, corrosion remains localized to the damaged area. The zeolite does not blister or delaminate from any damaged areas. It appears from the most recent test results that a consistent zeolite application has been achieved. After 2205 hours of salt fog exposure there is no visual difference between a rough or smooth zeolite surfaces.

A complete zeolite coating system passing 3100 hours of salt-fog exposure (ASTM B117) has been achieved. The chromated primer (Mil-PRF-23377) both with and without topcoat (Mil-

PRF-85285) showed no delamination of the primer or topcoat from the zeolite and there was no rust observed in the scribed areas after 3100 hours salt-fog exposure.

## Task 3-5: Examine substrate degradation and corrosion inhibition – EIS test
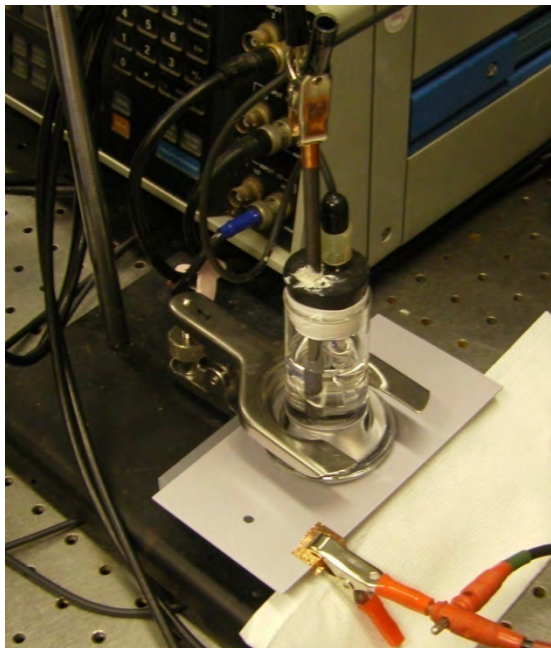


Figure 5-75 EIS test cell

EIS testing procedure

EIS testing was carried out at room temperature with Solartron potentiostat SI 1287 and Solartron impedance/gain-phase analyzer SI1260 in a three-electrode Cell (Gamry PTC1 Paint Test Cell) with a graphite rod counter electrode and a saturated calomel electrode (SCE) as the reference electrode (Figure 5-75). A ZSM-5 coated AA 2024-T3 was used as the working electrode with an exposed area of 15 cm$^2$. A small area of bare metal substrate is exposed on one side of the coated panel for electrical connection with copper conducting tape (as shown in *Figure* 5-24, right). The corrosive medium was 0.5 mol/L NaCl aqueous solution. The impedance measurements were performed at an open circuit potential with applied 10 mV sinusoidal perturbations in the frequency range of $10^{-2}$ -$2*10^5$ Hz with 10 steps per decades.

EIS measurement results

To date, a ten-day EIS test was measured. During this period, the spectra don't change much (Figure 5-76). The bode plot for the ZSM-5 coated AA 2024 has two distinguishable time-dependent processes. The time constant at high frequencies ($10^3$~$10^5$ Hz) is related to the capacitance of zeolite coating. The resistive plateau at $10^0$~$10^3$ Hz represents the pore resistance of the zeolite film. The time constant at low frequencies ($10^{-2}$~$10^0$ Hz) is attributed to the capacitance of an intermediate layer present at the AA/ZSM-5 interface. An intermediate layer was also reported for sol-gel coating[29] and chromate conversion coating[30], although the composition is not clear. It is believed that the intermediate layer is very important for the corrosion resistant coating since it is the last barrier for the corrosive species.

A three layer model (Figure 5-77) was used to fit the data and explain the protective and degradation mechanism of ZSM-5 coating. One simulation example was given in Figure 5-77, which shows perfect fitting results. Since a 10-day EIS test is not enough to show the degradation of ZSM-5 coatings, no further explanation was given here. A long-term EIS test is under investigation.
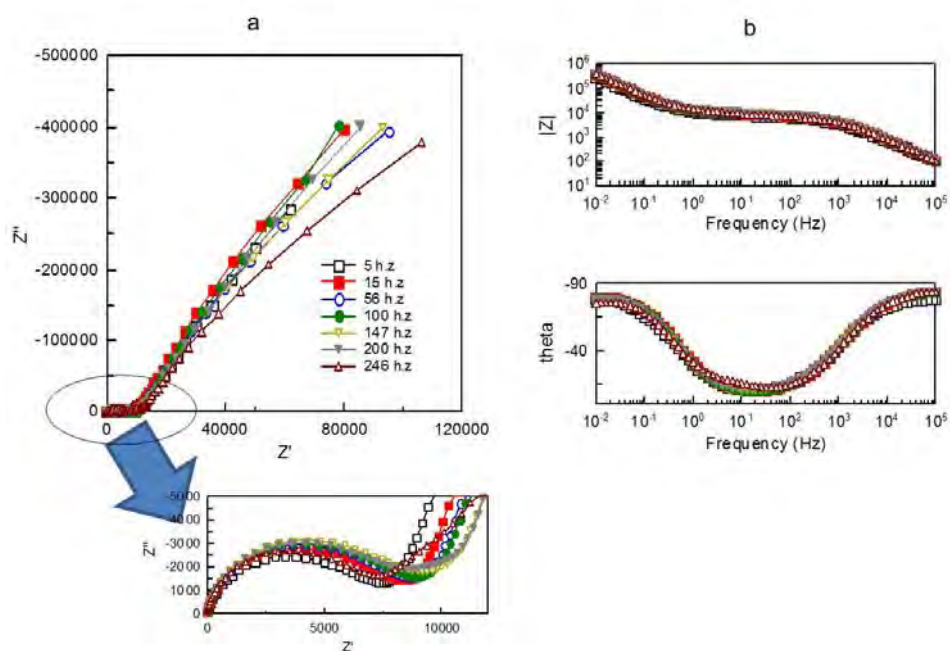
Figure 5-76 Impedance spectra during immersion in 0.5 mol/L NaCl solution. (a) Nyquist plot and (b) Bode plot
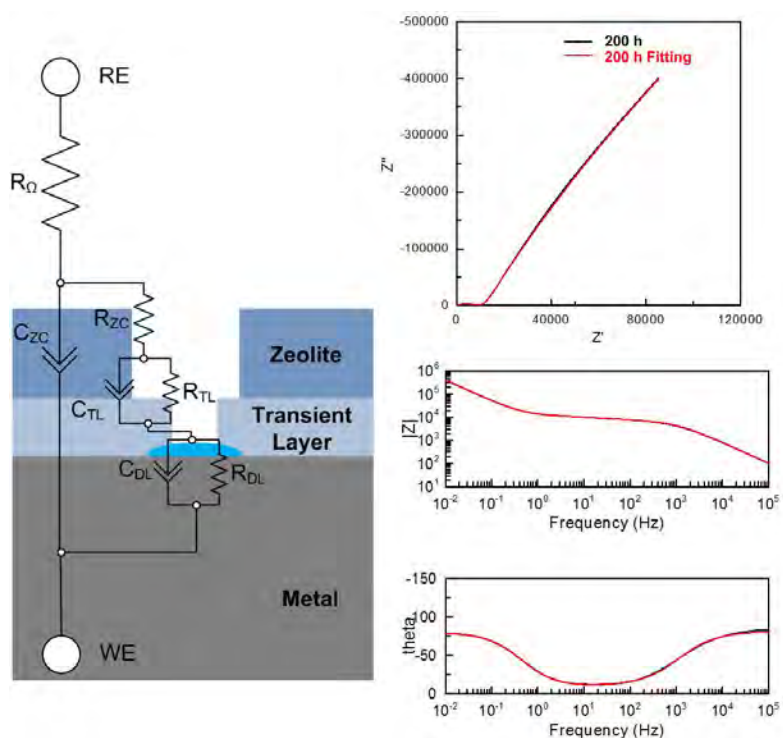


Figure 5-77 EIS model and fitting result

**Task 3-6: Marine atmosphere test/coating degradation studies**

Six zeolite coated 2024-T3 coupons, and five 2024-T3 bare aluminum substrates were furnished by the University of California at Riverside (UCR). The samples remained in an unscribed condition, and were exposed for 12 months at the NASA Beach Corrosion Test Site at the Kennedy Space Center (KSC).

The following evaluations were performed on the panels:
    A) Degree of Rusting on Painted Steel Surface (ASTM D 610)
    B) Degree of Blistering of Paints (ASTM D714)
    C) Color in CIE Lab format. (ASTM D 2244)
    D) Gloss (ASTM D 523)
    E) Overview photo-documentation of the samples.

The NASA Beach Corrosion Test Facility (Figure 5-78  NASA Beach Corrosion Test Site) is located approximately 150 feet from the Atlantic Ocean, and is approximately 1 mile south of the Space Shuttle launch sites. The facility includes an atmospheric exposure site, flowing seawater immersion tanks with spray-down capabilities, cathodic protection compatibility tank, weather station, on-site electrochemistry laboratory, monitoring station, and sample preparation and processing area.  The beachfront laboratory has the capability to provide real-time data access to monitor corrosion experiments and surrounding weather conditions.



Figure 5-78  NASA Beach Corrosion Test Site

Six zeolite coated 2024-T3 coupons and five uncoated 2024-T3 samples were labeled as shown in Table 5-5 Zeolite samples and bare AA 2024-T3 from UCR. The numbering sequence, provided in Table 5-5, is used throughout this report.

Table 5-5 Zeolite samples and bare AA 2024-T3 from UCR

| UCR Zeolite Samples | UCR AA 2024-T3 Samples |
|---|---|
| 080619B | |
| 080620A | 2024 T3-1 |
| 080620B | 2024 T3-2 |
| 080621A | 2024 T3-3 |
| 080621B | 2024 T3-4 |
| 080626A | 2024 T3-5 |

All samples were mounted on corrosion racks at the NASA Beach Corrosion Test Site, and remained in place for 12 months. Each rack was oriented so the face of each coupon was in direct exposure with the coastal marine atmospheric environment from the Atlantic Ocean (Figure 5-79 NAVAIR Panels at the NASA Beach Corrosion Test Site).



Figure 5-79 NAVAIR Panels at the NASA Beach Corrosion Test Site

Coating performance parameters, with respect to corrosion control, were ascertained using the following methodologies:
- ASTM D1654 - Standard Test Method for Evaluation of Painted or Coated Specimens Subjected to Corrosive Environments
- ASTM D610 - Standard Test Method for Evaluating Degree of Rusting on Painted Surfaces
- ASTM D714 - Standard Test Method for Evaluating Degree of Blistering of Paints

Gloss and color measurements were performed to determine aesthetic and technical parameters related to the coating systems.

ASTM D610 Standard Test Method for Evaluating Degree of Rusting on Painted Surfaces

All coupons were rated according to ASTM D 610 "*Standard Test Method for Evaluating Degree of Rusting on Painted Surfaces*". ASTM D 610 rates the degree of rusting on painted steel surfaces on a scale in which each rating number correlates to the area of a coupon that is corroded (Table 5-6 ASTM D 610 Rating Scale).

Table 5-6 ASTM D 610 Rating Scale

| Description | Rating |
|---|---|
| No rusting or less than 0.01% of surface rusted. | 10 |
| Minute rusting, less than 0.03% of surface rusted. | 9 |
| Few isolated rust spots, less than 0.1% of surface rusted. | 8 |
| Less than 0.3% of surface rusted. | 7 |
| Extensive rust spots, but less than 1% of surface rusted. | 6 |
| Rusting to the extent of 3% of surface rusted. | 5 |
| Rusting to the extent of 10% of surface rusted. | 4 |
| Approximately 1/6 of the surface rusted. | 3 |
| Approximately 1/3 of the surface rusted. | 2 |
| Approximately 1/2 of surface rusted. | 1 |
| Approximately 100% of surface rusted. | 0 |

To determine the degree of corrosion emanating from the unscribed metal surface, a series of pictorial examples from ASTM D 610 were used as a reference. These reference diagrams are shown in Figure 5-80 Pictorial examples of rust type and grade (7-9) from ASTM D 610.Figure 5-81, and Figure 5-82. In accord with these illustrations, the type of corrosion is reported as spot, general, pinpoint or hybrid; and the extent of corrosion is reported on a scale from 0-10 (worst-best).

A summary of the evaluations, according to ASTM D 610, is shown in Table 5-7 Summary of ASTM D 610 Ratings – Degree of Rusting on Painted SurfaceThe coating performance is color coded according to the extent of corrosion away from the scribe or edges of the samples. A perfect rating of 10 was color coded in green. A rating number from 7 to 10 (non inclusive of 10) was color coded in yellow. Finally, a rating below 7 was color coded in red.

Table 5-7 Summary of ASTM D 610 Ratings – Degree of Rusting on Painted Surface

| Substrate / Code | Conversion Coat | Primer | Topcoat | Panel ID #s | 4 Month | 6 Month | 9 Month | 12 Month |
|---|---|---|---|---|---|---|---|---|
| 2024 | UC Zeolite | None | None | 080619B | 6 | 5 | 5 | 2 |
| 2024 | UC Zeolite | None | None | 080620A | 10 | 10 | 10 | 8 |
| 2024 | UC Zeolite | None | None | 080620B | 10 | 8 | 8 | 7 |
| 2024 | UC Zeolite | None | None | 080621A | 7 | 7 | 6 | 6 |
| 2024 | UC Zeolite | None | None | 080621B | 7 | 7 | 6 | 6 |
| 2024 | UC Zeolite | None | None | 080626A | 6 | 5 | 5 | 5 |

The summary in Table 5-7 proves useful to show the degree of protection afforded by the different zeolite coated samples. All ratings that deviated from a perfect condition (10) were classified as pinpoint. It should be noted that neither a primer, nor a topcoat was used on the 2024-T3 zeolite samples.
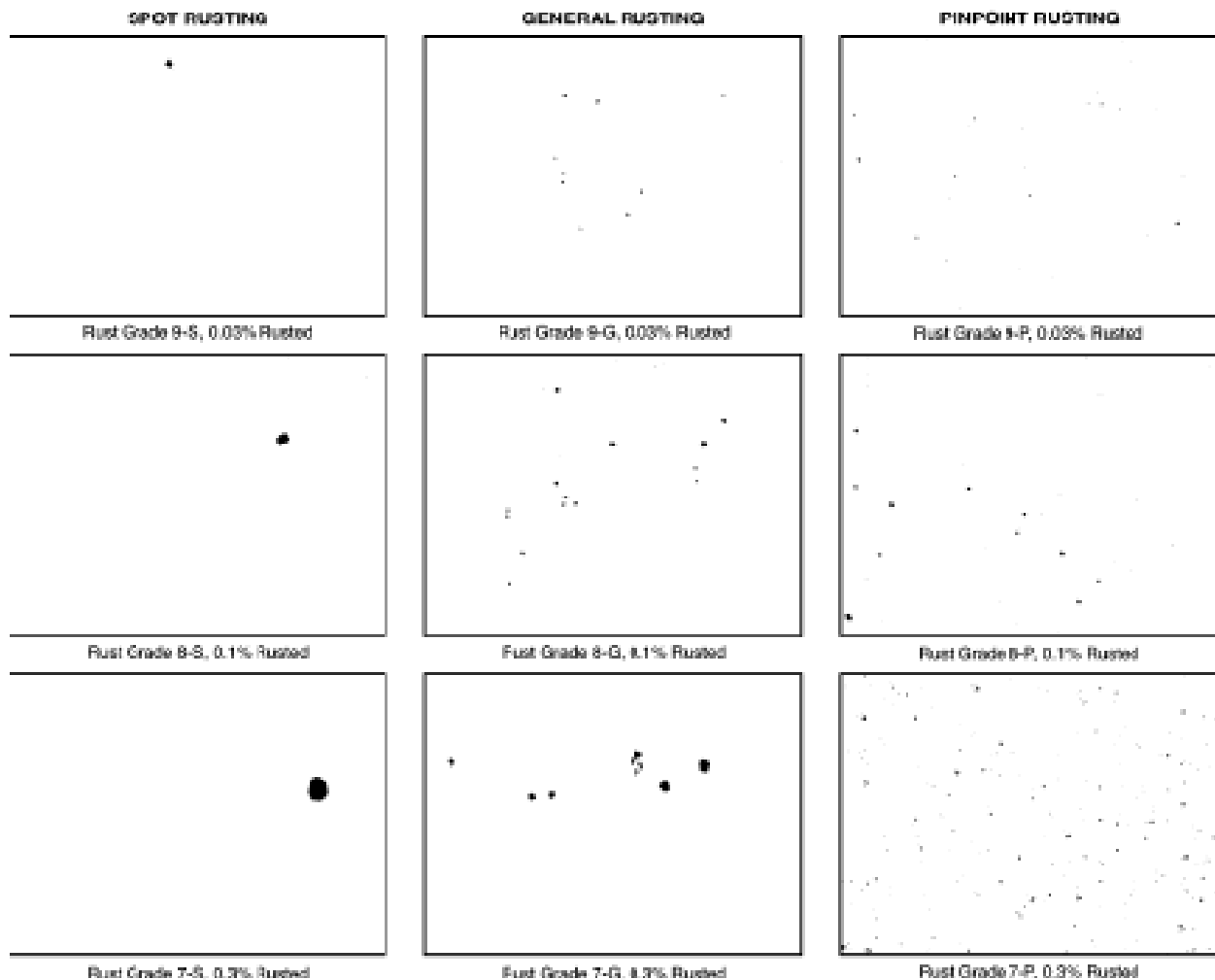


Figure 5-80 Pictorial examples of rust type and grade (7-9) from ASTM D 610.
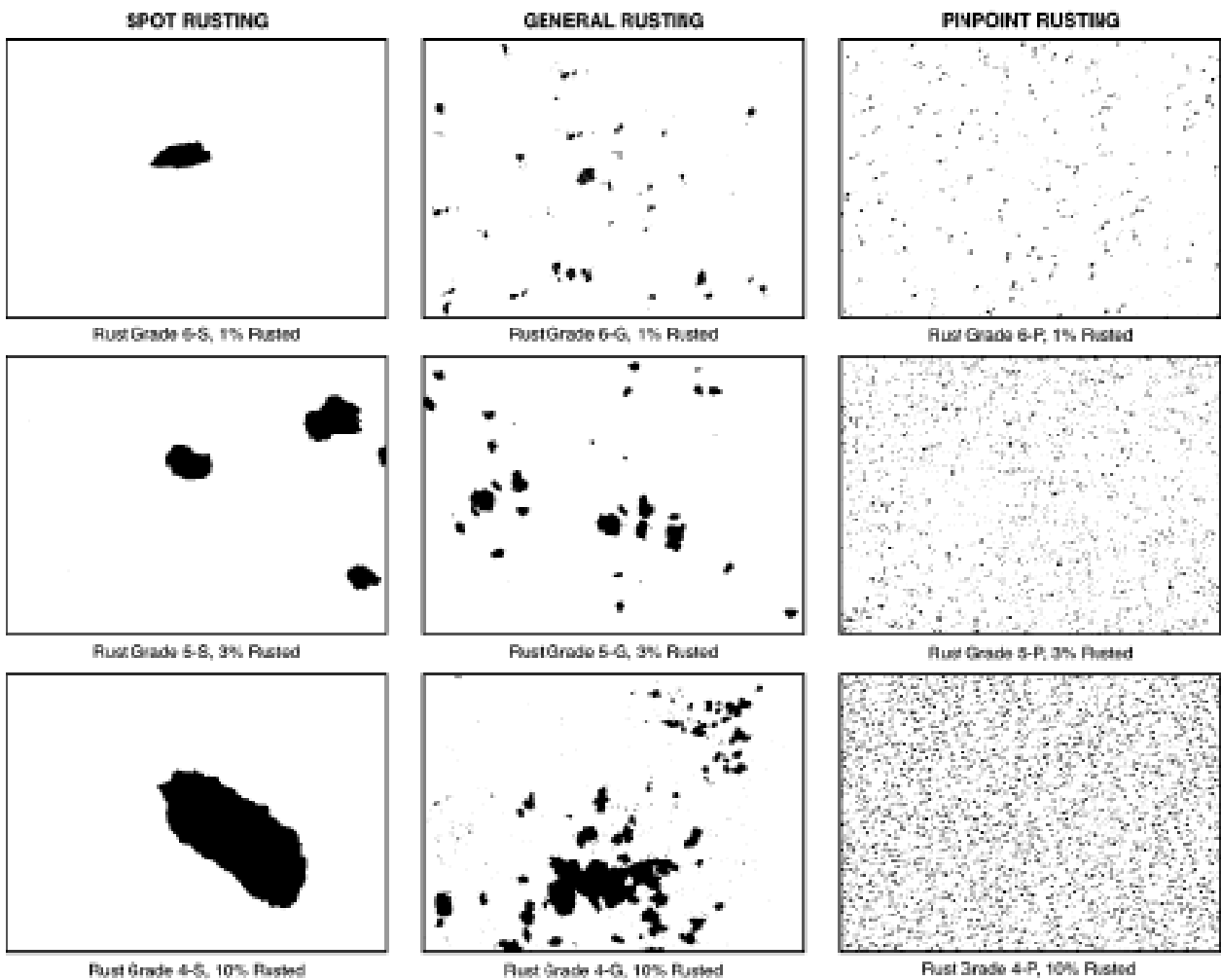
Figure 5-81 Pictorial examples of rust type and grade (4-6) from ASTM D 160

SPOT RUSTING    GENERAL RUSTING    PINPOINT RUSTING

Rust Grade 3-S, 16% Rusted    Rust Grade 3-G, 16% Rusted    Rust Grade 3-P, 16% Rusted

Rust Grade 2-S, 33% Rusted    Rust Grade 2-G, 33% Rusted    Rust Grade 2-P, 33% Rusted

Rust Grade 1-S, 50% Rusted    Rust Grade 1-G, 50% Rusted    Rust Grade 1-P, 50% Rusted
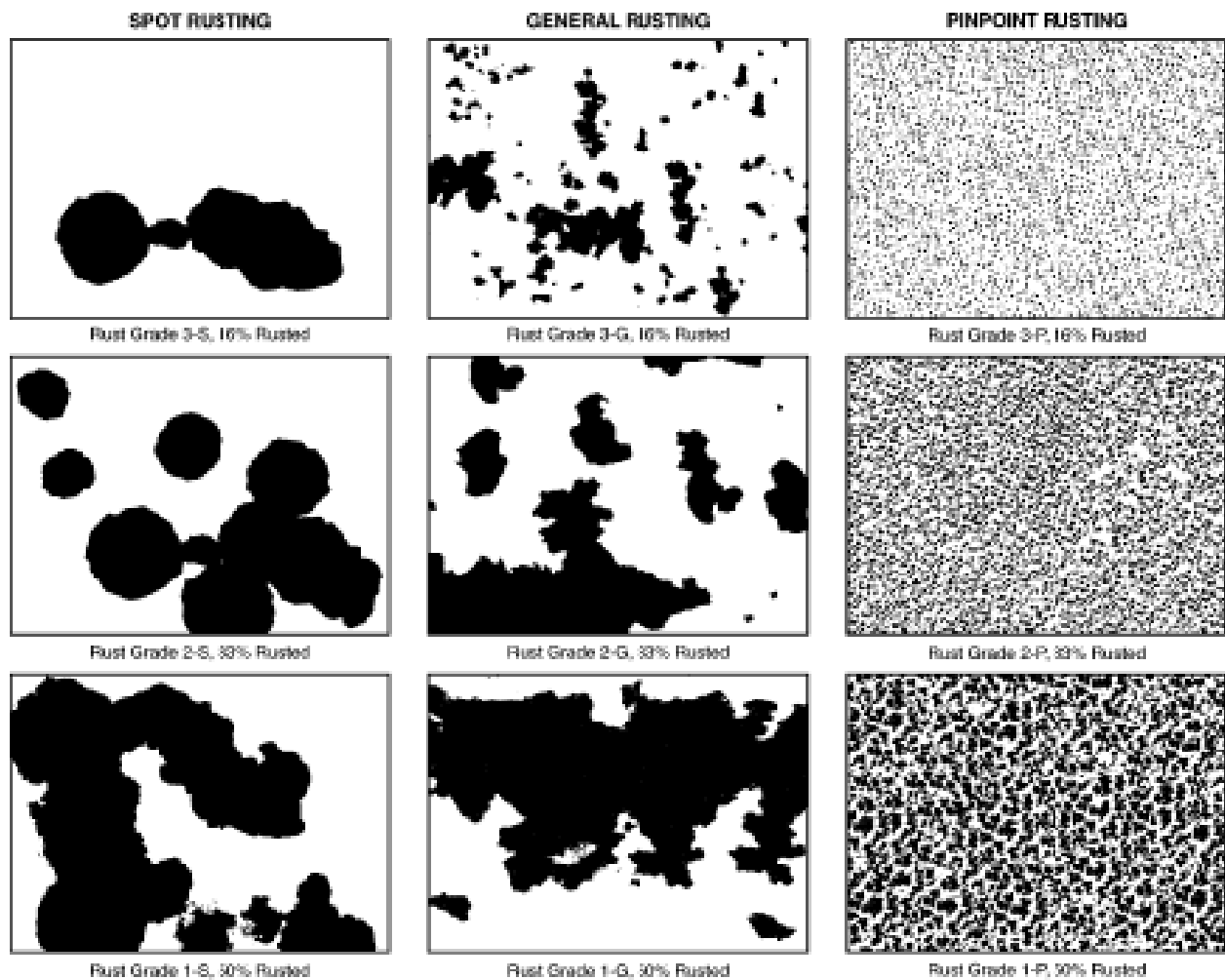
Figure 5-82 Pictorial examples of rust type and grade (1-3) from ASTM D 610

ASTM D714 Standard Test Method for Evaluating Degree of Blistering of Paints

ASTM D714 is a test method that uses photographic reference standards to evaluate the degree of blistering that may develop underneath a coating. The ratings are based upon the size of the blister, as well as the distribution of anomalies. Figure 5-83 ASTM D714-02 Blister Reference Photographs shows the template that was used to evaluate the size and distribution of blistering.
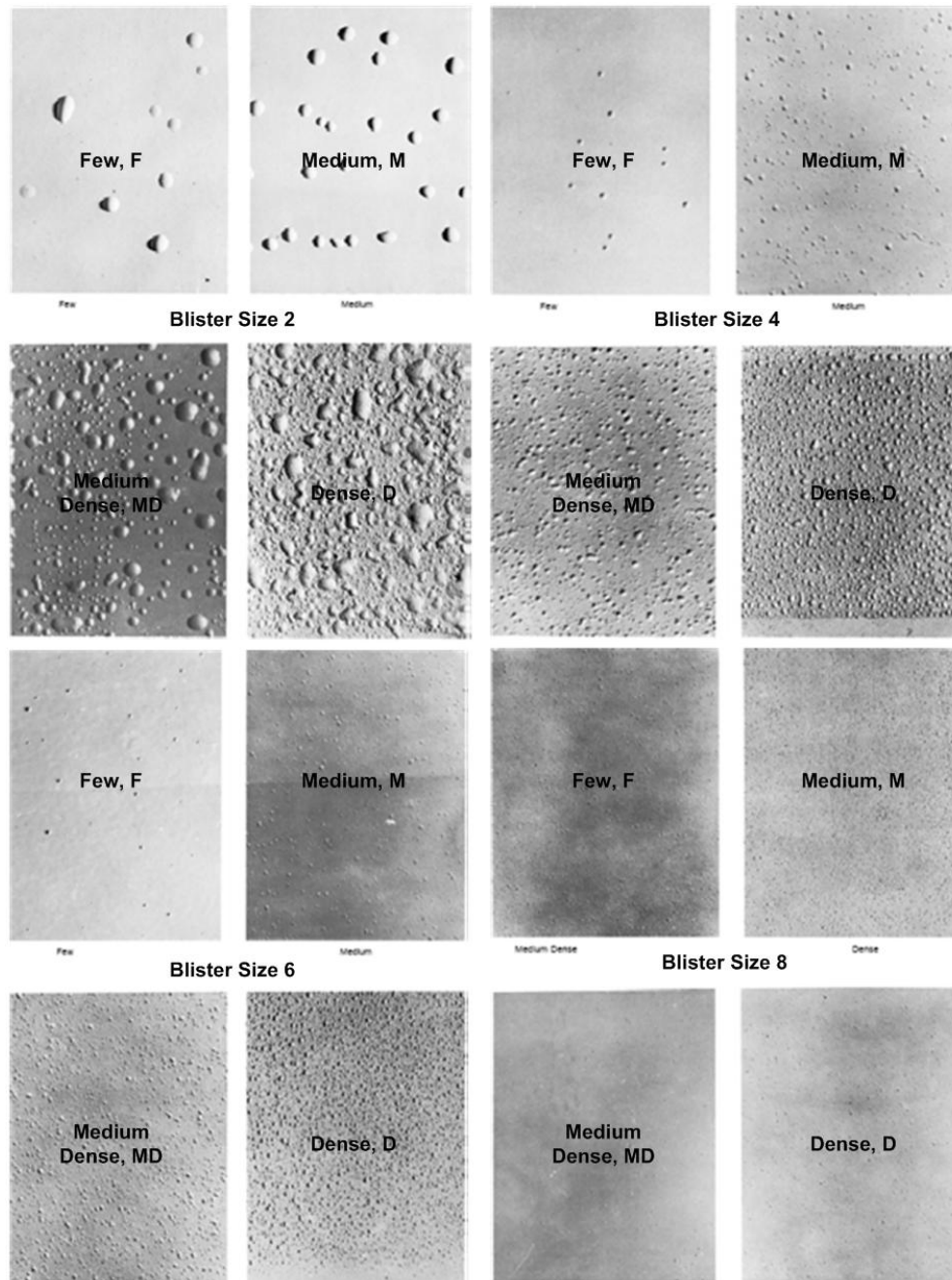
Figure 5-83 ASTM D714-02 Blister Reference Photographs

A summary of the ASTM D 714 blister ratings (by coating type) is shown in Table 5-8. A perfect rating value of 10 (indicating no blisters) was color coded in green. A system that exhibited blisters was color coded in red. Yellow indicates that the coating had previously blistered.

No blistering was evident on any of the zeolite coated aluminum substrates throughout the duration of exposure.

Table 5-9.  Summary of ASTM D 714 Ratings – Degree of Blistering

| System | Substrate / Code | Conversion Coat | Primer | Topcoat | Panel ID #s | 4 Month | 6 Month | 9 Month | 12 Month |
|--------|------------------|-----------------|--------|---------|-------------|---------|---------|---------|----------|
| UC | 2024 | UC Zeolite | None | None | 080619B | | | | |
| | 2024 | UC Zeolite | None | None | 080620A | | | | |
| | 2024 | UC Zeolite | None | None | 080620B | | | | |
| | 2024 | UC Zeolite | None | None | 080621A | | | | |
| | 2024 | UC Zeolite | None | None | 080621B | | | | |
| | 2024 | UC Zeolite | None | None | 080626A | | | | |

| Color Code | |
|------------|---|
| No Blisters | |
| Previously Blistered | |
| Blisters | |

## ASTM D2244 Color Measurements

Color can be a key aesthetic and technical consideration for a coating system.   Color measurements were recorded on a ColorTec-PCM handheld portable color meter using the CIE L*a*b* format, D-65 illuminant, and a 10° observer.

Briefly, a color's "lightness" (L*) runs from light (white) to dark (black).  A more reddish color will give a positive a* value and conversely, a more greenish color will give a negative a* value.  As with the a* values, the more bluish color will give a positive b* value, and a more yellowish color will give a negative b* value.

A single number indicator of overall color change (delta E) was calculated by taking the square root of the sum of the squares of the lightness and color difference according to the following equation:

$$\text{delta E} = \sqrt{\left(L_i - L_f\right)^2 + \left(a_i - a_f\right)^2 + \left(b_i - b_f\right)^2}$$

Where:

L$_i$ = initial Lightness value      a$_i$ = initial Red/Green value

L$_f$ = final Lightness value        a$_f$ = final Red/Green value

b$_i$ = initial Blue/Yellow value   b$_f$ = final Blue/Yellow value

As a general rule, a "*delta E*" value of 1 is discernable by the human eye in a side-by-side comparison.  However, in less than ideal lighting, a delta E value of 2 or 3 can still be considered the same color.   Delta E values were calculated from the initial, and time dependent measurements after each exposure period.

The delta E change in color for each coating type and duration of exposure is shown in Table 5-10.  Color values for individual coupons are reported in Tables 11-14.  Each value was based upon the average of three measurements for each sample.

As expected, significant changes in color were exhibited from white corrosion products that formed on the uncoated 2024-T3 aluminum substrates.  Significant changes in color were not seen (compared to the unprotected aluminum) for the zeolite coated specimens.

Since a topcoat was not used in conjunction with the zeolite pretreatment, color values may be irrelevant for the zeolite coated product when used in the field.

Table 5-10.  Average Delta E Color Calculations by Coating Type.

| Sample | Average Delta E Calculations by Group | | | |
| | 4 Month Delta E | 6 Month Delta E | 9 Month Delta E | 12 Month Delta E |
|---|---|---|---|---|
| **2024 T3** | 24.26 | 23.89 | 31.09 | 22.36 |
| | | | | |
| **080619B** | 5.92 | 5.69 | 5.34 | 5.78 |
| **080620A** | 6.74 | 6.87 | 6.43 | 6.37 |
| **080620B** | 6.16 | 6.04 | 5.81 | 5.75 |
| **080621A** | 3.31 | 3.30 | 3.45 | 3.40 |
| **080621B** | 3.39 | 3.27 | 3.16 | 3.07 |
| **080626A** | 5.18 | 5.26 | 6.04 | 5.76 |

Table 5-11.  Four Month Color Ratings

| Sample | 4 Month Delta E | Initial L | Intial a | Initial b | 4 month L | 4 month a | 4 month b |
|---|---|---|---|---|---|---|---|
| **2024 T3-1** | 22.441 | 51.84 | -3.59 | 8.34 | 73.72 | 1.12 | 6.70 |
| **2024 T3-2** | 23.528 | 56.03 | 11.27 | -7.51 | 72.08 | 0.97 | 6.27 |
| **2024 T3-3** | 34.792 | 51.43 | 11.09 | -20.77 | 70.65 | 1.00 | 6.42 |
| **2024 T3-4** | 12.815 | 55.43 | -0.60 | 2.70 | 67.94 | 0.80 | 5.10 |
| **2024 T3-5** | 27.711 | 53.89 | -12.85 | 18.68 | 74.82 | 1.14 | 7.10 |
| | | | | | | | |
| **080619B** | 5.916 | 74.93 | 6.42 | -2.93 | 75.45 | 2.12 | 1.10 |
| **080620A** | 6.743 | 74.44 | 6.16 | -6.22 | 76.27 | 2.56 | -0.82 |
| **080620B** | 6.162 | 74.76 | 6.34 | -4.91 | 76.56 | 3.22 | 0.09 |
| **080621A** | 3.314 | 75.65 | 4.31 | -3.26 | 75.57 | 2.27 | -0.65 |
| **080621B** | 3.392 | 77.71 | 4.27 | -2.52 | 78.17 | 2.49 | 0.33 |
| **080626A** | 5.182 | 68.44 | 3.02 | 1.08 | 71.51 | 0.70 | 4.55 |

Table 5-12.  Six Month Color Ratings

| Sample | Delta E | Initial L | Intial a | Initial b | 6 month L | 6 month a | 6 month b |
|---|---|---|---|---|---|---|---|
| **2024 T3-1** | 21.860 | 51.84 | -3.59 | 8.34 | 73.14 | 0.90 | 6.34 |
| **2024 T3-2** | 22.728 | 56.03 | 11.27 | -7.51 | 70.93 | 0.88 | 6.15 |
| **2024 T3-3** | 35.297 | 51.43 | 11.09 | -20.77 | 71.54 | 0.93 | 6.40 |
| **2024 T3-4** | 12.602 | 55.43 | -0.60 | 2.70 | 67.74 | 0.63 | 5.10 |
| **2024 T3-5** | 26.977 | 53.89 | -12.85 | 18.68 | 73.66 | 0.96 | 6.59 |
| | | | | | | | |
| **080619B** | 5.687 | 74.93 | 6.42 | -2.93 | 75.64 | 2.16 | 0.77 |
| **080620A** | 6.873 | 74.44 | 6.16 | -6.22 | 76.50 | 2.47 | -0.80 |
| **080620B** | 6.041 | 74.76 | 6.34 | -4.91 | 76.49 | 3.12 | -0.10 |
| **080621A** | 3.304 | 75.65 | 4.31 | -3.26 | 75.61 | 2.15 | -0.76 |
| **080621B** | 3.269 | 77.71 | 4.27 | -2.52 | 78.22 | 2.41 | 0.12 |
| **080626A** | 5.256 | 68.44 | 3.02 | 1.08 | 71.66 | 0.72 | 4.54 |

Table 5-13.  Nine Month Color Ratings

| Sample | Delta E | Initial L | Intial a | Initial b | 9 month L | 9 month a | 9 month b |
|---|---|---|---|---|---|---|---|
| 2024 T3-1 | 20.655 | 51.84 | -3.59 | 8.34 | 71.89 | 0.92 | 6.27 |
| 2024 T3-2 | 43.190 | 56.03 | 11.27 | -7.51 | 95.81 | -1.26 | 3.71 |
| 2024 T3-3 | 52.367 | 51.43 | 11.09 | -20.77 | 96.04 | -1.26 | 3.72 |
| 2024 T3-4 | 12.742 | 55.43 | -0.60 | 2.70 | 67.77 | 0.76 | 5.57 |
| 2024 T3-5 | 26.482 | 53.89 | -12.85 | 18.68 | 73.00 | 0.95 | 6.61 |
| | | | | | | | |
| 080619B | 5.342 | 74.93 | 6.42 | -2.93 | 76.88 | 1.88 | -0.90 |
| 080620A | 6.433 | 74.44 | 6.16 | -6.22 | 75.39 | 2.67 | -0.90 |
| 080620B | 5.813 | 74.76 | 6.34 | -4.91 | 75.56 | 3.30 | -0.02 |
| 080621A | 3.445 | 75.65 | 4.31 | -3.26 | 75.47 | 2.14 | -0.59 |
| 080621B | 3.158 | 77.71 | 4.27 | -2.52 | 77.55 | 2.47 | 0.07 |
| 080626A | 6.041 | 68.44 | 3.02 | 1.08 | 72.46 | 0.69 | 4.94 |

Table 5-14.  Twelve Month Color Ratings

| Sample | Delta E | Initial L | Intial a | Initial b | 12 month L | 12 month a | 12 month b |
|---|---|---|---|---|---|---|---|
| 2024 T3-1 | 19.168 | 51.84 | -3.59 | 8.34 | 70.27 | 0.98 | 5.72 |
| 2024 T3-2 | 21.435 | 56.03 | 11.27 | -7.51 | 69.15 | 1.06 | 6.02 |
| 2024 T3-3 | 32.962 | 51.43 | 11.09 | -20.77 | 68.59 | 0.89 | 5.46 |
| 2024 T3-4 | 12.481 | 55.43 | -0.60 | 2.70 | 67.65 | 0.81 | 4.81 |
| 2024 T3-5 | 25.737 | 53.89 | -12.85 | 18.68 | 71.48 | 1.05 | 6.04 |
| | | | | | | | |
| 080619B | 5.780 | 74.93 | 6.42 | -2.93 | 77.12 | 2.04 | 0.14 |
| 080620A | 6.371 | 74.44 | 6.16 | -6.22 | 74.98 | 2.65 | -0.93 |
| 080620B | 5.748 | 74.76 | 6.34 | -4.91 | 75.01 | 3.25 | -0.07 |
| 080621A | 3.402 | 75.65 | 4.31 | -3.26 | 75.04 | 2.19 | -0.67 |
| 080621B | 3.067 | 77.71 | 4.27 | -2.52 | 77.27 | 2.52 | -0.04 |
| 080626A | 5.760 | 68.44 | 3.02 | 1.08 | 72.13 | 0.69 | 4.84 |

## ASTM D523 Gloss Measurements

Gloss can be a key aesthetic and technical consideration for a coating system.  The gloss meter records the amount of reflective illuminated light at specified angles of 20°, 60°, or 85°; and gives a value in gloss units (GU).  The 60° geometry is used for most specimens, and is the initial angle used to determine whether the 20° or 85° angles may be more applicable. The 20° angle is used when the 60° angle gloss values are higher than 70 GU's, while the 85° angle is used when the 60° angle gloss values are less than 10 GU's.
Gloss measurements were recorded using a calibrated BYK Gardner Tri-Gloss portable gloss meter.  Measurements were recorded in three locations on the face of each coupon, and the average of those three measurements is reported in Table 5-15.

The gloss measurements for the bare aluminum substrates were heavily influenced by the corrosion products that formed on the face of the unprotected samples.  This phenomenon is as expected, and provides a control that might be used to form a comparison with the zeolite coated samples.

Table 5-15.  Gloss Measurements by Sample

| | Gloss Measurements | | | | |
|---|---|---|---|---|---|
| | Initial Gloss | 4 mo. Gloss | 6 mo. Gloss | 9 mo. Gloss | 12 mo. Gloss |
| 2024 T3-1 | 98.2 | 9.3 | 3.9 | 2.5 | 1.8 |
| 2024 T3-2 | 51.2 | 3.4 | 1.8 | 1.6 | 1.3 |
| 2024 T3-3 | 109.0 | 4.4 | 3.1 | 2.0 | 1.5 |
| 2024 T3-4 | 145.0 | 1.9 | 1.5 | 1.1 | 1.0 |
| 2024 T3-5 | 105.0 | 7.8 | 4.8 | 3.4 | 2.3 |
| | | | | | |
| 080619B | 9.4 | 7.8 | 6.6 | 8.1 | 8.2 |
| 080620A | 13.1 | 13.8 | 11.6 | 13.6 | 12.9 |
| 080620B | 10.2 | 13.7 | 12.8 | 14.5 | 13.2 |
| 080621A | 2.6 | 3.3 | 3.8 | 3.9 | 2.8 |
| 080621B | 40.8 | 37.8 | 28.3 | 32.6 | 22.2 |
| 080626A | 10.7 | 8.7 | 7.1 | 7.2 | 5.9 |

Figure 5-84~5-89 show the digital pictures of those zeolite coated and bare AA2024-T3 samples exposed at marine atmosphere on the rack up to 12 month (each sample's position is labeled in Figure 5-84 ).

| | A | B | C | D | E |
|---|---|---|---|---|---|
| 1 | Empty | 2024-T3-1 | 080619B | 080626A | Empty |
| 2 | Empty | 2024-T3-2 | 080620A | Empty | Empty |
| 3 | Empty | 2024-T3-3 | 080620B | Empty | Empty |
| 4 | Empty | 2024-T3-4 | 080621A | Empty | Empty |
| 5 | Empty | 2024-T3-5 | 080621B | Empty | Empty |

Figure 5-84 Sample position on rack



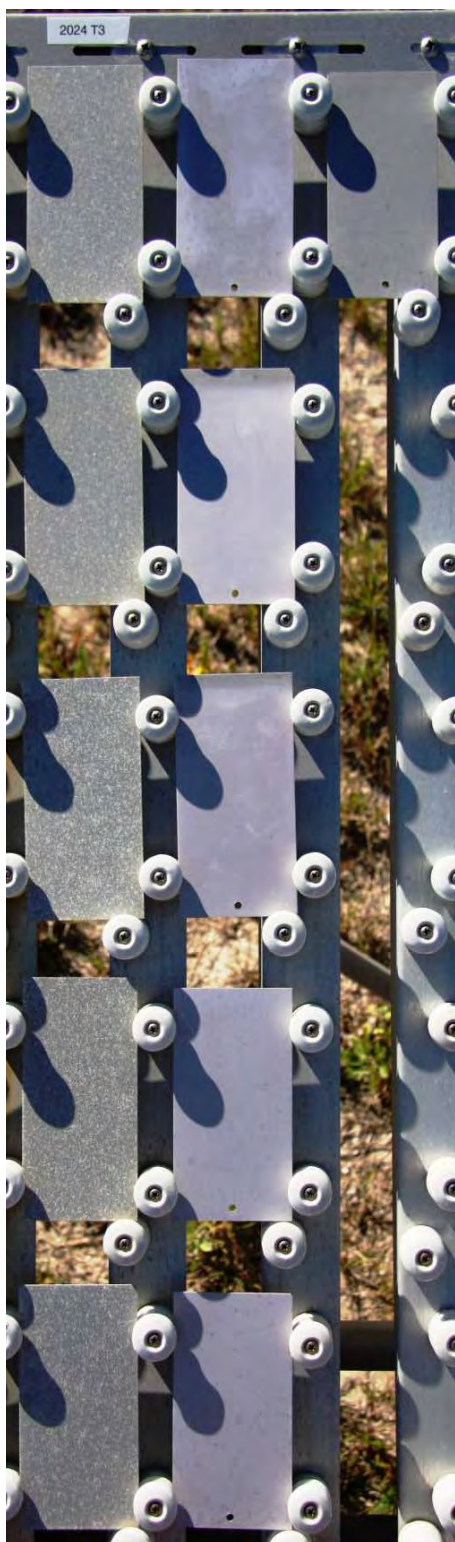Figure 5-85 Initial photo documentation

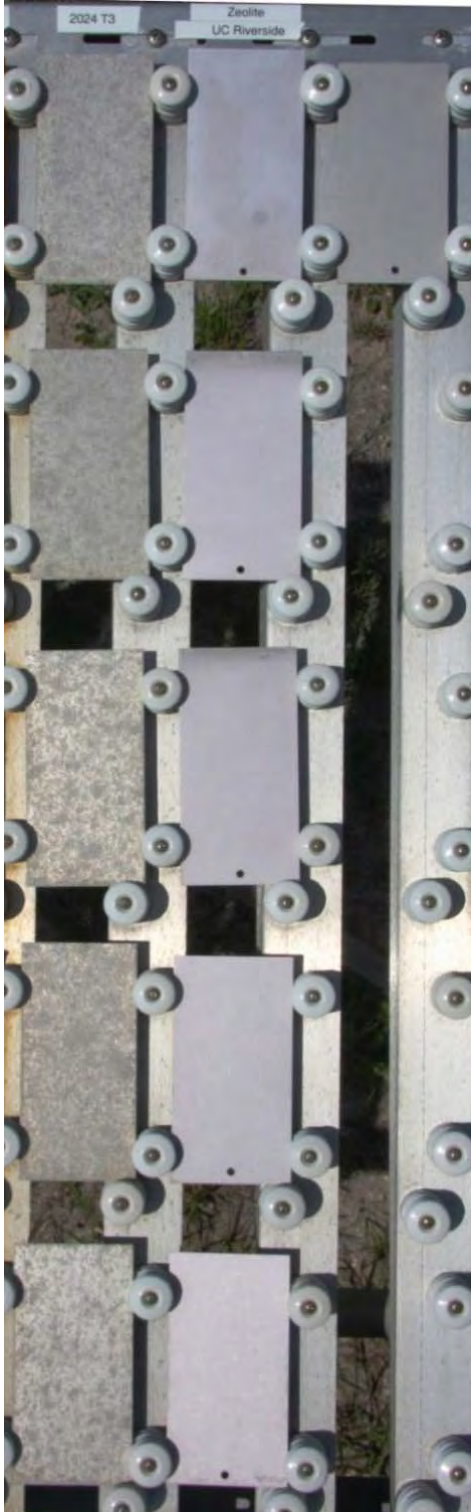Figure 5-86 Four month exposure



Figure 5-87 Six month exposure

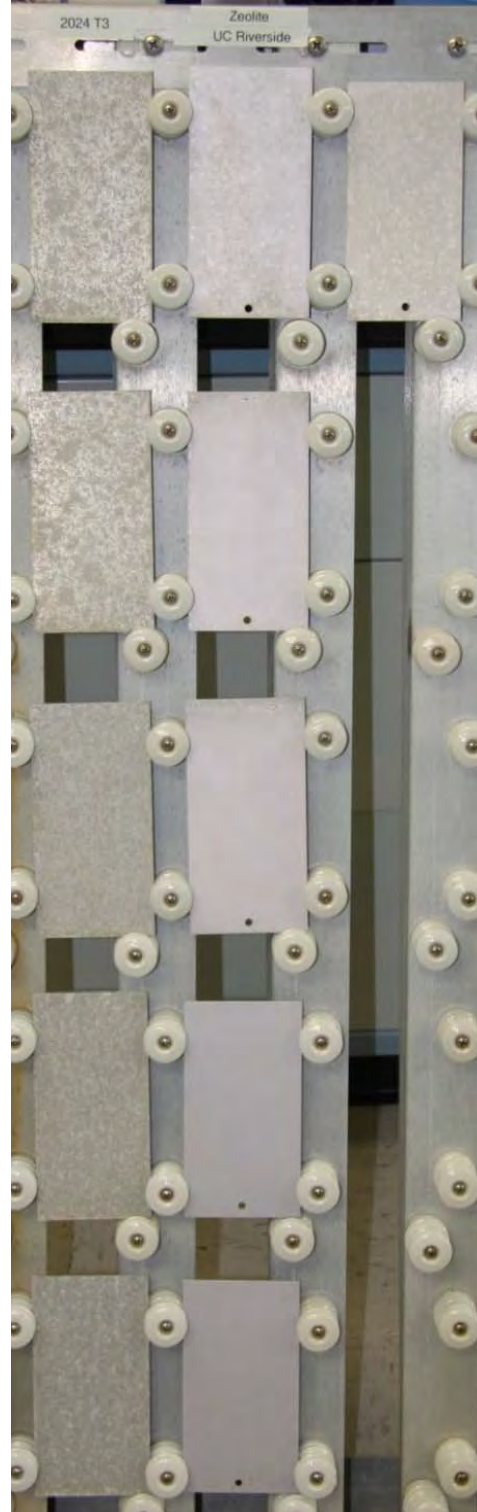Figure 5-88 Nine month exposure



Figure 5-89 Twelve month exposure

**Task 4: Technology Transition**

The corrosion resistant zeolite coating is protected by an issued US patent and one invention disclosure for the ionothermal synthesis process has been filed. There have been regular enquiries from companies about the technology (e.g., Metalast, VestaScience, UTEK Corporation, etc.). We have also submitted a demonstration pre-proposal lead by Navy China Lake to the ESTCP program. And now a full proposal is requested. We have recently demonstrated that zeolite could be possible replacement for hard chrome and cadmium. Since here mostly small parts are involved the pressured vessel is expected to be of less concern. This may open up more commercialization prospects.

## Appendix

Publications

1) Cheng, X.L., Z.B. Wang, and Y.S. Yan, *Corrosion-resistant zeolite coatings by in situ crystallization.* Electrochemical and Solid State Letters, 2001. **4**(5): p. B23-B26.

2) Wang, Z.B., et al., *Pure silica zeolite films as low-k dielectrics by spin-on of nanoparticle suspensions.* Advanced Materials, 2001. **13**(19): p. 1463.

3) Wang, Z.B. and Y.S. Yan, *Oriented zeolite MFI monolayer films on metal substrates by in situ crystallization.* Microporous and Mesoporous Materials, 2001. **48**(1-3): p. 229-238.

4) Mitra, A., et al., *Synthesis and corrosion resistance of high-silica zeolite MTW, BEA, and MFI coatings on steel and aluminum.* Journal of the Electrochemical Society, 2002. **149**(10): p. B472-B478.

5) Lai, Z.P., et al., *Microstructural optimization of a zeolite membrane for organic vapor separation.* Science, 2003. **300**(5618): p. 456-460.

6) Li, S., et al., *Micropatterned oriented zeolite monolayer films by direct in situ crystallization.* Chemistry of materials, 2003. **15**(14): p. 2687-2689.

7) Li, S., Z.J. Li, and Y.S. Yan, *Ultra-low-k pure-silica zeolite MFI films using cyclodextrin as porogen.* Advanced Materials, 2003. **15**(18): p. 1528.

8) Yan, Y., S. Li, and Z. Li, *Pure-Silica-Zeolite Low Dielectric Constant Films: Present and the Future.* Zeolite News letters, 2003. **20**: p. 110-119.

9) Li, S., et al., *TEM investigation of formation mechanism of monocrystal-thick b-oriented pure silica zeolite MFI film.* Journal of the American Chemical Society, 2004. **126**(34): p. 10732-10737.

10) Li, S., et al., *Evaluation of pore structure in pure silica zeolite MFI low-k thin films using positronium annihilation lifetime spectroscopy.* Journal of Physical Chemistry B, 2004. **108**(31): p. 11689-11692.

11) Li, S., et al., *Molecular sieving in a nanoporous b-oriented pure-silica-zeolite MFI monocrystal film.* Journal of the American Chemical Society, 2004. **126**(13): p. 4122-4123.

12) Li, Z.J., et al., *Effects of crystallinity in spin-on pure-silica-zeolite MFI low-dielectric-constant films.* Advanced Functional Materials, 2004. **14**(10): p. 1019-1024.

13) Mitra, A., et al., *Synthesis and evaluation of pure-silica-zeolite BEA as low dielectric constant material for microprocessors.* Industrial & Engineering Chemistry Research, 2004. **43**(12): p. 2946-2949.

14) Yan, Y.S. and H. Wang, *Nanostructured Zeolite Films*, in *Encyclopedia of nanoscience and nanotechnology*, H.S. Nalwa, Editor. 2004, American Scientific Publishers: Stevenson Ranch. p. 1-19.

15) Li, Z.J., et al., *Pure-silica-zeolite MEL low-k films from nanoparticle suspensions.* Journal of Physical Chemistry B, 2005. **109**(18): p. 8652-8658.

16) McDonnell, A.M.P., et al., *Hydrophilic and antimicrobial zeolite coatings for gravity-independent water separation.* Advanced Functional Materials, 2005. **15**(2): p. 336-340.

17) Munoz, R.A., D. Beving, and Y.S. Yan, *Hydrophilic zeolite coatings for improved heat transfer.* Industrial & Engineering Chemistry Research, 2005. **44**(12): p. 4310-4315.

18) Beving, D.E., et al., *Corrosion resistant high-silica-zeolite MFI coating - One general solution formulation for aluminum alloy AA-2024-T3, AA-5052-H32, AA-6061-T4, and AA-7075-T6.* Journal of the Electrochemical Society, 2006. **153**(8): p. B325-B329.

19) Hu, L.L., et al., *Interfacial adhesion of nanoporous zeolite thin films.* Journal of Materials Research, 2006. **21**(2): p. 505-511.

20) Li, Y.S., et al., *Microwave synthesis of LTA zeolite membranes without seeding.* Journal of Membrane Science, 2006. **277**(1-2): p. 230-239.
21) Li, Y.S., J. Liu, and W.S. Yang, *Formation mechanism of microwave synthesized LTA zeolite membranes.* Journal of Membrane Science, 2006. **281**(1-2): p. 646-657.
22) Li, Z.J., et al., *Mechanical and dielectric properties of pure-silica-zeolite low-k materials.* Angewandte Chemie-International Edition, 2006. **45**(38): p. 6329-6332.
23) O'Neill, C., et al., *Durability of hydrophilic and antimicrobial zeolite coatings under water immersion.* Aiche Journal, 2006. **52**(3): p. 1157-1161.
24) Johnson, M., et al., *Mechanical characterization of zeolite low dielectric constant thin films by nanoindentation.* Thin Solid Films, 2007. **515**(6): p. 3164-3170.
25) Cai, R., et al., *Ionothermal synthesis of oriented zeolite AEL films and their application as corrosion-resistant coatings.* Angewandte Chemie-International Edition, 2008. **47**(3): p. 525-528.
26) Cai, R. and Y. Yan, *Corrosion-resistant zeolite coatings.* Corrosion, 2008. **64**(3): p. 271-278.

Presentations

1) Beving D.; Yan Y. **2003.** Corrosion Resistant Zeolite Coatings: A General Coating for Aluminum Alloys. *The American Institute of Chemical Engineers National Meeting*, November 3-8, San Francisco, California.
2) Beving D.; McDonnell A.: Yan Y. **2004**, Corrosion Resistant Zeolite Coatings: A General Coating for Aluminum Alloys, American *Chemical Society 227th National Meeting*, March 28- April1, 2004, Anaheim, California.
3) Beving D.; McDonnell A.: Yan Y. **2004**, Corrosion Resistant Zeolite Coatings: A General Coating for Aluminum Alloys, *The American Institute of Chemical Engineers National Meeting*, November 7-12, Austin, Texas.
4) McDonnell A. M. P.; Beving D.; Wang A.; Chen W.; Yan Y. **2005.** Hydrophilic and antimicrobial zeolite coatings for gravity-independent water separation, *Adv. Functional Materials,* 15:336-339.
5) O'Neill C.; Beving D.; McDonnell A.; Chen W.; Yushan Y. **2005**, Hydrophilic and Antimicrobial Zeolite Coatings, *The American Institute of Chemical Engineers National Meeting*, October 30 - November 4, Cincinnati, Ohio.
6) O'Neill C.; Beving D.; McDonnell A.; Chen W.; Yushan Y. **2005**, Zeolite-A Coatings for Use in Condensing Heat Exchangers Onboard Manned Spacecraft, *The American Institute of Chemical Engineers National Meeting*, October 30 - November 4, Cincinnati, Ohio.
7) Mao Y.; Beving D.; Munoz R.; Yushan Y. **2005**, Hydrothermal Synthesis and Corrosion Resistance of Vanadium ZSM-5 Films, *The American Institute of Chemical Engineers National Meeting*, October 30 - November 4, Cincinnati, Ohio.
8) Mao Y.; Beving D.; Munoz R.; Yushan Y. **2005**, Hydrothermal Synthesis of Inorganic and Organic Nanocomposite ZSM-5 Films from Recycled Solution, *The American Institute of Chemical Engineers National Meeting*, October 30 - November 4, Cincinnati, Ohio.
9) Munoz R.; Beving D.; Mao Y.; Yushan Y. **2005**, Zeolite Y Coatings on Al-2024-T3 Substrate by a Novel Three-Step Synthesis Method, *The American Institute of Chemical Engineers National Meeting*, October 30 - November 4, Cincinnati, Ohio.

10) Lai Z.; Tsapatsis M.; Beving D.; Yan Y. **2005**, Fabrication of Zeolite Films Using Layer-by-Layer Depositions, *The American Institute of Chemical Engineers National Meeting*, October 30 - November 4, Cincinnati, Ohio.

11) Beving D.; Anderson N.; O'Neill C.; Yan Y. **2005**, Corrosion Resistant Zeolite Coatings: A General Coating for Aluminum Alloys, *The National Association of Corrosion Engineers Tri-Service Corrosion Conference*, November 14-18, Orlando, Florida.

12) Beving D.; Anderson N.; O'Neill C.; Yan Y. **2005**, Corrosion Resistant Zeolite Coatings: A General Coating for Aluminum Alloys, *The Electrochemical Society National Meeting*, October 16-21, Los Angeles, California.

13) Beving D.; Anderson N.; O'Neill C.; Yan Y. **2006**, Salt Fog Accelerated Weathering Testing of High-Silica-Zeolite MFI Coatings on Aluminum Alloy 2024-T3, *The Electrochemical Society Transactions*, 1(9):65-72.

14) Guthrie S.; Beving D.; Yan Y. **2006**, Zeolite Hybrid Coatings on Metal Alloys for Chemical Resistance, Hydrophilicity and Microbiocidal Activity, *The American Institute of Chemical Engineers National Meeting*, November 12 - 17, San Francisco, CA.

15) O'Neill C.; Beving D.; Flores D.; Chen W.; Yan Y. **2006**, Durability of Hydrophilic and Antimicrobial Zeolite Coatings, *The American Institute of Chemical Engineers National Meeting*, November 12 - 17, San Francisco, CA.

16) O'Neill C.; Beving D.; Chen W.; Yan Y. **2006**, Zeolite A/ZSM-5 Hybrid Coating, *The American Institute of Chemical Engineers National Meeting*, November 12 - 17, San Francisco, CA.

17) O'Neill C.; Beving D.; Chen W.; Yan Y. **2006**, Antimicrobial and Hydrophilic Zeolite Coating, *The American Institute of Chemical Engineers National Meeting*, November 12 - 17, San Francisco, CA.

18) R. Munoz, Y. Kim, D. Beving, Y. Yan **2006**. High Silica Zeolite (ZSM-5) Coated Aluminum (Al-20204-T3): Micro-Structural Characterization by Laser Confocal Microscopy and Electrochemical Studies, Oral Presentation at *210th Meeting of The Electrochemical Society*, October 29 – November 3, Cancun, Mexico.

19) R Munoz, J Liu, G Aguilar, Y Yan **2006**. Corrosion Resistant Hydrophilic Zeolite Coatings for Improved Heat Transfer, Poster Presentation at *210th Meeting of The Electrochemical Society*, October 29 – November 3, Cancun, Mexico.

20) R Cai, M Sun, Z Chen, D Beving, Y Yan, New synthesis route for corrosion resistant zeolite coatings, Poster Presentation at *212th ECS Meeting*, October 7-12, 2007, Washington, DC, USA.

21) D Beving, C O'Neill, N. Anderson, Y. Yan, Salt Fog Testing of Zeolite, Zeolite-Primer, and Zeolite-Primer-Topcoat Systems on AA-2024-T3, Oral Presentation at *212th ECS Meeting*, October 7-12, 2007, Washington, DC, USA.

22) R Beti, D Beving, Y Yan, Electronically Conductive Corrosion Resistant Zeolite Coatings by in-situ Crystallization, Poster Presentation at *213th ECS Meeting*, May 18-22, 2008, Phoenix, Arizona, USA.

## Reference

1) Kolcum, E.H., Aviation Week and Space Technology, 1991. **June 24**: p. 67.
2) Hegedus, C.R., et al., *A Review of Organic Coating Technology for United-States Naval Aircraft.* Journal of Coatings Technology, 1989. **61**(778): p. 31-42.
3) Waldrop, J.R. and M.W. Kendig, *Nucleation of chromate conversion coating on aluminum 2024-T3 investigated by atomic force microscopy.* Journal of the Electrochemical Society, 1998. **145**(1): p. L11-L13.
4) Wernick, S., R. Pinner, and P.G. Sheasby, *The Surface Treatment and Finishing of Aluminum and its Alloys*. 5th ed. 1987, Teddington, England: Finishing Publication Ltd.
5) Zhao, J., G. Frankel, and R.L. McCreery, *Corrosion protection of untreated AA-2024-T3 in chloride solution by a chromate conversion coating monitored with Raman spectroscopy.* Journal of the Electrochemical Society, 1998. **145**(7): p. 2258-2264.
6) Blasiak, J. and J. Kowalik, *A comparison of the in vitro genotoxicity of tri- and hexavalent chromium.* Mutation Research-Genetic Toxicology and Environmental Mutagenesis, 2000. **469**(1): p. 135-145.
7) Cornelius, K., *DoD Hazardous Waste Minimization Efforts.* Presentation at the Fifth Aerospace Hazardous Waste Minimization Conference, Costa Mesa, CA, 1990.
8) Breck, D.W., *Zeolite molecular sieves: Structure, chemistry, and use*. 1974, New York: Wiley. 771.
9) Szostak, R., *Handbook of molecular sieves*. 1992, New York: Van Nostrand Reinhold. xvi, 584.
10) Flanigen, E.M., et al., *Silicalite, a New Hydrophobic Crystalline Silica Molecular-Sieve.* Nature, 1978. **271**(5645): p. 512-516.
11) Young, S.W., et al., *Gadolinium Zeolite as an Oral Contrast Agent for Magnetic-Resonance-Imaging.* Jmri-Journal of Magnetic Resonance Imaging, 1995. **5**(5): p. 499-508.
12) Yan, Y., M.E. Davis, and G.R. Gavalas, *Preparation of Zeolite ZSM-5 Membranes by In-Situ Crystallization on Porous a-Al2O3.* Industrial & Engineering Chemistry Research, 1995. **34**(5): p. 1652-61.
13) Cheng, X., Z. Wang, and Y. Yan, *Corrosion-resistant zeolite coatings by in-situ crystallization.* Electrochemical and Solid-State Letters, 2001. **4**(5): p. B23-B26.
14) Yan, Y.S., X.L. Cheng, and Z.B. Wang, *Metal surfaces coated with molecular sieve for corrosion resistance*, in *US Patent 6521198*. 2003.
15) Wang, Z.B., et al., *Pure silica zeolite films as low-k dielectrics by spin-on of nanoparticle suspensions.* Advanced Materials, 2001. **13**(19): p. 1463-+.
16) Kendall, G., et al., *Power-law phenomena in adhesive de-bonding.* Materials Research Society Symposium Proceedings, 1997. **458**(Interfacial Engineering for Optimized Properties): p. 357-362.
17) Moulder, J.C., E. Uzal, and J.H. Rose, *Thickness and conductivity of metallic layers from eddy current measurements.* Review of Scientific Instruments, 1992. **63**: p. 3455.
18) Leonowicz, M.E., et al., *MCM-22 - A MOLECULAR-SIEVE WITH 2 INDEPENDENT MULTIDIMENSIONAL CHANNEL SYSTEMS.* Science, 1994. **264**(5167): p. 1910-1913.
19) Corma, A., et al., *Delaminated zeolite precursors as selective acidic catalysts.* Nature, 1998. **396**(6709): p. 353-356.
20) Wang, H.T., Z.B. Wang, and Y.S. Yan, *Colloidal suspensions of template-removed zeolite nanocrystals.* Chemical Communications, 2000(23): p. 2333-2334.

21) Corma, A., et al., *Delaminated zeolites: Combining the benefits of zeolites and mesoporous materials for catalytic uses.* Journal of Catalysis, 1999. **186**(1): p. 57-63.

22) Roth, W.J. and J.C. Vartuli, *Preparation of exfoliated zeolites from layered precursors: The role of pH and nature of intercalating media*, in *Nanoporous Materials Iii*. 2002. p. 273-279.

23) Ha, K., et al., *Facile assembly of zeolite monolayers on glass, silica, alumina, and other zeolites using 3-halopropylsilyl reagents as covalent linkers.* Advanced Materials, 2000. **12**(15): p. 1114-+.

24) Lai, Z.P., et al., *Microstructural optimization of a zeolite membrane for organic vapor separation.* Science, 2003. **300**(5618): p. 456-460.

25) Cooper, E.R., et al., *Ionic liquids and eutectic mixtures as solvent and template in synthesis of zeolite analogues.* Nature, 2004. **430**(7003): p. 1012-1016.

26) Xu, Y.P., et al., *Microwave-enhanced ionothermal synthesis of aluminophosphate molecular sieves.* Angewandte Chemie-International Edition, 2006. **45**(24): p. 3965-3970.

27) van Ooij, W.J. and D. Zhu, *Electrochemical impedance spectroscopy of bis-[triethoxysilypropyl]tetrasulfide on Al 2024-T3 substrates.* Corrosion, 2001. **57**(5): p. 413-427.

28) Galvele, J.R. and S.M. de De Micheli, *MECHANISM OF INTERGRANULAR CORROSION OF AL-CU ALLOYS.* Corrosion Science, 1970. **10**(11): p. 795-807.

29) Shchukin, D.G., et al., *Layer-by-layer assembled nanocontainers for self-healing corrosion protection.* Advanced Materials, 2006. **18**(13): p. 1672-+.

30) Campestrini, P., et al., *Chromate conversion coating on aluminum alloys - III. Corrosion protection.* Journal of the Electrochemical Society, 2004. **151**(6): p. B370-B377.